Title
Characterizing Gray Matter Atrophy and Preservation in Experimental Autoimmune Encephalomyelitis

Author
Meyer, Cassandra

Publication Date
2021

Peer reviewed|Thesis/dissertation

UNIVERSITY OF CALIFORNIA

Los Angeles

Characterizing Gray Matter Atrophy and Preservation in Experimental Autoimmune Encephalomyelitis

A dissertation submitted in partial satisfaction of the

requirements for the degree Doctor of Philosophy in

Neuroscience

by

Cassandra Meyer

2021

ABSTRACT OF THE DISSERTATION

Characterizing Gray Matter Atrophy and Preservation in Experimental Autoimmune Encephalomyelitis

by

Cassandra Meyer

Doctor of Philosophy in Neuroscience

University of California, Los Angeles, 2021

Professor Allan MacKenzie-Graham, Chair

Gray matter (GM) atrophy is considered one of the best predictors of disability accumulation in multiple sclerosis (MS) yet the mechanisms underlying its progression are poorly understood. Currently, there are no directly neuroprotective therapies in MS that can halt the progression of GM atrophy. While GM atrophy has been established in the most commonly used mouse model for MS, experimental autoimmune encephalomyelitis (EAE), there is a lack of studies directly investigating associated pathologies of GM atrophy and methods of sparing GM volume.

The projects in this dissertation were designed with the goal of characterizing changes in GM volume and associated pathology. In the second chapter, I investigated baseline sex differences in the C57BL/6 mouse brain. This was an important step in establishing the use of magnetic resonance imaging (MRI) and voxel-based morphometry (VBM) to identify differences in GM volume. Moreover, it highlighted the importance of performing experimental analyses within sex as we determined that

differences exist in the brain in healthy mice. In the third chapter, I sought to utilize VBM to localize atrophy *in vivo* in a chronic mouse model of EAE and to identify the spatial relationship between downstream axonal damage in the spinal cord and gray matter loss. I found substantial GM volume loss throughout the brain particularly within the cortex, caudoputamen, and thalamus during EAE. Further, I found axonal damage in the spinal cord was negatively correlated to GM volume in motor and sensorimotor regions of the cerebral cortex. In the fourth chapter, I describe a network of pathology associated with GM atrophy that is disrupted by estriol treatment. I further identified ligation of ERβ as method of inducing remyelination in GM. Lastly, in chapter five, I used VBM to identify sex differences in GM atrophy during EAE. Using voxel-wise regression analysis I found a sex-specific relationship between disability and GM atrophy in the somatosensory cortex in males. I further found evidence of increased neuronal loss and increased axonal transection in males with EAE compared to their healthy controls than females with EAE compared to their healthy controls.

Localizing atrophy and related pathology will allow for us to investigate the molecular underpinnings of GM volume loss and potentially lead to the development of better neuroprotective therapies for patients with MS.

The dissertation of Cassandra Meyer is approved.

Arthur Arnold

David Shattuck

Ye Zhang

Rhonda Voskuhl

Allan MacKenzie-Graham, Committee Chair

University of California, Los Angeles

2021

TABLE OF CONTENTS

Abstract of the Dissertation ii

Table of Contents v

List of Figures and Tables viii

Acknowledgements xi

VITA xvi

Chapter 1. Introduction and background 1

1.1 Multiple Sclerosis 2

1.2 Gray matter atrophy in multiple sclerosis 3

1.3 Experimental autoimmune encephalomyelitis 4

1.4 Sex differences in multiple sclerosis 6

1.5 Estriol as a treatment in multiple sclerosis 9

1.6 *In vivo* magnetic resonance imaging in mouse models 10

1.7 Clear Lipid-exchanged Acrylamide-hybridized Rigid Imaging-compatible Tissue hYdrogel (CLARITY) 11

1.8 Overview of experiments 12

1.9 References 13

Chapter 2. *In vivo* magnetic resonance images reveal neuroanatomical sex differences through the application of voxel-based morphometry in C57BL/6 mice 28

2.1 Abstract 29

2.2 Introduction 29

2.3 Methods 32

2.4 Results 36
2.5 Discussion 38
2.6 Conclusion 43
2.7 References 50
Chapter 3. Axonal damage in spinal cord is associated with gray matter atrophy in sensorimotor cortex in experimental autoimmune encephalomyelitis 60
3.1 Abstract 61
3.2 Introduction 61
3.3 Materials and Methods 63
3.4 Results 66
3.5 Discussion 70
3.6 References 80
Chapter 4. Neuroprotective mechanisms underlying mitigation of cerebral cortex atrophy by estriol treatment 84
4.1 Abstract 85
4.2 Introduction 85
4.3 Materials and Methods 87
4.4 Results 89
4.5 Discussion 94
4.6 References 109
Chapter 5. Increased neurodegeneration in male C57BL/6 mice with experimental autoimmune encephalomyelitis 114
5.1 Abstract 115

5.2 Introduction 115
5.3 Materials and Methods 117
5.4 Results 121
5.5 Discussion 124
5.6 References 137
Chapter 6. Conclusions, limitations, and future directions 145

List of Figures and Tables

Chapter 2:

Figure 2-1 Tissue probability maps 44

Figure 2-2 Localized sex differences in gray matter volume. 45

Figure 2-3 Minimum deformation atlas with region delineations.....46

Figure 2-4 Atlas-based morphometry supports VBM results 47

Table 2-1 Regional volumes for male and female C57BL/6 mice 48

Table 2-2 Regional volumes for male and female C57BL/6 mice normalized to male and female mean whole brain volume respectively 48

Table 2-3 Prominent regions displaying sexual dimorphism in this study compared to mouse and human literature.....49

Chapter 3:

Figure 3-1 EAE clinical scores.....73

Figure 3-2 Axonal transection in the spinal cord correlates with GM atrophy in sensorimotor cortex.....74

Table 3-1 Volume comparisons for mice with EAE as compared to normal controls 76

Figure 3-3 Reduced cortical layer V neuronal number in sensorimotor cortex during EAE.....77

Figure 3-4 Demyelination in sensorimotor cortex during EAE 78

Figure 3-5 Activated microglia in sensorimotor cortex during EAE.....79

Chapter 4:

Figure 4-1 Therapeutic estriol treatment reduces EAE scores 97

Figure 4-2 Estriol treatment reduces cortical gray matter atrophy and mitigates underlying neurodegeneration in cerebral cortex during EAE 98

Figure 4-3 Estriol treatment reduces microglial activation and preserves myelin in cerebral cortex during EAE 100

Figure 4-4 Estriol treatment abrogates associations between cortical GM atrophy and underlying neuropathology during EAE 101

Table 4-1 Pearson correlation coefficients and FDR corrected p values for relationships between different pathological measures 102

Figure 4-5 ERβ-ligand treatment is neuroprotective in the cerebral cortex during EAE 104

Figure 4-6 ERβ-ligand treatment promotes remyelination in the cerebral cortex during EAE 105

Figure 4-7 Estriol pre-treatment prevents gray matter atrophy and induces neuroprotection in EAE 107

Chapter 5:

Figure 5-1 EAE scores 130

Figure 5-2 Voxel-based morphometry reveal more gray matter atrophy in males with EAE 131

Figure 5-3 Worse disability correlates with worse gray matter atrophy in somatosensory cortex in males but not females 132

Figure 5-4 Male mice demonstrate worse neurodegeneration during EAE than females 133

Figure 5-5 Male and female mice demonstrate similar inflammation and demyelination in the cerebral cortex during EAE.....135

Figure 5-6 Supporting data.....136

ACKNOWLEDGEMENTS

Firstly, I would like to thank my mentor, Allan Mackenzie-Graham, for providing an environment that allowed me to grow personally and as a scientist. Your passion for mentorship and teaching is apparent and I feel lucky to have had the opportunity to learn under your guidance. I will always cherish your kindness and support in my many and varied endeavors.

The Voskuhl lab has been such an important part of my graduate experience and has provided me with invaluable aid and companionship over the years. Dr. Voskuhl, thank you for graciously offering your time and mentorship which has driven me to develop as a scientist. I have learned so much about scientific thinking and storytelling from you. I greatly value your opinion and am grateful to have learned from you. To Noriko, I have never been more impressed by anyone's work ethic! You work so hard yet still find the time to give your help to others. You have been a voice of kindness and a necessary source of knowledge for me in my studies. I can genuinely say I would not have gotten to where I am today without you. And thank you to the current and past members of the Voskuhl lab (Lisa Golden, Roy Kim, Alessia Tassoni, and Laura Kammel) and Mackenzie-graham Lab (Stephano Lepore, Mandavi Oberoi, Peter Boyle, and Haley Hrncir) for all of your advice and friendship.

The members of my committee have all provided much needed support at various times in my graduate career. Dr. Arnold, your passion for science and commitment to mentorship comes through in all of your interactions with students. I value all that I have learned in your classes and through my meetings with you. Dr. Zhang, I have always felt comfortable going to you for advice. Thank you so much for providing a welcoming environment for me. Dr. Shattuck, thank you so much for being available when both Dr. MacKenzie-Graham and I were unsure how to proceed in our imaging analysis. Your creative and inventive approach toward problem solving is always so inspiring!

I have had the privilege of working with so many hardworking, motivated, and intelligent undergraduate students. Over the course of my graduate career I have worked with 8

undergrads and 1 high school student: Josephine Gao, James Cheng, Mackenzie Thurston, Dayana Lujan, Aitana Padilla-Requerey, Han Ngo, Andrew Smith, Christina Lee, and Quynh-Anh Nguyen. Over the years they have given so much of their time to these projects. I could not have done this work alone and am so grateful for everything they have done. I have enjoyed watching each and every one of them grow and am so proud of all that they have accomplished. Thank you for your hard work and for inspiring me with your curiosity and drive.

I would also like thank the broader neuroscience community at UCLA. Jennifer Lee in particular sets the tone for a positive and supportive community. Thank you for being available and opening your doors when students are struggling and need someone to talk to. You make me proud to be in this department. To my wonderful cohort and friends that I have been lucky to meet at UCLA, you make even the hardest days worth every minute.

I would like to offer my most sincere thanks to my family and friends who have supported me throughout the course of my PhD. My parents, Robert Meyer and Sharon Shofner-Meyer, have believed in me and encouraged me since childhood. During my PhD they have provided a wonderful safety net of love when I felt challenged and were always available to listen to my talks. My grandparents, Dana and Milton Shofner, who give all of their grandchildren the fullest extent of their love and pride, continuously provide my motivation and inspiration for research. My sisters, Rachel Meyer and Rebecca Meyer, thank you for being the best friends I could possibly have asked for and for always lending an ear when I needed to talk.

To my partner and dearest friend, Akshat Arneja. It’s wild to think of all that we’ve been through together! I don’t know what I would have done had you not been on this journey with me. You have always been my biggest cheerleader. Thank you for providing me with the encouragement and reason that I needed when I doubted myself along the way. Thank you for the countless hours that you spent listening to my talks and reading my papers when I needed feedback. You are the reason I am here and the reason I have joy in every day.

Chapter 2 was originally published in *NeuroImage* in December of 2017 with the title "*In vivo* magnetic resonance images reveal neuroanatomical sex differences through the application of voxel-based morphometry in C57BL/6 mice" (Volume 163, pages 197-205). As the primary author, I collected MR images, completed all atlas-based morphometry analyses and wrote the first draft of the manuscript. The second author, Florian Kurth created the tissue probability maps used in this study and performed the voxel-based morphometry. Stefano Lepore and Josephine Gao aided in data collection and image analysis. Hadley Johnsonbaugh and Mandavi Oberoi performed animal husbandry and mouse care. Stephen Sawiak provided input and review of the final manuscript. Allan MacKenzie-Graham was the senior author and project director.

Chapter 3 was originally published in *Multiple Sclerosis Journal* in March of 2019 with the title "Axonal damage in spinal cord is associated with gray matter atrophy in sensorimotor cortex in experimental autoimmune encephalomyelitis" (Volume 26, pages 294-303). I was the primary author of this work and collected most of the data and conducted all major analysis. I also synthesized and interpreted all of the results, constructed all accompanying graphics and tables, and wrote the first draft of the manuscript. Other co-authors who contributed in data collection of MR images and immunohistochemistry, animal husbandry and care, and review of the final manuscript included Josephine Gao, James Cheng, Mandavi Oberoi, Hadley Johnsonbaugh, Stefano Lepore, Florian Kurth, Mackenzie Thurston, Noriko Itoh, and Kevin Patel. Rhonda Voskuhl contributed substantial advice throughout the project and provided input in the final version of the manuscript. Allan Mackenzie-Graham was the senior author and project director.

Chapter 4 has been submitted for publication with the title "Neuroprotective mechanisms underlying mitigation of cerebral cortex atrophy by estriol treatment". I am the primary author on this publication and again performed data collection, conducted all major analyses, interpreted results, and wrote the first draft of the manuscript. As the second author, Aitana Padilla-

Requerey aided in EAE induction, estriol treatment, animal care, tissue processing, immunohistochemistry and data analysis. Vista Farkhondeh performed EAE induction for the ERβ ligation experiments. Noriko Itoh provided substantial advice throughout the project. Yuichiro Itoh created the correlation figure (Figure 4-4). Josephine L. Gao, Katelyn H. Ngo, Quynhanh Nguyen, and Mandavi R. Oberoi all helped with data collection and animal care. Rhonda Voskuhl contributed substantially to the written manuscript and provided input throughout the project. Allan Mackenzie-Graham was the senior author and project director. Chapter 5 is new and unpublished work. I have performed data collection, conducted all major analyses, and interpreted results presented in this dissertation. Andrew Smith and Haley Hrncir aided in research and data collection. Aitana Padilla-Requerey aided in data analysis. Rhonda Voskuhl has provided substantial advice. Allan Mackenzie-Graham is the project director.

I would also like to acknowledge my funding sources which have made this research possible. This work was generously supported by NINDS/NIH R01NS086981 (A.M.G.), NINDS/NIH 1F31NS105387 (C.E.M), the Conrad N. Hilton Foundation 201918394 (R.V. and A.M.G.)), the Tom Sherak MS Hope Foundation (R.V.), the Rhoda Goetz Foundation for MS (R.V.), the Dunk MS Foundation, UCLA Laboratory of Neuroendocrinology NIH training grant 5T32HD007228 (C.E.M), Achievement Rewards for College Students (ARCS) Foundation (C.E.M.), and by the UCLA Brain Research Institute Knaub Fellowship in Multiple Sclerosis Research (C.E.M.). I am grateful for the generous support provided to the labs of R.V. and A.M.G. from the Brain Mapping Medical Research Organization, Brain Mapping Support Foundation, Pierson-Lovelace Foundation, The Ahmanson Foundation, Capital Group Companies Charitable Foundation, William M. and Linda R. Dietel Philanthropic Fund, and Northstar Fund. Research reported in this dissertation was also partially supported by the National Center for Research Resources and by the Office of the Director of the National Institutes of Health under award numbers C06RR012169, C06RR015431, and S10OD011939.

Lastly, and perhaps most importantly, thank you to all of the mice who gave their life for this research. Without them, none of these discoveries would have been possible.

VITA

EDUCATION

2014-present **University of California, Los Angeles, CA**
Ph.D Candidate in Interdepartmental Program for Neuroscience
Current Cumulative GPA 3.784

2010-2014 **University of Minnesota, Twin Cities, Minneapolis, MN**
Bachelor of Science in Neuroscience
Cumulative GPA 3.619

RESEARCH EXPERIENCE

University of California, Los Angeles, CA 2015-present
Laboratory of Dr. Allan MacKenzie-Graham

University of Minnesota, Twin Cities, Minneapolis, MN September 2013- July 2014
Laboratory of Dr. Lorene Lanier, Department of Neuroscience

University of Minnesota—Twin Cities, Minneapolis, MN September 2011-May 2014
Laboratory of Dr. Teresa Nick, Department of Neuroscience

TEACHING GRANTS AND FELLOWSHIPS

2018	UCLA mini-grant for instructional development

RESEARCH GRANTS AND FELLOWSHIPS

2015-2016	Laboratory of Neuroendocrinology UCLA training grant
2016-present	Achievement Rewards for College Scientists (ARCS) Foundation Award
2018	The Brain Research Institute Knaub Graduate Student Fellowship in Multiple Sclerosis Research
2018-2021	Ruth L. Kirschstein National Research Service Award (NRSA) Individual Predoctoral Fellowship (Parent F31) NINDS 1F31NS105387

HONORS AND AWARDS

2016	Second place for data blitz presentation at NSIDP retreat
2016	Brain Research Institute and Semel Institute for Neuroscience & Human Behavior travel award
2016-2017	Graduate Division Award
2017	Second Place for poster presentation at UCLA Neurology Day
2018	Dr. Eva Kavan Prize for Excellence in Neuroscience Research

2020	Americas Committee for Treatment and Research in Multiple Sclerosis (ACTRIMS) educational award for travel
2020	Second place in campus wide UCLA Grad Slam competition

PUBLICATIONS

Research Papers

Meyer CE, Boroda E, Nick TA. Sexually dimorphic perineuronal net expression in the songbird. Basal Ganglia. 2014;3(4):229-37. doi: 10.1016/j.baga.2013.10.002.

Meyer CE, Kurth F, Lepore S, Gao JL, Johnsonbaugh H, Oberoi MR, Sawiak SJ, MacKenzie-Graham A. In vivo magnetic resonance images reveal neuroanatomical sex differences through the application of voxel-based morphometry in C57BL/6 mice. Neuroimage. 2017;163:197-205. Epub 2017/09/20. doi: 10.1016/j.neuroimage.2017.09.027. PubMed PMID: 28923275.

MacKenzie-Graham A, Brook J, Kurth F, Itoh Y, **Meyer C**, Montag MJ, Wang HJ, Elashoff R, Voskuhl RR. Estriol-mediated neuroprotection in multiple sclerosis localized by voxel-based morphometry. Brain and behavior. 2018:e01086. Epub 2018/08/26. doi: 10.1002/brb3.1086. PubMed PMID: 30144306.

Meyer, C.E., Gao, J.L., Cheng, J.Y., Oberoi, M.R., Johnsonbaugh, H., Lepore, S., Kurth, F., Thurston, M.J., Itoh, N., Patel, K.R., Voskuhl, R.R., MacKenzie-Graham, A., 2019. Axonal damage in spinal cord is associated with gray matter atrophy in sensorimotor cortex in experimental autoimmune encephalomyelitis. Mult Scler, 1352458519830614.

Meyer C.E., Padilla-Requery A., Farkondeh V., Itoh N., Itoh Y., Gao J., Ngo H., Nguyen Q., Oberoi M., Voskuhl R., MacKenzie-Graham A. (2020) Neuroprotective mechanisms underlying mitigation of cerebral cortex atrophy by estriol treatment. (*submitted*)

Selected Abstracts

Meyer, C. E., Johnsonbaugh H., Gao J., Oberoi M., Lepore S., Ito N., Voskuhl R., MacKenzie-Graham A. (2016) *Estriol preserves axonal integrity and cortical volume in experimental autoimmune encephalomyelitis.* Society for Neuroscience.

Meyer C. E., Kurth F., Lepore S., Gao J., Johnsonbaugh H., Oberoi M., Sawiak S., MacKenzie-Graham A. (2017*) In vivo magnetic resonance imaging reveals neuroanatomical sex differences through the application of voxel-based morphometry in C57BL/6 mice.* Center for Neurobiology of Stress and Resilience Symposium.

Meyer C. E., Gao J., Cheng J., Oberoi M., Johnsonbaugh H., Lepore S., Kurth F., Thurston M. J., Itoh N., Voskuhl R., MacKenzie-Graham A. (2018) *Axonal damage in spinal cord is associated with gray matter atrophy in sensorimotor cortex in mice with experimental autoimmune encephalomyelitis.* American Society for Neurochemistry.

Meyer C. E., Padilla-Requery A., Tassoni A., Farkhondeh V., Itoh N., Gao J., Ngo H., Oberoi M., Voskuhl R., MacKenzie-Graham A. (2020*) Mechanism of Estriol-Mediated Neuroprotection in Cerebral Cortex During Experimental Autoimmune Encephalomyelitis (EAE).* Americas Committee for Treatment and Research in Multiple Sclerosis

Chapter 1

Introduction and background

1.1 Multiple Sclerosis

Multiple sclerosis (MS) presents a global challenge as the most common neurological disorder affecting young adults as symptoms first manifest between the ages of 20-40 (Browne et al., 2014). In recent years, MS diagnosis has been on the rise, potentially due to environmental factors. It is currently estimated that there are nearly 1 million people in the US living with MS (Wallin et al., 2019). MS is a progressive and often disabling disease of the central nervous system (CNS). It is an immune-mediated disorder where activated T lymphocytes migrate into the central nervous system (CNS) and initiate widespread inflammation, gliosis, demyelination, and neurodegeneration (Dendrou et al., 2015). Though the etiology of the disease is unknown, it is thought that a combination of genetic and environmental factors contribute to disease susceptibility (Winquist et al., 2007). Patients with MS experience a wide variety of symptoms including loss of motor and sensory abilities, vision loss, fatigue and cognitive dysfunction which can dramatically effect quality of life.

Based on the manifestation and progression of symptoms, MS can be classified into three main types. Relapsing-remitting MS (RRMS) is the most common. Approximately 85% of MS patients are initially diagnosed with this type (Fox and Cohen, 2001). RRMS involves periodic relapses, where existing symptoms are exacerbated or new symptoms develop, and remissions, where the patient demonstrates partial recovery. Most patients with RRMS will eventually transition into the Secondary Progressive form of MS (SPMS). This form is characterized by progressively worsening symptoms with no periods of remission. During SPMS, patients are often less responsive to treatment and disability accumulates quickly (Galboiz et al., 2001; Li et al., 2001; Molyneux et al., 2000; Paz Soldán et al., 2015). 10-15% of MS patients present the Primary Progressive form (PPMS), where symptoms worsen from the onset of disease with no initial relapsing-remitting period (Thompson et al., 1997).

MS involves both inflammation and neurodegeneration which are thought to contribute to clinical disability. Neurodegeneration in MS is a complex process that includes dysfunction and

loss of axons, neurons, and synapses. While it is thought that neurodegeneration initially occurs as a response to inflammation and demyelination, the specific mechanisms of neurodegeneration remain unclear. In the early stages of MS, neurodegeneration is often subclinical (Trapp et al., 2016). Later in the course of disease, during SPMS, neurodegeneration becomes more aggressive and irreversible disability accumulates (Confavreux and Vukusic, 2014). There is evidence to suggest that neurodegeneration is not necessarily a direct effect of the immune response (Confavreux and Vukusic, 2006; Trapp and Nave, 2008). This is supported by the observation that treatments that suppress the immune response and reduce relapses do not halt the progression of disability (Coles et al., 1999; Kappos et al., 2006; Molyneux et al., 2000). While immunomodulatory treatments can slow disability accumulation, there is a lack of directly neuroprotective treatments for MS patients. Understanding how and why neurodegeneration occurs in MS can help identify therapeutic targets that can be treated with neuroprotective agents.

1.2 Gray matter atrophy in Multiple Sclerosis

Magnetic resonance imaging (MRI) provides a non-invasive method of evaluating neurodegenerative damage in the CNS of MS patients and a means to investigate the underlying pathology of disability. MRI has been used in the past to identify white matter (WM) lesions, indicating disease burden, and gadolinium-enhancing lesions, indicating active inflammatory lesions, as a method of monitoring disease progression (Kirshner et al., 1985; McFarland et al., 1992; Thompson et al., 1992). While these measures provide valuable information about inflammatory activity, they have been found to be only modest indicators of overall disease disability (Fisher et al., 2008; Fisniku et al., 2008; Fulton et al., 1999; Kappos et al., 1999; Zivadinov and Leist, 2005). Gray matter (GM) atrophy, however, has been shown to be strongly associated with disability (Benedict et al., 2002; Filippi et al., 2013; Jacobsen et al., 2014; Sanfilipo et al., 2005).

GM atrophy is characterized by loss of neurons, axons, glial cells, extracellular matrix, and myelin within the gray matter tissue of the brain (Dutta and Trapp, 2011). Even though it is often subclinical, brain atrophy begins to accumulate even in early years of the disease (Chard et al., 2004; Rudick et al., 1999; Simon et al., 1999) and becomes more aggressive during SPMS (Calabrese et al., 2015; Fisher et al., 2008; Fisniku et al., 2008). GM atrophy has been found to be better than white matter atrophy, white matter lesion load, or gadolinium-enhancing lesions at predicting disability (Barkhof, 2002; Eijlers et al., 2018; Filippi et al., 2013; Fisniku et al., 2008). The rate of GM atrophy that occurs early in disease is highly predictive of future clinical status (Fisher et al., 2002; Summers et al., 2008). Regional GM atrophy, particularly in deep GM structures, is closely tied with enhanced disability status score (EDSS) worsening (Eshaghi et al., 2018b) and cognitive dysfunction (Schoonheim et al., 2012). Our group has shown that localized GM atrophy is associated with clinically eloquent disability. For example, worse performance on the 9-hole peg test, a test that measures arm and hand dexterity, was associated with worse GM atrophy in a region of the brain involved in arm and hand motion (MacKenzie-Graham et al., 2016).

Despite the growing body of literature highlighting the robust ability of GM atrophy to predict disability progression in MS, it is still unclear what pathological measures lead to permanent GM volume loss. Therapies for MS are primarily immunomodulatory and have been shown to have no effect (Eshaghi et al., 2018a) or a only a modest effect on preventing GM atrophy (Cohen et al., 2010; Filippi et al., 2004; Molyneux et al., 2000). Investigating mechanisms of GM atrophy is a critical step in identifying novel therapeutic targets that can be acted upon by neuroprotective agents.

1.3 Experimental autoimmune encephalomyelitis

The most commonly used mouse model of MS, experimental autoimmune encephalomyelitis (EAE) provides a useful method to investigate the mechanisms that underlie GM atrophy and

potentially neuroprotective treatments. Much of the research that has been done investigating treatments for MS have been done using EAE. EAE can be induced through either an active or passive method (Gold et al., 2000). In the passive, adoptive transfer, method the induction phase (activation of T cells) is separate from the effector phase (inflammation and neurodegeneration). Passive induction is done by first injecting a myelin protein (myelin basic protein (MBP), proteolipid protein (PLP), or myelin oligodendrocyte glycoprotein (MOG)) and the immune stimulants, complete Freund's adjuvant (CFA) and tuberculosis bacterium (TB), in one mouse and then harvesting the lymph nodes or spleen from that mouse and transferring activated, myelin specific T-cells into a naïve animal. In the active C57BL/6 model, the model used in the projects with this dissertation, both the induction and effector phase occur in the same mouse. Mice are immunized with a myelin peptide, MOG35-55 , and immune stimulators, CFA and TB. Pertussis toxin is also given to increase the permeability of the blood brain barrier (BBB). The activated T-cells enter the CNS, recruit further immune activity, and lead to demyelination. As in MS, this is followed by neurodegeneration, including synaptic loss, axonal damage, and neuronal death.

The disease course of EAE differs depending that the strain of mouse that is used (Gold et al., 2000). When EAE is induced in the SJL strain, the disease course is relapse-remitting, while induction in C57BL/6 mice initiates a chronic disease course. In both strains, disability is measured as ascending paralysis affecting the tail and hindlimbs. The clinical disability scale used in the projects associated with this dissertation is as follows: 0 – healthy; 1 – tail limpness; 2 – limb weakness; 3 - partial paralysis of at least one limb; 4 – complete paralysis of at least one limb; 5 – moribund (Pettinelli and McFarlin, 1981).

GM atrophy has been described in chronic EAE both *ex vivo* and *in vivo* (MacKenzie-Graham et al., 2012a; MacKenzie-Graham et al., 2006; MacKenzie-Graham et al., 2009; Meyer et al., 2019; Spence et al., 2014). MacKenzie-Graham et al. (2012) found that cortical and cerebellar GM volume progressively decreased over the course of disease and was associated

with neuropathology in EAE. Evaluating mechanisms of GM atrophy in EAE can provide insight into neurodegenerative processes in MS.

1.4 Sex differences in multiple sclerosis

Investigating the sexually dimorphic nature of MS can provide clues about the etiology of the disease as well as identify novel therapeutic targets. It is well established that MS is a sexually dimorphic disease. Women demonstrate increased susceptibility to MS and are 3 times more likely to develop MS than men (Orton et al., 2006; Whitacre et al., 1999). Furthermore, several clinical observations indicate that women tend to display increased inflammatory activity in RRMS compared to males. Examples include a higher relapse rate (Kalincik et al., 2013) and greater number of gadolinium-enhancing lesions (Pozzilli et al., 2003; Tomassini et al., 2005) in females with MS. Evidence suggests that women have a more robust immune response than men, contributing to autoimmune disease susceptibility (Bao et al., 2002; Choudhry et al., 2006; Cruz-Orengo et al., 2014; Klein and Flanagan, 2016; Purtilo and Sullivan, 1979). Indeed, females show increased susceptibility to many autoimmune disorders including systemic lupus erythematosus, Hashimoto's thyroiditis, and rheumatoid arthritis (Gleicher and Barad, 2007). The biological effect of sex can be due to sex hormones, sex chromosomes, or an interaction of the two.

The role of sex hormones and sex chromosomes in autoimmune susceptibility is complex. Genetic factors likely play a key role in the origin of the observed female preponderance in MS as both estrogens and androgens tend to suppress the inflammatory response and ameliorate disease in EAE and MS (Bebo et al., 2001; Bebo et al., 1999; Bove et al., 2014b; Sicotte et al., 2002; Voskuhl, 2011; Voskuhl, 2020). Some have postulated that differences in the expression of genes on the X chromosome may contribute to autoimmune susceptibility (Golden et al., 2019; Selmi et al., 2012). In the four core genotype mouse model, the testis-determining region (Sry) is removed from the Y chromosome and added to an autosome. This allows for both XX

and XY^- gonadal males as well as XX and XY^- gonadal females to be created, therefore decoupling the effect of sex hormones and sex chromosomes (Arnold and Chen, 2009; De Vries et al., 2002). Using the four core genotype model, it was shown that XX mice, regardless of gonadal sex, were more susceptible to EAE and lupus than XY^- mice (Smith-Bouvier et al., 2008). In a recent study, it was found that the X escapee gene, Kdm6a, was expressed at higher levels in XX mice compared to XY^- mice and the deletion of Kdm6a ameliorated EAE (Itoh et al., 2019). Together, these studies and others (Elsheikh et al., 2001; Lu et al., 2007) provide support for the hypothesis that the XX chromosome complement contributes to the female preponderance in autoimmune disorders.

However, when males do develop MS, they tend to demonstrate worse disease progression than females. Despite being less susceptible to disease onset, males are more likely to progress from RRMS to SPMS than females and do so in a shorter time span (Alroughani et al., 2015; Kalincik et al., 2013; Koch et al., 2010; Weinshenker et al., 1996). While there are no sex differences in PPMS progression, males appear to be more prone to PPMS (Golden and Voskuhl, 2017; Kantarci et al., 1998). Males demonstrate more gray matter atrophy than females, particularly in deep GM structures (Antulov et al., 2009; Sanchis-Segura et al., 2016; Schoonheim et al., 2012; Voskuhl et al., 2020). Furthermore, several studies have found that male sex is a strong predictor of more severe disability (Beatty and Aupperle, 2002; Benedict and Zivadinov, 2011; Ribbons et al., 2015; Savettieri et al., 2004; Schoonheim et al., 2012). A study done by Schoonheim et al. (2012) examined cognition in RRMS patients throughout the six years following diagnosis. Although there were no sex differences in disease duration, T1 or T2 lesion volumes, males demonstrated significant cognitive decline in several cognitive domains, while females did not. This was found in conjunction with significantly worse gray matter atrophy in males than in females (Schoonheim et al., 2012). This suggests that more pronounced cognitive disability and gray matter atrophy are visible in males even early in disease. In another study, males were found to perform worse on the 9-hole peg test (a

measure of hand and arm dexterity) than females. There was a direct correlation between worse 9-hole peg test performance and less thalamic volume in males, but not in females (Voskuhl et al., 2020). Together, these studies indicate worse disease progression in males than females.

The faster disease progression in males opposes the increased susceptibility and increased inflammatory activity seen in females. This indicates that males may have an increased neurodegenerative response to inflammation in MS than females. There are several possible explanations for this observation. One possibility is that testosterone exacerbates disease course. This, however, is unlikely as testosterone has been found to be protective in MS and EAE (Bove et al., 2014a; Dalal et al., 1997; Kurth et al., 2014; Ziehn et al., 2012b). Another possibility is that endogenous estrogens are protective against neurodegeneration. There is a large body of evidence indicating that estrogens are neuroprotective (Behl, 2002; Christianson et al., 2015; Garcia-Segura et al., 2001; Suzuki et al., 2006). 54% of postmenopausal women, after an abrupt decrease in circulating estradiol levels, report worsening of MS symptoms, suggesting that endogenous estradiol ameliorates disease. In this same study, 75% of women reported an improvement of symptoms with estradiol treatment (Smith and Studd, 1992). Studies have further shown that exogenous estradiol treatment ameliorates disease, shifts cytokine production, and is neuroprotective in EAE (Bebo et al., 2001; Gold and Voskuhl, 2009; Ito et al., 2001; MacKenzie-Graham et al., 2012b). Lastly, recent evidence suggest a likely role for sex chromosomes in influencing disease progression. A study using bone marrow chimeras and the four core genotype mouse model utilized both XX and XY^- mice with the same gonadal background and the same peripheral immune cells. This ensured that the CNS was either XX or XY^- and that the results were not confounded by either sex hormones or a difference in peripheral immune response. This study eloquently demonstrated that mice with the XY chromosome complement in the CNS have worse disease progression and increased neurodegeneration (Du et al., 2014). It is still unknown whether wild-type males with chronic

EAE experience increased neurodegeneration. It will be important to determine the mechanisms of increased neurodegeneration associated with sex-specific factors in males in order to identify potential neuroprotective treatments in MS.

1.5 Estriol as a treatment in multiple sclerosis

Studies investigating sex-specific factors have identified estriol, an estrogen produced by the placenta during pregnancy, as a promising neuroprotective agent. Pregnant women with MS demonstrate a significant reduction in relapses, particularly during the third trimester when estriol levels are highest (Confavreux et al., 1998). A similar effect was demonstrated using the most commonly used mouse model of MS, experimental autoimmune encephalomyelitis (EAE). Pregnant mice showed disease amelioration and a reduction in relapses (Kim et al., 1999). Furthermore, it was found that exogenous treatment with estriol ameliorated disease and shifted cytokine production in male and female mice with EAE (Kim et al., 1999; Palaszynski et al., 2004). Several clinical trials have demonstrated that therapeutic treatment with estriol also ameliorates disease in female patients with MS (MacKenzie-Graham et al., 2018; Sicotte et al., 2002; Soldan et al., 2003; Voskuhl et al., 2016). In a recent study, MacKenzie-Graham et al. (2018) demonstrated that estriol treatment was associated with protection against GM atrophy which was accompanied with an improvement in cognitive testing. The cellular mechanisms through which estriol is working to reduce atrophy are still unclear. To date, very few studies have characterized the effect of estriol on GM tissue in EAE. One study demonstrated that estriol treatment was neuroprotective by preserving synaptic function in the hippocampus of mice with EAE (Ziehn et al., 2012a), but the specific mechanisms of estriol-mediated neuroprotection in GM tissue remains unknown. Understanding the relationship between GM preservation and associated changes in pathology will aid in the development of better treatment options for patients with MS.

Some treatments, like Natalizumab, do appear to be moderately neuroprotective in MS, but administering the drug is strenuous for patients (Mattioli et al., 2015). Estriol is attractive as a treatment option for patients for several reasons: 1) It is a naturally occurring estrogen that can be administered orally and crosses the blood brain barrier, 2) it is an inexpensive alternative to current treatments, and 3) it is known to bind both to estrogen receptor (ER)α and Erβ, but binds with a higher affinity to ERβ (Kuiper et al., 1997). Estrogens that bind with a higher affinity for ERα have been associated with adverse side effects such as breast and uterine cancer, while estriol is considered safe when administered to humans (Lauritzen, 1987; Takahashi et al., 2000). Investigating neuroprotective mechanisms of estriol is an important step in developing better neuroprotective therapies that are effective, safe, and easily administered.

1.6 *In vivo* magnetic resonance imaging in mouse models

Structural Magnetic resonance imaging (MRI) in mouse models has been extensively used to examine changes in brain volume. However, it is only relatively recently that technology has advanced to allow the benefits of structural *in vivo* imaging to be recognized (Lerch et al., 2012; Mackenzie-Graham, 2012). *In vivo* MRI in mice provides the opportunity to assess atrophy in longitudinal studies of disease. *In vivo* imaging ensures that biologically relevant brain conditions are being captured, such as full ventricles and no distortion of neuroanatomy upon death (MacKenzie-Graham et al., 2012a). Furthermore, evaluating atrophy using similar methods in both EAE and MS provides a direct comparison of outcome measures in patients and mouse models.

Atlas-based morphometry (ABM) is one of the most common and reliable methods of evaluating changes in structure volume in mice (Toga and Mazziotta, 2002). It involves using atlas-based guidelines to delineate structures of interest on MR images and measure volume. It is an invaluable hypothesis-based method to use when the region of interest is known.

ABM is beneficial in that it allows for the quantification of volume change. However, it requires manual delineation making this technique time intensive. Voxel-based morphometry (VBM), on the other hand, can address some of the limitations of ABM. In VBM, volume differences are compared on a voxel-by-voxel basis (Ashburner and Friston, 2000). A voxel, or 3D pixel, represents a small point in an MRI image. While commonly used in humans (MacKenzie-Graham et al., 2018; MacKenzie-Graham et al., 2016; Matías-Guiu et al., 2018; Rothstein, 2020; Singh et al., 2020), VBM has not been used extensively in mice (Cutuli et al., 2016; Hikishima et al., 2017; Sawiak et al., 2009). VBM can provide a powerful method to localize regions of volume difference. However, VBM cannot readily quantify those volume differences, although it can indicate regions demonstrating atrophy between two groups more precisely. Since VBM does not rely on manual delineation, it can be used to analyze volume differences throughout the entire brain, ensuring that results emerge based on biology and not investigator bias. Furthermore, VBM is sensitive to smaller volume differences and changes that are not bounded by discrete anatomical structures than ABM. Identifying regions that are particularly susceptible to atrophy with VBM can indicate regions to examine further using *ex vivo* biological methods.

1.7 Clear Lipid-exchanged Acrylamide-hybridized Rigid Imaging-compatible Tissue hYdrogel (CLARITY)

Clear Lipid-exchanged Acrylamide-hybridized Rigid Imaging-compatible Tissue-hYdrogel (CLARITY) provides a particularly valuable method of investigating *ex vivo* pathology of the brain. CLARITY (Chung et al., 2013; Spence et al., 2014) is a recently developed optical clearing methodology that permits the intact imaging of the entire brain. This approach embeds the brain in a porous matrix that provides structural integrity to proteins, nucleic acids, and small molecules, while leaving lipids unbound. The lipids are then removed, culminating in an optically cleared brain that can be easily visualized and probed using commonly available techniques.

Using CLARITY we can conduct analyses not possible with traditional immunohistochemistry. For example, we can quantify all of the layer V pyramidal neurons in the cerebral cortex and assess damage across the entire length of an axon or dendrite.

1.8 Overview of experiments

There is an ever-growing need to investigate the pathological mechanisms underlying GM atrophy in MS in order to identify potential therapeutic targets that can be acted upon by neuroprotective agents. The overarching goal, with the projects detailed in this dissertation was to utilize MR imaging in mice to evaluate changes in GM volume and then apply the use of CLARITY and immunohistochemistry to identify associated changes in pathology in EAE. In the first chapter, I establish the use of VBM to evaluate sex differences in neuroanatomy in C57BL/6 mice. In the second chapter, I apply the use of VBM to EAE and identify the cerebral cortex as a region of interest that is associated with neuropathology. In the third chapter, I extensively investigate pathology associated with GM atrophy in the cerebral cortex and identify an estriol-mediated pathway of neuroprotection. Lastly, I utilize VBM to identify sex differences in GM atrophy during EAE.

The results in these studies advance upon previous literature by more extensively characterizing GM atrophy in EAE. They further elucidate mechanisms of GM atrophy and neuroprotection that may be used more broadly to understand disease progression and provide neuroprotective therapies for patients with MS.

1.9 References

Alroughani, R.A., Akhtar, S., Ahmed, S.F., Al-Hashel, J.Y., 2015. Clinical predictors of disease progression in multiple sclerosis patients with relapsing onset in a nation-wide cohort. Int J Neurosci 125, 831-837.

Antulov, R., Weinstock-Guttman, B., Cox, J.L., Hussein, S., Durfee, J., Caiola, C., Dwyer, M.G., Bergsland, N., Abdelrahman, N., Stosic, M., Hojnacki, D., Munschauer, F.E., Miletic, D., Zivadinov, R., 2009. Gender-related differences in MS: a study of conventional and nonconventional MRI measures. Mult Scler 15, 345-354.

Arnold, A.P., Chen, X., 2009. What does the "four core genotypes" mouse model tell us about sex differences in the brain and other tissues? Front Neuroendocrinol 30, 1-9.

Ashburner, J., Friston, K.J., 2000. Voxel-based morphometry--the methods. Neuroimage 11, 805-821.

Bao, M., Yang, Y., Jun, H.S., Yoon, J.W., 2002. Molecular mechanisms for gender differences in susceptibility to T cell-mediated autoimmune diabetes in nonobese diabetic mice. J Immunol 168, 5369-5375.

Barkhof, F., 2002. The clinico-radiological paradox in multiple sclerosis revisited. Current opinion in neurology 15.

Beatty, W.W., Aupperle, R.L., 2002. Sex differences in cognitive impairment in multiple sclerosis. Clin Neuropsychol 16, 472-480.

Bebo, B.F., Jr., Fyfe-Johnson, A., Adlard, K., Beam, A.G., Vandenbark, A.A., Offner, H., 2001. Low-dose estrogen therapy ameliorates experimental autoimmune encephalomyelitis in two different inbred mouse strains. Journal of Immunology 166, 2080-2089.

Bebo, B.F., Jr., Schuster, J.C., Vandenbark, A.A., Offner, H., 1999. Androgens alter the cytokine profile and reduce encephalitogenicity of myelin-reactive T cells. J Immunol 162, 35-40.

Behl, C., 2002. Oestrogen as a neuroprotective hormone. Nat Rev Neurosci 3, 433-442.

Benedict, R.H., Bakshi, R., Simon, J.H., Priore, R., Miller, C., Munschauer, F., 2002. Frontal

cortex atrophy predicts cognitive impairment in multiple sclerosis. Journal of Neuropsychiatry and Clinical Neurosciences 14, 44-51.

Benedict, R.H., Zivadinov, R., 2011. Risk factors for and management of cognitive dysfunction in multiple sclerosis. Nat Rev Neurol 7, 332-342.

Bove, R., Musallam, A., Healy, B., Raghavan, K., Glanz, B., Bakshi, R., Weiner, H., De Jager, P., Miller, K., Chitnis, T., 2014a. Low testosterone is associated with disability in men with multiple sclerosis. Mult Scler 20, 1584-1592.

Bove, R., Musallam, A., Healy, B.C., Raghavan, K., Glanz, B.I., Bakshi, R., Weiner, H., De Jager, P.L., Miller, K.K., Chitnis, T., 2014b. Low testosterone is associated with disability in men with multiple sclerosis. Mult Scler 20, 1584-1592.

Browne, P., Chandraratna, D., Angood, C., Tremlett, H., Baker, C., Taylor, B., Thompson, A., 2014. Atlas of Multiple Sclerosis 2013: A growing global problem with widespread inequity. Neurology 83.

Calabrese, M., Reynolds, R., Magliozzi, R., Castellaro, M., Morra, A., Scalfari, A., Farina, G., Romualdi, C., Gajofatto, A., Pitteri, M., Benedetti, M.D., Monaco, S., 2015. Regional Distribution and Evolution of Gray Matter Damage in Different Populations of Multiple Sclerosis Patients. PLoS ONE 10, e0135428.

Chard, D.T., Griffin, C.M., Rashid, W., Davies, G.R., Altmann, D.R., Kapoor, R., Barker, G.J., Thompson, A.J., Miller, D.H., 2004. Progressive grey matter atrophy in clinically early relapsing-remitting multiple sclerosis. Mult Scler 10, 387-391.

Choudhry, M.A., Bland, K.I., Chaudry, I.H., 2006. Gender and susceptibility to sepsis following trauma. Endocr Metab Immune Disord Drug Targets 6, 127-135.

Christianson, M.S., Mensah, V.A., Shen, W., 2015. Multiple sclerosis at menopause: Potential neuroprotective effects of estrogen. Maturitas 80, 133-139.

Chung, K., Wallace, J., Kim, S.Y., Kalyanasundaram, S., Andalman, A.S., Davidson, T.J.,

Mirzabekov, J.J., Zalocusky, K.A., Mattis, J., Denisin, A.K., Pak, S., Bernstein, H., Ramakrishnan, C., Grosenick, L., Gradinaru, V., Deisseroth, K., 2013. Structural and molecular interrogation of intact biological systems. Nature 497, 332-337.

Cohen, J., Barkhof, F., Comi, G., Hartung, H., Khatri, B., Montalban, X., Pelletier, J., Capra, R., Gallo, P., Izquierdo, G., Tiel-Wilck, K., de Vera, A., Jin, J., Stites, T., Wu, S., Aradhye, S., Kappos, L., 2010. Oral fingolimod or intramuscular interferon for relapsing multiple sclerosis. The New England journal of medicine 362.

Coles, A.J., Wing, M.G., Molyneux, P., Paolillo, A., Davie, C.M., Hale, G., Miller, D., Waldmann, H., Compston, A., 1999. Monoclonal antibody treatment exposes three mechanisms underlying the clinical course of multiple sclerosis. Ann Neurol 46, 296-304.

Confavreux, C., Hutchinson, M., Hours, M.M., Cortinovis-Tourniaire, P., Moreau, T., 1998. Rate of pregnancy-related relapse in multiple sclerosis. Pregnancy in Multiple Sclerosis Group [see comments]. New England Journal of Medicine 339, 285-291.

Confavreux, C., Vukusic, S., 2006. Accumulation of irreversible disability in multiple sclerosis: from epidemiology to treatment. Clinical neurology and neurosurgery 108.

Confavreux, C., Vukusic, S., 2014. The clinical course of multiple sclerosis. Handbook of clinical neurology 122.

Cruz-Orengo, L., Daniels, B.P., Dorsey, D., Basak, S.A., Grajales-Reyes, J.G., McCandless, E.E., Piccio, L., Schmidt, R.E., Cross, A.H., Crosby, S.D., Klein, R.S., 2014. Enhanced sphingosine-1-phosphate receptor 2 expression underlies female CNS autoimmunity susceptibility. J Clin Invest 124, 2571-2584.

Cutuli, D., Pagani, M., Caporali, P., Galbusera, A., Laricchiuta, D., Foti, F., Neri, C., Spalletta, G., Caltagirone, C., Petrosini, L., Gozzi, A., 2016. Effects of Omega-3 Fatty Acid Supplementation on Cognitive Functions and Neural Substrates: A Voxel-Based Morphometry Study in Aged Mice. Front Aging Neurosci 8.

Dalal, M., Kim, S., Voskuhl, R.R., 1997. Testosterone therapy ameliorates experimental

autoimmune encephalomyelitis and induces a T helper 2 bias in the autoantigen-specific T lymphocyte response. Journal of Immunology 159, 3-6.

De Vries, G.J., Rissman, E.F., Simerly, R.B., Yang, L.Y., Scordalakes, E.M., Auger, C.J., Swain, A., Lovell-Badge, R., Burgoyne, P.S., Arnold, A.P., 2002. A model system for study of sex chromosome effects on sexually dimorphic neural and behavioral traits. Journal of Neuroscience 22, 9005-9014.

Dendrou, C.A., Fugger, L., Friese, M.A., 2015. Immunopathology of multiple sclerosis. Nat Rev Immunol 15, 545-558.

Du, S., Itoh, N., Askarinam, S., Hill, H., Arnold, A.P., Voskuhl, R.R., 2014. XY sex chromosome complement, compared with XX, in the CNS confers greater neurodegeneration during experimental autoimmune encephalomyelitis. Proceedings of the National Academy of Sciences of the United States of America 111, 2806-2811.

Dutta, R., Trapp, B.D., 2011. Mechanisms of neuronal dysfunction and degeneration in multiple sclerosis. Prog Neurobiol 93, 1-12.

Eijlers, A., van Geest, Q., Dekker, I., Steenwijk, M., Meijer, K., Hulst, H., Barkhof, F., Uitdehaag, B., Schoonheim, M., Geurts, J., 2018. Predicting cognitive decline in multiple sclerosis: a 5-year follow-up study. Brain : a journal of neurology 141.

Elsheikh, M., Wass, J.A., Conway, G.S., 2001. Autoimmune thyroid syndrome in women with Turner's syndrome--the association with karyotype. Clin Endocrinol (Oxf) 55, 223-226.

Eshaghi, A., Marinescu, R., Young, A., Firth, N., Prados, F., Jorge Cardoso, M., Tur, C., De Angelis, F., Cawley, N., Brownlee, W., De Stefano, N., Laura Stromillo, M., Battaglini, M., Ruggieri, S., Gasperini, C., Filippi, M., Rocca, M., Rovira, A., Sastre-Garriga, J., Geurts, J., Vrenken, H., Wottschel, V., Leurs, C., Uitdehaag, B., Pirpamer, L., Enzinger, C., Ourselin, S., Gandini Wheeler-Kingshott, C., Chard, D., Thompson, A., Barkhof, F., Alexander, D., Ciccarelli, O., 2018a. Progression of regional grey matter atrophy in multiple sclerosis. Brain : a journal of neurology 141.

Eshaghi, A., Prados, F., Brownlee, W., Altmann, D., Tur, C., Cardoso, M., De Angelis, F., van de Pavert, S., Cawley, N., De Stefano, N., Stromillo, M., Battaglini, M., Ruggieri, S., Gasperini, C., Filippi, M., Rocca, M., Rovira, A., Sastre-Garriga, J., Vrenken, H., Leurs, C., Killestein, J., Pirpamer, L., Enzinger, C., Ourselin, S., Wheeler-Kingshott, C., Chard, D., Thompson, A., Alexander, D., Barkhof, F., Ciccarelli, O., 2018b. Deep gray matter volume loss drives disability worsening in multiple sclerosis. Annals of neurology 83.

Filippi, M., Preziosa, P., Copetti, M., Riccitelli, G., Horsfield, M.A., Martinelli, V., Comi, G., Rocca, M.A., 2013. Gray matter damage predicts the accumulation of disability 13 years later in MS. Neurology 81, 1759-1767.

Filippi, M., Rovaris, M., Inglese, M., Barkhof, F., De Stefano, N., Smith, S., Comi, G., 2004. Interferon beta-1a for brain tissue loss in patients at presentation with syndromes suggestive of multiple sclerosis: a randomised, double-blind, placebo-controlled trial. Lancet (London, England) 364.

Fisher, E., Lee, J.C., Nakamura, K., Rudick, R.A., 2008. Gray matter atrophy in multiple sclerosis: a longitudinal study. Ann Neurol 64, 255-265.

Fisher, E., Rudick, R.A., Simon, J.H., Cutter, G., Baier, M., Lee, J.C., Miller, D., Weinstock-Guttman, B., Mass, M.K., Dougherty, D.S., Simonian, N.A., 2002. Eight-year follow-up study of brain atrophy in patients with MS. Neurology 59, 1412-1420.

Fisniku, L.K., Chard, D.T., Jackson, J.S., Anderson, V.M., Altmann, D.R., Miszkiel, K.A., Thompson, A.J., Miller, D.H., 2008. Gray matter atrophy is related to long-term disability in multiple sclerosis. Ann Neurol 64, 247-254.

Fox, R.J., Cohen, J.A., 2001. Multiple sclerosis: the importance of early recognition and treatment. Cleve Clin J Med 68, 157-171.

Fulton, J.C., Grossman, R.I., Udupa, J., Mannon, L.J., Grossman, M., Wei, L., Polansky, M., Kolson, D.L., 1999. MR lesion load and cognitive function in patients with relapsing-remitting multiple sclerosis. Ajnr. American Journal of Neuroradiology 20, 1951-1955.

Galboiz, Y., Shapiro, S., Lahat, N., Rawashdeh, H., Miller, A., 2001. Matrix metalloproteinases and their tissue inhibitors as markers of disease subtype and response to interferon-beta therapy in relapsing and secondary-progressive multiple sclerosis patients. Ann Neurol 50, 443-451.

Garcia-Segura, L.M., Azcoitia, I., DonCarlos, L.L., 2001. Neuroprotection by estradiol. Prog Neurobiol 63, 29-60.

Gleicher, N., Barad, D.H., 2007. Gender as risk factor for autoimmune diseases. J Autoimmun 28, 1-6.

Gold, R., Hartung, H.P., Toyka, K.V., 2000. Animal models for autoimmune demyelinating disorders of the nervous system. Mol Med Today 6, 88-91.

Gold, S.M., Voskuhl, R.R., 2009. Estrogen treatment in multiple sclerosis. Journal of the Neurological Sciences 286, 99-103.

Golden, L., Itoh, Y., Itoh, N., Iyengar, S., Coit, P., Salama, Y., Arnold, A., Sawalha, A., Voskuhl, R., 2019. Parent-of-origin differences in DNA methylation of X chromosome genes in T lymphocytes. Proceedings of the National Academy of Sciences of the United States of America 116.

Golden, L.C., Voskuhl, R., 2017. The importance of studying sex differences in disease: The example of multiple sclerosis. Journal of Neuroscience Research 95, 633-643.

Hikishima, K., Komaki, Y., Seki, F., Ohnishi, Y., Okano, H., Okano, H., 2017. In vivo microscopic voxel-based morphometry with a brain template to characterize strain-specific structures in the mouse brain. Scientific reports 7.

Ito, A., Bebo, B.F., Jr., Matejuk, A., Zamora, A., Silverman, M., Fyfe-Johnson, A., Offner, H., 2001. Estrogen treatment down-regulates TNF-alpha production and reduces the severity of experimental autoimmune encephalomyelitis in cytokine knockout mice. J Immunol 167, 542-552.

Itoh, Y., Golden, L., Itoh, N., Matsukawa, M., Ren, E., Tse, V., Arnold, A., Voskuhl, R., 2019.

The X-linked histone demethylase Kdm6a in CD4+ T lymphocytes modulates autoimmunity. The Journal of clinical investigation 129.

Jacobsen, C., Hagemeier, J., Myhr, K.M., Nyland, H., Lode, K., Bergsland, N., Ramasamy, D.P., Dalaker, T.O., Larsen, J.P., Farbu, E., Zivadinov, R., 2014. Brain atrophy and disability progression in multiple sclerosis patients: a 10-year follow-up study. Journal of Neurology, Neurosurgery and Psychiatry 85, 1109-1115.

Kalincik, T., Vivek, V., Jokubaitis, V., Lechner-Scott, J., Trojano, M., Izquierdo, G., Lugaresi, A., Grand'maison, F., Hupperts, R., Oreja-Guevara, C., Bergamaschi, R., Iuliano, G., Alroughani, R., Van Pesch, V., Amato, M.P., Slee, M., Verheul, F., Fernandez-Bolanos, R., Fiol, M., Spitaleri, D.L., Cristiano, E., Gray, O., Cabrera-Gomez, J.A., Shaygannejad, V., Herbert, J., Vucic, S., Needham, M., Petkovska-Boskova, T., Sirbu, C.A., Duquette, P., Girard, M., Grammond, P., Boz, C., Giuliani, G., Rio, M.E., Barnett, M., Flechter, S., Moore, F., Singhal, B., Bacile, E.A., Saladino, M.L., Shaw, C., Skromne, E., Poehlau, D., Vella, N., Spelman, T., Liew, D., Kilpatrick, T.J., Butzkueven, H., 2013. Sex as a determinant of relapse incidence and progressive course of multiple sclerosis. Brain 136, 3609-3617.

Kantarci, O., Siva, A., Eraksoy, M., Karabudak, R., Sutlas, N., Agaoglu, J., Turan, F., Ozmenoglu, M., Togrul, E., Demirkiran, M., 1998. Survival and predictors of disability in Turkish MS patients. Turkish Multiple Sclerosis Study Group (TUMSSG). Neurology 51, 765-772.

Kappos, L., Moeri, D., Radue, E.W., Schoetzau, A., Schweikert, K., Barkhof, F., Miller, D., Guttmann, C.R., Weiner, H.L., Gasperini, C., Filippi, M., 1999. Predictive value of gadolinium-enhanced magnetic resonance imaging for relapse rate and changes in disability or impairment in multiple sclerosis: a meta-analysis. Gadolinium MRI Meta-analysis Group. Lancet 353, 964-969.

Kappos, L., Traboulsee, A., Constantinescu, C., Eralinna, J.P., Forrestal, F., Jongen, P.,

Pollard, J., Sandberg-Wollheim, M., Sindic, C., Stubinski, B., Uitdehaag, B., Li, D., 2006. Long-term subcutaneous interferon beta-1a therapy in patients with relapsing-remitting MS. Neurology 67, 944-953.

Kim, S., Liva, S.M., Dalal, M.A., Verity, M.A., Voskuhl, R.R., 1999. Estriol ameliorates autoimmune demyelinating disease: implications for multiple sclerosis. Neurology 52, 1230-1238.

Kirshner, H.S., Tsai, S.I., Runge, V.M., Price, A.C., 1985. Magnetic resonance imaging and other techniques in the diagnosis of multiple sclerosis. Arch Neurol 42, 859-863.

Klein, S., Flanagan, K., 2016. Sex differences in immune responses. Nature reviews. Immunology 16.

Koch, M., Kingwell, E., Rieckmann, P., Tremlett, H., Neurologists, U.M.C., 2010. The natural history of secondary progressive multiple sclerosis. Journal of Neurology, Neurosurgery and Psychiatry 81, 1039-1043.

Kuiper, G.G., Carlsson, B., Grandien, K., Enmark, E., Haggblad, J., Nilsson, S., Gustafsson, J.A., 1997. Comparison of the ligand binding specificity and transcript tissue distribution of estrogen receptors alpha and beta. Endocrinology 138, 863-870.

Kurth, F., Luders, E., Sicotte, N.L., Gaser, C., Giesser, B.S., Swerdloff, R.S., Montag, M.J., Voskuhl, R.R., Mackenzie-Graham, A., 2014. Neuroprotective effects of testosterone treatment in men with multiple sclerosis. Neuroimage Clin 4, 454-460.

Lauritzen, C., 1987. Results of a 5 years prospective study of estriol succinate treatment in patients with climacteric complaints. Horm Metab Res 19, 579-584.

Lerch, J.P., Gazdzinski, L., Germann, J., Sled, J.G., Henkelman, R.M., Nieman, B.J., 2012. Wanted dead or alive? The tradeoff between in-vivo versus ex-vivo MR brain imaging in the mouse. Frontiers in Neuroinformatics 6.

Li, D.K., Zhao, G.J., Paty, D.W., 2001. Randomized controlled trial of interferon-beta-1a in secondary progressive MS: MRI results. Neurology 56, 1505-1513.

Lu, Q., Wu, A., Tesmer, L., Ray, D., Yousif, N., Richardson, B., 2007. Demethylation of CD40LG on the inactive X in T cells from women with lupus. J Immunol 179, 6352-6358.

Mackenzie-Graham, A., 2012. In vivo vs. ex vivo Magnetic Resonance Imaging In Mice. Front Neuroinform 6, 19.

MacKenzie-Graham, A., Brook, J., Kurth, F., Itoh, Y., Meyer, C., Montag, M.J., Wang, H.J., Elashoff, R., Voskuhl, R.R., 2018. Estriol-mediated neuroprotection in multiple sclerosis localized by voxel-based morphometry. Brain Behav 8, e01086.

MacKenzie-Graham, A., Kurth, F., Itoh, Y., Wang, H.J., Montag, M.J., Elashoff, R., Voskuhl, R.R., 2016. Disability-Specific Atlases of Gray Matter Loss in Relapsing-Remitting Multiple Sclerosis. JAMA Neurology 73, 944-953.

MacKenzie-Graham, A., Rinek, G.A., Avedisian, A., Gold, S.M., Frew, A.J., Aguilar, C., Lin, D.R., Umeda, E., Voskuhl, R.R., Alger, J.R., 2012a. Cortical atrophy in experimental autoimmune encephalomyelitis: in vivo imaging. Neuroimage 60, 95-104.

MacKenzie-Graham, A., Tinsley, M.R., Shah, K.P., Aguilar, C., Strickland, L.V., Boline, J., Martin, M., Morales, L., Shattuck, D.W., Jacobs, R.E., Voskuhl, R.R., Toga, A.W., 2006. Cerebellar cortical atrophy in experimental autoimmune encephalomyelitis. Neuroimage 32, 1016-1023.

MacKenzie-Graham, A., Tiwari-Woodruff, S.K., Sharma, G., Aguilar, C., Vo, K.T., Strickland, L.V., Morales, L., Fubara, B., Martin, M., Jacobs, R.E., Johnson, G.A., Toga, A.W., Voskuhl, R.R., 2009. Purkinje cell loss in experimental autoimmune encephalomyelitis. Neuroimage 48, 637-651.

MacKenzie-Graham, A.J., Rinek, G.A., Avedisian, A., Morales, L.B., Umeda, E., Boulat, B., Jacobs, R.E., Toga, A.W., Voskuhl, R.R., 2012b. Estrogen treatment prevents gray matter atrophy in experimental autoimmune encephalomyelitis. Journal of Neuroscience Research 90, 1310-1323.

Matías-Guiu, J., Cortés-Martínez, A., Montero, P., Pytel, V., Moreno-Ramos, T., Jorquera, M.,

Yus, M., Arrazola, J., Matías-Guiu, J., 2018. Identification of Cortical and Subcortical Correlates of Cognitive Performance in Multiple Sclerosis Using Voxel-Based Morphometry. Frontiers in neurology 9.

Mattioli, F., Stampatori, C., Bellomi, F., Scarpazza, C., Capra, R., 2015. Natalizumab Significantly Improves Cognitive Impairment over Three Years in MS: Pattern of Disability Progression and Preliminary MRI Findings. PLoS ONE 10, e0131803.

McFarland, H.F., Frank, J.A., Albert, P.S., Smith, M.E., Martin, R., Harris, J.O., Patronas, N., Maloni, H., McFarlin, D.E., 1992. Using gadolinium-enhanced magnetic resonance imaging lesions to monitor disease activity in multiple sclerosis. Ann Neurol 32, 758-766.

Meyer, C.E., Gao, J.L., Cheng, J.Y., Oberoi, M.R., Johnsonbaugh, H., Lepore, S., Kurth, F., Thurston, M.J., Itoh, N., Patel, K.R., Voskuhl, R.R., MacKenzie-Graham, A., 2019. Axonal damage in spinal cord is associated with gray matter atrophy in sensorimotor cortex in experimental autoimmune encephalomyelitis. Mult Scler, 1352458519830614.

Molyneux, P.D., Kappos, L., Polman, C., Pozzilli, C., Barkhof, F., Filippi, M., Yousry, T., Hahn, D., Wagner, K., Ghazi, M., Beckmann, K., Dahlke, F., Losseff, N., Barker, G.J., Thompson, A.J., Miller, D.H., 2000. The effect of interferon beta-1b treatment on MRI measures of cerebral atrophy in secondary progressive multiple sclerosis [In Process Citation]. Brain, 2256-2263.

Orton, S.M., Herrera, B.M., Yee, I.M., Valdar, W., Ramagopalan, S.V., Sadovnick, A.D., Ebers, G.C., Canadian Collaborative Study, G., 2006. Sex ratio of multiple sclerosis in Canada: a longitudinal study. Lancet Neurol 5, 932-936.

Palaszynski, K.M., Liu, H., Loo, K.K., Voskuhl, R.R., 2004. Estriol treatment ameliorates disease in males with experimental autoimmune encephalomyelitis: implications for multiple sclerosis. J Neuroimmunol 149, 84-89.

Paz Soldán, M.M., Novotna, M., Abou Zeid, N., Kale, N., Tutuncu, M., Crusan, D.J., Atkinson,

E.J., Siva, A., Keegan, B.M., Pirko, I., Pittock, S.J., Lucchinetti, C.F., Weinshenker, B.G., Rodriguez, M., Kantarci, O.H., 2015. Relapses and disability accumulation in progressive multiple sclerosis. Neurology, pp. 81-88.

Pettinelli, C.B., McFarlin, D.E., 1981. Adoptive transfer of experimental allergic encephalomyelitis in SJL/J mice after in vitro activation of lymph node cells by myelin basic protein: requirement for Lyt 1+ 2- T lymphocytes. J Immunol 127, 1420-1423.

Pozzilli, C., Tomassini, V., Marinelli, F., Paolillo, A., Gasperini, C., Bastianello, S., 2003. 'Gender gap' in multiple sclerosis: magnetic resonance imaging evidence. Eur J Neurol 10, 95-97.

Purtilo, D.T., Sullivan, J.L., 1979. Immunological bases for superior survival of females. Am J Dis Child 133, 1251-1253.

Ribbons, K., McElduff, P., Boz, C., Trojano, M., Izquierdo, G., Duquette, P., Girard, M., Grand'Maison, F., Hupperts, R., Grammond, P., Oreja-Guevara, C., Petersen, T., Bergamaschi, R., Giuliani, G., Barnett, M., van Pesch, V., Amato, M., Iuliano, G., Fiol, M., Slee, M., Verheul, F., Cristiano, E., Fernandez-Bolanos, R., Saladino, M., Rio, M., Cabrera-Gomez, J., Butzkueven, H., van Munster, E., Den Braber-Moerland, L., La Spitaleri, D., Lugaresi, A., Shaygannejad, V., Gray, O., Deri, N., Alroughani, R., Lechner-Scott, J., 2015. Male Sex Is Independently Associated with Faster Disability Accumulation in Relapse-Onset MS but Not in Primary Progressive MS. PLoS ONE 10.

Rothstein, T., 2020. Gray Matter Matters: A Longitudinal Magnetic Resonance Voxel-Based Morphometry Study of Primary Progressive Multiple Sclerosis. Frontiers in neurology 11.

Rudick, R.A., Fisher, E., Lee, J.C., Simon, J., Jacobs, L., 1999. Use of the brain parenchymal fraction to measure whole brain atrophy in relapsing-remitting MS. Multiple Sclerosis Collaborative Research Group. Neurology 53, 1698-1704.

Sanchis-Segura, C., Cruz-Gomez, A.J., Belenguer, A., Fittipaldi Marquez, M.S., Avila, C., Forn,

C., 2016. Increased regional gray matter atrophy and enhanced functional connectivity in male multiple sclerosis patients. Neuroscience Letters 630, 154-157.

Sanfilipo, M.P., Benedict, R.H., Sharma, J., Weinstock-Guttman, B., Bakshi, R., 2005. The relationship between whole brain volume and disability in multiple sclerosis: a comparison of normalized gray vs. white matter with misclassification correction. Neuroimage 26, 1068-1077.

Savettieri, G., Messina, D., Andreoli, V., Bonavita, S., Caltagirone, C., Cittadella, R., Farina, D., Fazio, M.C., Girlanda, P., Le Pira, F., Liguori, M., Lugaresi, A., Nocentini, U., Reggio, A., Salemi, G., Tedeschi, G., Trojano, M., Valentino, P., Quattrone, A., 2004. Gender-related effect of clinical and genetic variables on the cognitive impairment in multiple sclerosis. J Neurol 251, 1208-1214.

Sawiak, S.J., Wood, N.I., Williams, G.B., Morton, A.J., Carpenter, T.A., 2009. Voxel-based morphometry in the R6/2 transgenic mouse reveals differences between genotypes not seen with manual 2D morphometry. Neurobiol Dis 33, 20-27.

Schoonheim, M.M., Popescu, V., Rueda Lopes, F.C., Wiebenga, O.T., Vrenken, H., Douw, L., Polman, C.H., Geurts, J.J., Barkhof, F., 2012. Subcortical atrophy and cognition: sex effects in multiple sclerosis. Neurology 79, 1754-1761.

Selmi, C., Brunetta, E., Raimondo, M.G., Meroni, P.L., 2012. The X chromosome and the sex ratio of autoimmunity. Autoimmun Rev 11, A531-537.

Sicotte, N.L., Liva, S.M., Klutch, R., Pfeiffer, P., Bouvier, S., Odesa, S., Wu, T.C., Voskuhl, R.R., 2002. Treatment of multiple sclerosis with the pregnancy hormone estriol. Ann Neurol 52, 421-428.

Simon, J.H., Jacobs, L.D., Campion, M.K., Rudick, R.A., Cookfair, D.L., Herndon, R.M., Richert, J.R., Salazar, A.M., Fischer, J.S., Goodkin, D.E., Simonian, N., Lajaunie, M., Miller, D.E., Wende, K., Martens-Davidson, A., Kinkel, R.P., Munschauer, F.E., 3rd, Brownscheidle,

C.M., 1999. A longitudinal study of brain atrophy in relapsing multiple sclerosis. The Multiple Sclerosis Collaborative Research Group (MSCRG). Neurology 53, 139-148.

Singh, S., Tench, C., Tanasescu, R., Constantinescu, C., 2020. Localised Grey Matter Atrophy in Multiple Sclerosis and Clinically Isolated Syndrome-A Coordinate-Based Meta-Analysis, Meta-Analysis of Networks, and Meta-Regression of Voxel-Based Morphometry Studies. Brain sciences 10.

Smith, R., Studd, J.W., 1992. A pilot study of the effect upon multiple sclerosis of the menopause, hormone replacement therapy and the menstrual cycle. J R Soc Med 85, 612-613.

Smith-Bouvier, D.L., Divekar, A.A., Sasidhar, M., Du, S., Tiwari-Woodruff, S.K., King, J.K., Arnold, A.P., Singh, R.R., Voskuhl, R.R., 2008. A role for sex chromosome complement in the female bias in autoimmune disease. J Exp Med 205, 1099-1108.

Soldan, S.S., Alvarez Retuerto, A.I., Sicotte, N.L., Voskuhl, R.R., 2003. Immune modulation in multiple sclerosis patients treated with the pregnancy hormone estriol. J Immunol 171, 6267-6274.

Spence, R.D., Kurth, F., Itoh, N., Mongerson, C.R., Wailes, S.H., Peng, M.S., MacKenzie-Graham, A.J., 2014. Bringing CLARITY to gray matter atrophy. Neuroimage 101, 625-632.

Summers, M., Fisniku, L., Anderson, V., Miller, D., Cipolotti, L., Ron, M., 2008. Cognitive impairment in relapsing-remitting multiple sclerosis can be predicted by imaging performed several years earlier. Multiple sclerosis 14, 197-204.

Suzuki, S., Brown, C.M., Wise, P.M., 2006. Mechanisms of neuroprotection by estrogen. Endocrine 29, 209-215.

Takahashi, K., Manabe, A., Okada, M., Kurioka, H., Kanasaki, H., Miyazaki, K., 2000. Efficacy and safety of oral estriol for managing postmenopausal symptoms. Maturitas 34, 169-177.

Thompson, A.J., Miller, D., Youl, B., MacManus, D., Moore, S., Kingsley, D., Kendall, B., Feinstein, A., McDonald, W.I., 1992. Serial gadolinium-enhanced MRI in relapsing/remitting multiple sclerosis of varying disease duration. Neurology 42, 60-63.

Thompson, A.J., Polman, C.H., Miller, D.H., McDonald, W.I., Brochet, B., Filippi, M.M.X., De Sa, J., 1997. Primary progressive multiple sclerosis. Brain 120 (Pt 6), 1085-1096.

Toga, A., Mazziotta, J., 2002. Brain Mapping: The Methods - 2nd Edition. Academic Press.

Tomassini, V., Onesti, E., Mainero, C., Giugni, E., Paolillo, A., Salvetti, M., Nicoletti, F., Pozzilli, C., 2005. Sex hormones modulate brain damage in multiple sclerosis: MRI evidence. Journal of Neurology, Neurosurgery and Psychiatry 76, 272-275.

Trapp, B.D., Nave, K.A., 2008. Multiple sclerosis: an immune or neurodegenerative disorder? Annu Rev Neurosci 31, 247-269.

Trapp, B.D., Ransohoff, R.M., Fisher, E., Rudick, R.A., 2016. Neurodegeneration in Multiple Sclerosis: Relationship to Neurological Disability:. http://dx.doi.org/10.1177/107385849900500107.

Voskuhl, R., 2011. Sex differences in autoimmune diseases. Biol Sex Differ 2, 1.

Voskuhl, R., 2020. The effect of sex on multiple sclerosis risk and disease progression. Multiple sclerosis (Houndmills, Basingstoke, England) 26.

Voskuhl, R., Patel, K., Paul, F., Gold, S., Scheel, M., Kuchling, J., Cooper, G., Asseyer, S., Chien, C., Brandt, A., Meyer, C., MacKenzie-Graham, A., 2020. Sex differences in brain atrophy in multiple sclerosis. Biology of sex differences 11.

Voskuhl, R.R., Wang, H., Wu, T.C., Sicotte, N.L., Nakamura, K., Kurth, F., Itoh, N., Bardens, J., Bernard, J.T., Corboy, J.R., Cross, A.H., Dhib-Jalbut, S., Ford, C.C., Frohman, E.M., Giesser, B., Jacobs, D., Kasper, L.H., Lynch, S., Parry, G., Racke, M.K., Reder, A.T., Rose, J., Wingerchuk, D.M., MacKenzie-Graham, A.J., Arnold, D.L., Tseng, C.H., Elashoff, R., 2016. Estriol combined with glatiramer acetate for women with relapsing-

remitting multiple sclerosis: a randomised, placebo-controlled, phase 2 trial. Lancet Neurol 15, 35-46.

Wallin, M., Culpepper, W., Campbell, J., Nelson, L., Langer-Gould, A., Marrie, R., Cutter, G., Kaye, W., Wagner, L., Tremlett, H., Buka, S., Dilokthornsakul, P., Topol, B., Chen, L., LaRocca, N., 2019. The prevalence of MS in the United States: A population-based estimate using health claims data. Neurology 92.

Weinshenker, B.G., Issa, M., Baskerville, J., 1996. Long-term and short-term outcome of multiple sclerosis: a 3-year follow-up study. Arch Neurol 53, 353-358.

Whitacre, C.C., Reingold, S.C., O'Looney, P.A., 1999. A gender gap in autoimmunity. Science 283, 1277-1278.

Winquist, R.J., Kwong, A., Ramachandran, R., Jain, J., 2007. The complex etiology of multiple sclerosis. Biochem Pharmacol 74, 1321-1329.

Ziehn, M.O., Avedisian, A.A., Dervin, S.M., O'Dell, T.J., Voskuhl, R.R., 2012a. Estriol preserves synaptic transmission in the hippocampus during autoimmune demyelinating disease. Lab Invest 92, 1234-1245.

Ziehn, M.O., Avedisian, A.A., Dervin, S.M., Umeda, E.A., O'Dell, T.J., Voskuhl, R.R., 2012b. Therapeutic testosterone administration preserves excitatory synaptic transmission in the hippocampus during autoimmune demyelinating disease. Journal of Neuroscience 32, 12312-12324.

Zivadinov, R., Leist, T.P., 2005. Clinical-magnetic resonance imaging correlations in multiple sclerosis. J Neuroimaging 15, 10s-21s.

Chapter 2

In vivo magnetic resonance images reveal neuroanatomical sex differences through the application of voxel-based morphometry in C57BL/6 mice

1.1 Abstract

Behaviorally relevant sex differences are often associated with structural differences in the brain and many diseases are sexually dimorphic in prevalence and progression. Characterizing sex differences is imperative to gaining a complete understanding of behavior and disease which will, in turn, allow for a balanced approach to scientific research and the development of therapies. In this study, we generated novel tissue probability maps (TPMs) based on 30 male and 30 female *in vivo* C57BL/6 mouse brain magnetic resonance images and used voxel-based morphometry (VBM) to analyze sex differences. Females displayed larger anterior hippocampus, basolateral amygdala, and lateral cerebellar cortex volumes, while males exhibited larger cerebral cortex, medial amygdala, and medial cerebellar cortex volumes. Atlas-based morphometry (ABM) revealed a statistically significant sex difference in cortical volume and no difference in whole cerebellar volume. This validated our VBM findings that showed a larger cerebral cortex in male mice and a pattern of dimorphism in the cerebellum where the lateral portion was larger in females and the medial portion was larger in males. These results are consonant with previous *ex vivo* studies examining sex differences, but also suggest further regions of interest.

1.2 Introduction

The difference in brain size is one of the oldest and best known sexual dimorphisms in neuroscience. In fact, studies have demonstrated that sex differences exist in the central nervous system (CNS) at virtually every level of anatomical detail (Arnold, 2004) and it has become increasingly evident that considering sex differences is vital to understanding the brain (Beery and Zucker, 2011; Clayton and Collins, 2014; McCarthy and Arnold, 2011). Historically, in biological research, sex differences were deemed insignificant and experiments performed in only one sex. This frequently led to an overemphasis of results in one sex while neglecting

possible differences that could illuminate our understanding of biological processes. Current research suggests that sex differences are substantial and may bias conclusions if both sexes are not represented (Arnold, 2010).

Neuroimaging studies in humans have shown sex differences in whole brain (Blatter et al., 1995; Luders and Toga, 2010) as well as numerous neuroanatomical structures including the cerebral cortex (Schlaepfer et al., 1995), amygdala (Goldstein et al., 2001), and hypothalamus (Swaab et al., 1985). Gray and white matter volumes were reported as larger in males (Blatter et al., 1995; Luders et al., 2002), but when gray matter was computed as a percentage of total brain volume, females showed a larger gray matter ratio (Gur et al., 1999). These studies demonstrate that sexual dimorphism in the brain extends beyond anatomical structures that are involved in reproductive behavior, in fact occurring throughout the brain (Luders et al., 2004).

Clinically significant sexual dimorphisms in brain function are also well documented (Cahill, 2006). They are found in learning and memory (Andreano and Cahill, 2009), nociception (Berkley, 1997), and analgesia (Gioiosa et al., 2008) to name a few. In cognition, males have been shown to have an advantage in some spatial measures (Lejbak et al., 2011; Voyer et al., 1995) and females to have an advantage in some verbal (Norman et al., 2000; Weiss et al., 2006) and object-location memory measures (Tottenham et al., 2003; Voyer et al., 2007). This cognitive sexual dimorphism raises the possibility that these effects may be connected to structural brain differences between the sexes.

Interest in examining neuroanatomical sex differences has been stimulated by the recognition of widespread sexual dimorphism in disease (Beery and Zucker, 2011). For instance, males show much higher incidence of schizophrenia and developmental disorders (Fombonne, 2005; Gonthier and Lyon, 2004). Females, however, are more susceptible to neurodegenerative disorders and mood disorders (Barnes et al., 2005; Hebert et al., 2013; Piccinelli and Wilkinson, 2000; Zhao et al., 2016). Even when no preponderance is observed, disease progression or response to treatment may vary (Arnold, 2010). Sex differences have

been shown in the incidence and course of numerous neurological disorders such as multiple sclerosis (Whitacre et al., 1999), Parkinson's disease (Shulman and Bhat, 2006), and Alzheimer's disease (Webber et al., 2005). The incidence and progression of some psychiatric disorders have also been shown to exhibit sex differences. For example, males suffer from schizophrenia more than 2.5 times more often than females. Males also experience an earlier onset of schizophrenia and exhibit more structural brain abnormalities than females. Relapses are more severe and their response to neuroleptic medication is less favorable (Castle and Murray, 1991).

The underlying mechanisms of sex differences in brain structure are not entirely clear. The organizational-activational hypothesis emphasizes the importance of sex hormones and the timing of their activity in brain architecture (Arnold, 2009b; Morris et al., 2004; Phoenix et al., 1959). Recently, more emphasis has been placed on factors outside of gonadal hormones in the formation of neural sex (Arnold, 2009a). For example, sex chromosomes, epigenetics, and environmental factors have all been shown to produce sex differences in the brain (McCarthy and Arnold, 2011; Raznahan et al., 2013). Striving to uncover the basis of neural sex differences will lead to an improved understanding of sexually dimorphic behavior and disease.

Clearly, there are many elements contributing to differences in neural anatomy. In fact, numerous conflicting results exist in human studies describing opposing effects (Ruigrok et al., 2014). For this reason, mice are excellent models for identifying sex differences (Arnold, 2009a; Kovacevic et al., 2005). And although sex differences in mice may not be a perfect proxy for sex differences in humans, mouse models may yield some insight into sex differences without the multiple confounds found in human studies. For example, males and females of the same mouse strain have the same genetic makeup and are housed in similar environments, and controlling for as many variables as possible may allow observed differences in male and female brain structure to be attributed strictly to sex. However, only a few prior studies have provided a thorough analysis of neural sex differences in mice (Corre et al., 2014; Raznahan et

al., 2013; Spring et al., 2007). These watershed studies provide invaluable information about sexual dimorphism in the brain, but it is also important to validate and expand this work with carefully-controlled, well-powered studies with meaningful differences in image acquisition and analysis.

Voxel-based morphometry (VBM) is a well-established and well-validated image analysis technique (Ashburner and Friston, 2000, 2005; Good et al., 2001; Luders et al., 2009). It can provide an unbiased and comprehensive assessment of anatomical differences throughout the brain. As such, sexual dimorphism of structures that would not have been expected can be identified. If sex differences across the brain are not homogenous, then regional measures, like VBM, may detect greater local change than measures averaged across the whole brain and thus provide more sensitive indices of change. VBM has been used extensively in humans and is now being used to evaluate gray matter changes in the mouse brain (Keifer et al., 2015; Sasaki et al., 2015; Sawiak et al., 2009, 2013).

In this project, we examined differences in the neural anatomy of 30 female and 30 male C57BL/6 mice. Voxel-based morphometry was used to identify regions where gray matter volume differed significantly. For our analysis, we generated new *in vivo* C57BL/6 tissue probability maps (TPMs) that improved image registration and segmentation in this mouse strain. Our analysis allowed us to identify regions that are sexually dimorphic and can be used to inform further investigation of sex differences in the living brain.

1.3 Methods

Animals and Study Design

60 C57BL/6J mice ranging from 8-12 weeks old (30 male / 30 female) bred (3 generations or less) at UCLA from stock purchased from the Jackson Laboratories (Bar Harbor ME) were analyzed using voxel-based morphometry (VBM). Animals were maintained in a 12 h dark/light cycle with access to food and water *ad libidum*. All procedures were performed in accordance to

the guidelines of the National Institutes of Health and the Chancellor's Animal Research Committee of the University of California, Los Angeles Office for the Protection of Research Subjects.

Image Acquisition

All animals were scanned *in vivo* at the Ahmanson-Lovelace Brain Mapping Center at UCLA on a 7T Bruker imaging spectrometer with a micro-imaging gradient insert with a maximum gradient strength of 100 G/cm (Bruker Instruments, Billerica, MA). An actively decoupled quadrature surface coil array was used for signal reception and a 72-mm birdcage coil was used for transmission. For image acquisition, mice were anesthetized with isoflurane and their heads secured with bite and ear bars. Respiration rate was monitored and the mice were maintained at 37° C using a circulating water pump. Each animal was scanned using a rapid-acquisition with relaxation enhancement (RARE) sequence with the following parameters: TR/TE_{eff} 3500/32 ms, ETL 16, matrix: 256 x 192 x 100, voxel dimensions: 100 x 100 x 100 μm^3. Total imaging time was 93 minutes. Images were acquired and reconstructed using ParaVision 5.1 software.

Creating C57BL/6 in vivo tissue probability maps

Magnetic resonance images were processed using statistical parametric mapping 8 (SPM8, http://www.fil.ion.ucl.ac.uk/spm) and the SPMMouse toolbox (Sawiak et al., 2009, 2013) within MATLAB 2013a (Mathworks, Natick, MA). The standard preprocessing steps for VBM were carefully adapted as described below to accommodate the analysis of the C57BL/6 mouse brain images acquired *in vivo*.

The *in vivo* tissue probability maps provided with SPMMouse were created from R6/2 mice (Sawiak et al., 2009, 2013), therefore some spatial mismatch between these prior TPMs and the brains of the C57BL/6 mice used in the current study is to be expected. Thus, to avoid potential bias from systematic differences between the different mouse strains, customized TPMs were

created for the current sample as described previously in humans (Kurth et al., 2015; Luders et al., 2004). For this, the acquired images were skull-stripped using hand-drawn masks by one rater (CEM), bias corrected, and spatially transformed into the same space as the R6/2 TPMs provided with SPMMouse by applying affine transformations using SPM routines. All images were subsequently resliced to match the R6/2 TPMs with respect to orientation and resolution. As this new "native" space is consistent with the reference space, new TPMs can directly be obtained using these resliced images (Kurth et al., 2015; Luders et al., 2004). More specifically, the registered and resliced images were segmented using SPMMouse to obtain gray matter (GM), white matter (WM), and cerebrospinal fluid (CSF) segments without any linear or non-linear deformations that would encode the shape of the tissue probability maps provided with SPMMouse. Subsequently, these tissue segments were averaged over all 60 animals and smoothed with a Gaussian Kernel of 200 μm full-width-half-maximum (FWHM). This resulted in a new sample-derived set of TPMs. However, seeing that the first segmentation step was performed using the TPMs provided with SPMMouse that were obtained from a different strain, we repeated the process once more with the newly created TPMs. That is, the new TPMs were used in a second iteration to align the skull-stripped and bias-corrected images to the reference space and tissue segment these images into GM, WM, and CSF. Once more, these resulting segments were averaged and smoothed with a Gaussian Kernel of 200 μm FWHM to generate the final set of TPMs for *in vivo* image analysis of C57BL/6 mice (Fig. 2-1). We named the space defined by these TPMs "Mortimer Space" and they are available for download at http://www.bmap.ucla.edu/portfolio/atlases/MSA.

Voxel-based Morphometry

The magnetic resonance images of all 60 mice were manually registered to the newly created TPMs using 6 parameter linear transformations. The images were bias corrected and tissue segmented into GM, WM, and CSF using the unified segmentation algorithm (Ashburner

and Friston, 2005) with the newly created TPMs. The resulting tissue segments were used to create a DARTEL template (Ashburner, 2007) and the individual GM segments were warped to this template and modulated. The size of an optimal smoothing kernel should be on the order of the signal expected (Siegmund and Worsley, 1995) and isotropic smoothing kernels between 5-10 times voxel size are common in the literature (Lerch et al., 2011; Sawiak et al., 2013). We selected a value 6-times our voxel size, or a 600 μm FWHM Gaussian kernel to smooth the normalized and modulated GM segments. The resulting smoothed images constituted the input for the statistical analysis. In addition, bias-corrected images were skull-stripped, warped to the DARTEL template, and averaged to create a mean template for visualization, which we named the Mortimer Space Atlas (MSA). The Mortimer Space Atlas is available for download at http://www.bmap.ucla.edu/portfolio/atlases/MSA.

Atlas-based Morphometry

A minimum deformation atlas (MDA) was created with the magnetic resonance images from all subjects (30 males and 30 females) used in this study as described (MacKenzie-Graham et al., 2009). The cortex and cerebellum were manually labelled on the MDA using BrainSuite 16a (Shattuck and Leahy, 2002) (http://brainsuite.org/) as described (MacKenzie-Graham et al., 2012). Briefly, our cerebral cortex label was bounded ventrally by the plane inferior to the most anterior point of the corpus callosum at midline. Anterior and posterior boundaries were drawn in the plane before the corpus callosum was no longer continuous across the midline. These boundaries were selected to rely on unambiguous landmarks ensuring that no regions outside of the cerebral cortex were included in our delineations. Cerebellar labels were drawn to include the entirety of the cerebellum, bounded by the inferior colliculus and the vestibular nuclei. The anterior hippocampus label was bounded dorsally by the corpus callosum and ventrally by the most dorsal horizontal section where the anterior commissure was visible. The posterior boundary was the plane where the corpus callosum was no longer continuous across the

midline. The posterior hippocampus label was bound anteriorly by the anterior hippocampus label and extended posteriorly until the semicircular canals were visible. It was bound dorsally by the corpus callosum and extended to the most ventral portion of the hippocampus. These labels were then warped out to the individual images and manually corrected by a blinded operator to correct for discrepancies in the automated registration. BrainSuite was used to calculate the corresponding volumes.

Statistical Analyses

Sex differences in local GM volume were examined with a general linear model in which the smoothed, normalized GM segments constituted the dependent variable and sex the independent variable. In addition, whole brain volume was included as covariate to account for the variance associated with brain size and to prevent potential effects due to differences in brain size. Within this model significant differences in local GM volume between males and females were determined via student's t-tests. All findings were corrected for multiple comparisons by controlling the false discovery rate (Hochberg and Benjamini, 1990) and significance maps with a threshold at $q \leq 0.05$. Surviving clusters were then overlaid onto the mean template for anatomic localization and visualization.

Whole brain (BR), GM, WM, CSF, and atlas-based morphometry (ABM) data were analyzed in R (https://www.r-project.org/). Volumes were compared with a student's t-test (two-tailed) and reported without multiple comparison corrections. 95% confidence intervals were found by resampling (10,000 bootstraps).

1.4 Results

Analysis of BR, and normalized and modulated GM, WM, and CSF produced by SPMMouse indicated that males had more gray matter and CSF than females (Table 2-1). However, females demonstrated larger WM volume. Interestingly, although it did not reach statistical significance, males exhibited a statistical trend towards larger whole brain volumes (Fig. 2-4A). When normalizing for whole brain volume, their comparisons remained statistically significant (Table 2-2).

Voxel-based morphometry revealed multiple regions of sexually dimorphic gray matter volume throughout the brain (Fig. 2-2). Several prominent regions were significantly larger in females including the anterior hippocampus, basolateral amygdala, and a dorsal region of the caudoputamen. Females also exhibited larger anatomy in the periaqueductal grey, as well as the paraflocculus and paramedian lobule in the cerebellar cortex.

Males displayed larger cortical volume, as well as in the bed nucleus of the stria terminalis, posterior hypothalamus, inferior colliculus, inferior portion of caudoputamen, and medial amygdala. Several clusters denoting more GM in males also emerged in the thalamus and medial regions of the cerebellar cortex. Nearly all significant differences were bilateral, indicating left-right symmetry in the organization of sexually dimorphic neural anatomy.

Delineations of cerebral cortex and cerebellum, as well as anterior, posterior, and whole hippocampus were created for all subjects (Fig. 2-3) and used to calculate volumes (Table 2-1). Without spatial normalization, male mice had larger cerebral cortex volumes than females (Fig. 2-4B). Cerebellar volumes, however, did not show significant sex differences (Fig. 2-4C). Male mice had larger posterior and whole hippocampus volumes (Fig 2-4 D & E), whereas female mice had larger anterior hippocampus volumes than males (Fig 2-4F). When the structure volumes were calculated as percentages of whole brain volume (normalizing for brain volume), male mice had larger GM, CSF, cerebral cortex, and posterior hippocampus volumes than females (Table 2-2). Females had larger WM and anterior hippocampus volumes than males. These results are consistent with our VBM results, since the cerebral cortex and posterior

hippocampus were shown to be larger in males and anterior hippocampus was shown to be larger in females. Interestingly, the lateral cerebellum was larger in females and the medial cerebellum was larger in males, effectively offsetting each other in our ABM results.

1.5 Discussion

Voxel-based morphometry, while extensively used in human neuroimaging research, is novel in rodent image analysis. The use of VBM allowed for an objective and comprehensive analysis of sex differences in C57BL/6 mouse brains. It is not subject to human error or bias and is sensitive to subtle changes that may not be detected with atlas-based morphometry (Ashburner and Friston, 2000, 2001). Additionally, the process is considerably less time consuming than manual analysis and allows for the investigation of all available data (Sawiak et al., 2009, 2013). Our results are consonant and expand upon current literature demonstrating sex differences in the brain (Corre et al., 2014; Dorr et al., 2008; Spring et al., 2007). Though much higher resolution can be achieved in *ex vivo* imaging, our results indicate that VBM can be used to reliably identify sex differences *in vivo*.

In this study, we employed novel tissue probability maps (TPMs) generated from 30 male and 30 female live C57BL/6 mice to examine sex-differences in brain structure using voxel-based morphometry. Since an equal number of males and females were used to create the TPMs, it can readily be applied to either sex in an unbiased fashion. The use of these TPMs improved the accuracy of our VBM examination of *in vivo* C57BL/6 mouse brains.

We observed that males had a statistical trend towards larger whole brain volumes, but this did not reach significance. This is consonant with previous studies in mice, where males have demonstrated 2.5% larger whole brain volumes and human studies where male whole brain volume has been reported as 13-15% larger than females (Gur et al., 1999; Leonard et al., 2008; Luders et al., 2009; Luders et al., 2005) (Table 2-3). Segment volume analysis revealed that male mice have larger GM and CSF compartments, while females have more WM. Since

sex differences in compartment volumes have not previously been explored in rodent studies, it is not clear whether these effects are conserved across strains.

We observed larger volumes in the female anterior hippocampus, which is consistent with the literature (Spring et al., 2007). Sex hormones have been known to alter the anatomy of the hippocampus in rodent models (McEwen and Woolley, 1994; Roof and Havens, 1992), but conflicting results exist on the precise nature of these differences (Corre et al., 2014; Isgor and Sengelaub, 1998). The hippocampus has been heavily implicated in sexually dimorphic behaviors including spatial memory (Jacobs et al., 1990) and fear conditioning (Gupta et al., 2001). Furthermore, hippocampal dysfunction is sexually dimorphic in several diseases including anxiety and dementia (Lebron-Milad et al., 2012; Murphy et al., 1996). Differences between anterior and posterior hippocampal function and anatomy have been identified in humans in a sex-dependent manner (Chua et al., 2007; Persson et al., 2014) but, again, inconsistencies in literature suggest that the specifics of these differences are not entirely clear (Goldstein et al., 2001; Ruigrok et al., 2014). Despite the variability in the characterization of sex differences in the hippocampus, it is clear differences exist. A larger anterior hippocampus was demonstrated in female mice relative to males using two different analyses (Corre et al., 2014; Spring et al., 2007). This may contribute to hippocampal-dependent sex differences observed in behavior and disease.

Our results also demonstrated that cortical and basolateral amygdala regions appear larger in female mice. This region is known to exhibit a sexually dimorphic pattern of gene expression in humans and mice (Lin et al., 2011). While morphometric differences have been shown in sections of the basal forebrain just anterior to our findings (Dorr et al., 2008; Spring et al., 2007), sex differences have not previously been shown in the more lateral amygdalar regions in mice. This region has been associated with sexually dimorphic behaviors such as pheromone processing, anxiety, and aggression (Akhmadeev et al., 2016). Developing female rats have been shown to display increased rates of cell proliferation (Krebs-Kraft et al., 2010) in the

amygdala, but not much is known about the origin of this difference. We also observed a larger medial amygdala and bed nucleus of the stria terminalis in males, consistent with previous findings (Corre et al., 2014; Hines et al., 1992). Both hormones and sex chromosomes have been implicated in contributing to this difference (Corre et al., 2014; Shah et al., 2004). The medial amygdala is known to be involved male reproductive behavior (Newman, 1999) and aggression (Wang et al., 2013), as well as social recognition in both sexes (Ferguson et al., 2001). The results in this study support findings in multiple species, indicating that structural differences in the amygdala are present in a sexually dimorphic pattern.

We found that sex differences in the cerebellum were, intriguingly, heterogeneously arranged. The medial portion of the cerebellar cortex was larger in males while the lateral regions, including the paraflocculus and paramedian lobule were larger in females. This heterogeneity was consistent with Spring et al. (2007). Remarkably, these findings were demonstrated in a human study as well (Fan et al., 2010). Fan et al. found that the medial cerebellum, including lobules V and VIIIb, was significantly larger in human males. Human females were shown in this study to have larger lateral cerebellum, including Crus II. These findings demonstrate nearly the exact pattern of sexual dimorphism in our results. The similarity in our findings suggests conservation of sex differences in the cerebellum across species. Little is known about functional sex differences in the cerebellum. There is evidence, however, linking these regions to behaviors that may be functionally relevant to sexual dimorphism (Stoodley and Schmahmann, 2009; Stoodley et al., 2012). Functional MRI suggests lobules IV-V and VII, all of which were shown to be larger in males, are involved in sensorimotor tasks. Language tasks have been associated with Crus II, which is larger in females (Stoodley and Schmahmann, 2009; Stoodley et al., 2012). Further characterizing these differences will be invaluable as human studies have linked sex differences in cerebellar structure to differences in cognitive function (Gur et al., 1999), social behavior (Wang et al., 2014) and disease (Keller et al., 2003).

Additionally, we found that the dorsal region of the caudoputamen was larger in females while the ventral region, as well as the nucleus accumbens, was larger in males. The striatum is known to have many functional sexually dimorphic properties, but the literature describing structural sex differences in this region is scarce (Becker and Hu, 2008; Bobzean et al., 2014). What literature does exist is inconsistent (Corre et al., 2014; Spring et al., 2007; Wong et al., 2015). Spring et al. (2007) did not find volume differences in the caudoputamen, but did identify sex differences in its shape. Corre et al. (2014) did report, however, that gonadal hormones were associated with volume differences in several regions within the caudoputamen. Regardless of sex chromosome complement, gonadal females displayed regions of greater volume, but the specific pattern of these differences was unclear. Our results demonstrate, for the first time, a robust bilateral pattern of sexual dimorphism in the striatum. These structural differences could contribute to the sexually dimorphic behaviors that are regulated by the striatum including motivation, reward, and impulse control (Becker and Hu, 2008; Bobzean et al., 2014). Sex hormones seem to play a pivotal role in manipulating these behaviors. Estrogens, for example, enhance neuronal excitability in the striatum and increase dopamine receptor availability (Yoest et al., 2014). Females and males react differently to substance abuse as a result of these properties and a better understanding of the associated neural differences may lead to more successful methods of treating the condition.

As a validation of our VBM results, we analyzed the data using atlas-based morphometry. Consistent with our VBM results, ABM revealed that cerebral cortex was larger in males. Interestingly, no sex differences were observed in the volume of the cerebellum. However, given the sexual dimorphic pattern of GM volume in the cerebellum noted with VBM, this is, again, consistent with our findings. VBM indicated that the medial portion of the cerebellum was larger in males, but the lateral portion was larger in females. It is possible that the sex differences offset one another so that the net cerebellar volume is not statistically different between the sexes. This result highlights one of the strengths of this approach, that VBM allows us to

perform sophisticated voxelwise statistical analyses. In this report, we used a general linear model to perform the statistical analysis, permitting us to use total intracranial volume (TIV) as a covariate. In this way, each voxel can have its own relationship with the covariates, unveiling the regional cerebellar differences between females and males we observed. Furthermore, the consistency between our results and Spring et al., despite different analysis techniques, is noteworthy and likely represents biologically meaningful effects. There were some differences between our results and other reports in the literature (Corre et al., 2014; Spring et al., 2007), but these discrepancies may be due to differences in imaging resolution and contrast, differences in the nature of the analyses (deformation based morphometry vs. voxel-based morphometry), or even differences in the size of the smoothing kernel used for the analysis.

The tissue probability maps that we generated appear to over-represent white matter in the brainstem. This may limit the ability to detect changes in brainstem nuclei, although experiments with other, similar TPMs have demonstrated that differences in the brainstem can be visualized (Sawiak et al., 2009).

It is important to acknowledge that sex differences may vary across different mouse strains. In rodents, it seems that both sex hormones and sex chromosomes contribute to sex differences in anatomy (Arnold, 2009a; McCarthy and Arnold, 2011). Furthermore, epigenetics and environmental factors have also been known to alter neural structure (Champagne, 2008; McCarthy and Arnold, 2011). Recently, investigation into the effects of sex chromosomes using the four core genotypes (Arnold and Chen, 2009) has suggested significant differences in the neuroanatomy of mice possessing different sex chromosome complement (XX or XY), but the same gonadal sex (Corre et al., 2014). Considering how anatomical differences in the four core genotypes translate to disease models presents an intriguing line of future research.

Though VBM is a powerful analysis tool, it is unable to determine the basis of morphological differences. We cannot distinguish whether our observed results are due to differences in neuronal number, neuronal size, or even cellular composition. To fully understand the anatomy

underlying neural sex differences, future analysis should include a histological component, perhaps with use of modern optical clearing technologies to visualize entire brains (Chung et al., 2013; Spence et al., 2014).

1.6 Conclusion

Voxel-based morphometry has not previously been used to analyze sex differences in mice. Our approach was particularly well suited to the study of sex differences through the use of novel TPMs that equally represented both sexes. Males exhibited larger cerebral cortex, medial amygdala, and medial cerebellar cortex volumes, whereas females displayed larger anterior hippocampus, basolateral amygdala, and lateral cerebellar cortex volumes. The results presented are consonant with previous findings that demonstrated sexually dimorphic brain morphometry (Corre et al., 2014; Spring et al., 2007) signifying a robust effect across studies. Much is still left to be discovered about the basis of anatomical sex differences in the brain, but it is clear that the differences are measurable and therefore cannot be considered negligible. They can, however, inform our understanding of the brain and sexually dimorphic behavior and disease.

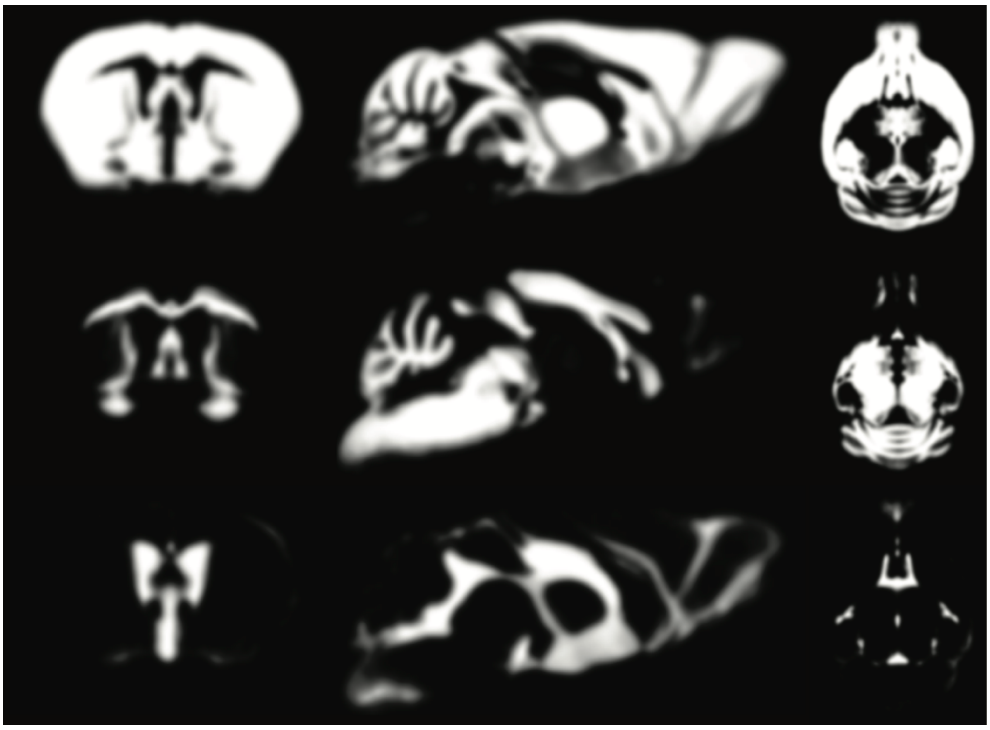

Fig. 2-1. Tissue probability maps. Tissue probability maps for gray matter (top), white matter (middle), and cerebrospinal fluid (bottom). Coronal (left), sagittal (middle), and axial (right) sections through each map represent the probability that a given voxel belongs to that class of tissue. Maps were created using T2-weighted magnetic resonance images from 30 male and 30 female adult C57BL/6 mice.

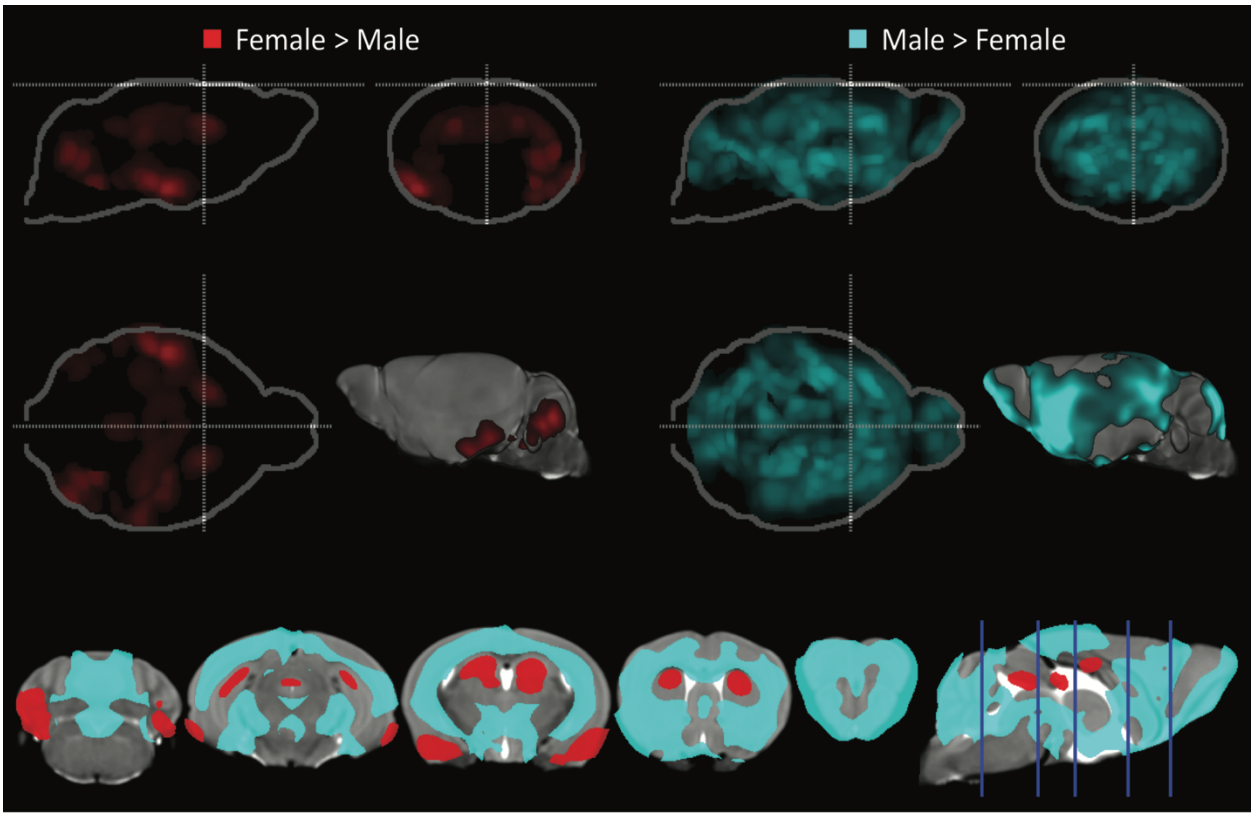

Fig. 2-2. Localized sex differences in gray matter volume. VBM revealed regions that were significantly ($p \leq 0.05$, FDR corrected) larger in females (red) or males (aqua). Maximum intensity projections are overlain on the Mortimer Space Atlas standard glass brains where the dotted line represents bregma. Surface views of significant regions are shown over a 3D rendering of the mean template. Coronal sections (bottom row) demonstrate regions larger in females (anterior hippocampus, basolateral amygdala, and lateral cerebellar cortex) or larger in males (cerebral cortex, medial amygdala, and medial cerebellar cortex). Blue lines on the sagittal section indicate the position of the coronal slices from left to right respectively.

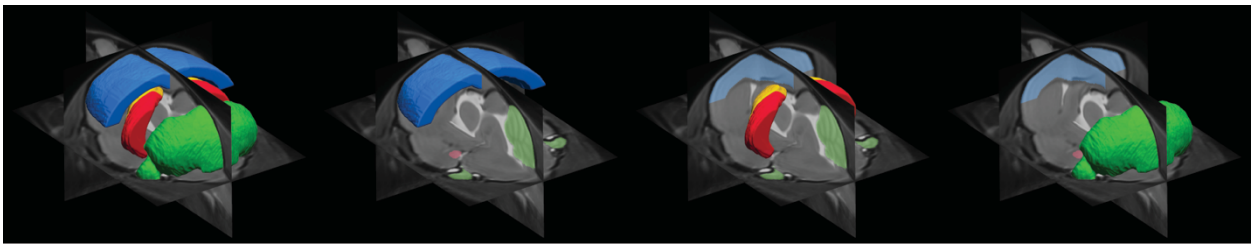

Fig. 2-3. Minimum deformation atlas with region delineations. Surface views of cerebral cortex (blue), anterior hippocampus (yellow), posterior hippocampus (red), and cerebellum (green) delineations are overlaid on the minimum deformation atlas created from the T2-weighted magnetic resonance images of 30 male and 30 female C57BL/6 mice used in this study.

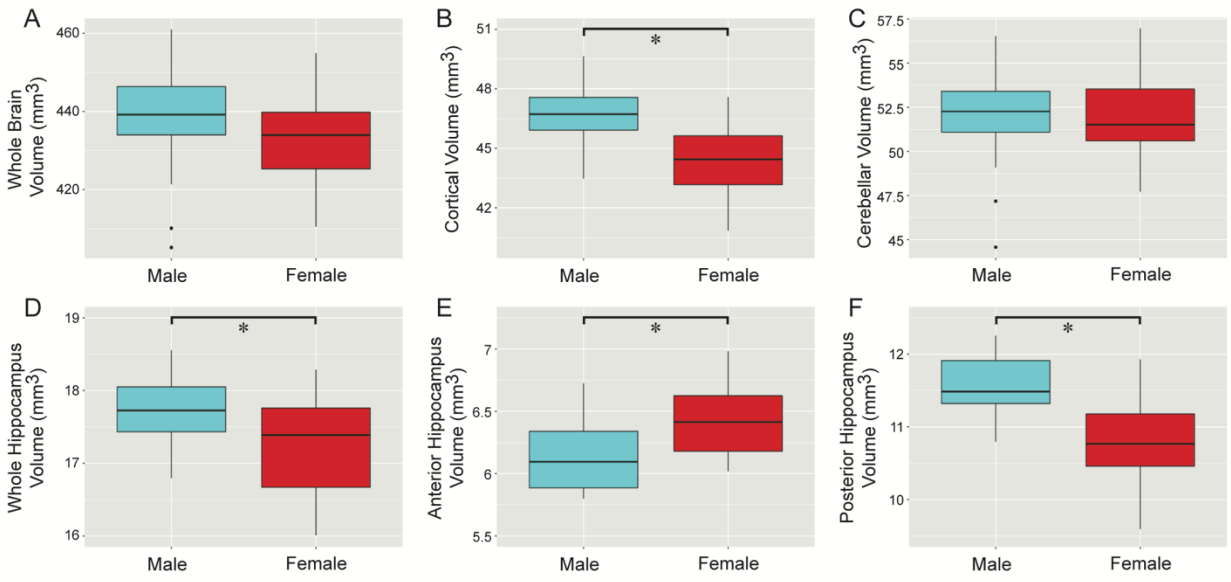

Fig. 2-4. Atlas-based morphometry supports VBM results. (A) Whole brain volume showed a statistical trend towards being larger in males (aqua) than females (red) ($p = 0.07$). (B) Cortical volume was larger in males ($p = 2.96 \times 10^{-6}$). (C) No statistically significant sex difference was found in cerebellar volume. (D) Whole hippocampus volume was larger in males ($p = 2.47 \times 10^{-3}$). (E) Anterior hippocampus volume was larger in females ($p = 1.71 \times 10^{-4}$) while (F) Posterior hippocampus volume was larger in males ($p = 8.25 \times 10^{-7}$). All p-values are FDR-corrected for multiple comparisons.

Region	Mean (mm^3)		Effect Size (mm^3)	*P* value
	Male	Female		
Whole brain	438.43 [434.05, 442.42]	432.48 [428.31, 436.63]	5.95 [-0.06, 11.65]	0.07
Gray matter	262.25 [257.00, 267.26]	251.00 [247.62, 254.39]	11.25 [5.01, 17.21]	1.41×10^{-3}
White matter	130.60 [126.93, 133.97]	143.20 [140.86, 145.53]	12.60 [16.94, 8.41]	2.94×10^{-6}
Cerebrospinal fluid	45.58 [43.18, 47.98]	38.29 [36.50, 40.07]	7.29 [4.37, 10.23]	4.60×10^{-5}
Cerebral cortex	46.72 [46.20, 47.21]	44.32 [43.67, 44.97]	2.39 [1.58, 3.24]	2.96×10^{-6}
Cerebellum	51.89 [50.99, 52.73]	51.84 [51.11, 52.58]	0.05 [-1.09, 1.17]	0.93
Whole Hippocampus	17.71 [17.54, 17.88]	17.22 [16.98, 17.45]	0.49 [0.21, 0.78]	2.47×10^{-3}
Anterior Hippocampus	6.13 [6.04, 6.22]	6.42 [6.33, 6.52]	0.29 [0.16, 0.43]	1.71×10^{-4}
Posterior Hippocampus	11.58 [11.44, 11.72]	10.80 [10.60, 11.00]	0.78 [0.54, 1.02]	8.25×10^{-7}

Table 2-1. Regional volumes for male and female C57BL/6 mice. All reported p-values are FDR-corrected for multiple comparisons. 95% confidence interval in brackets. (n = 30 males, 30 females)

Region	Mean Percentage of Total Brain Volume		Effect Size	*P* value
	Male	Female		
Gray matter	59.82 [58.62, 60.96]	58.04 [57.25, 58.82]	1.78 [0.36, 3.16]	0.02
White matter	29.79 [28.96, 30.56]	33.11 [32.57, 33.65]	3.32 [2.40, 4.32]	3.72×10^{-7}
Cerebrospinal fluid	10.40 [9.85, 10.95]	8.85 [8.44, 9.27]	1.54 [0.84, 2.23]	1.37×10^{-4}
Cerebral cortex	10.66 [10.54, 10.77]	10.24 [10.10, 10.40]	0.41 [0.22, 0.60]	2.05×10^{-4}
Cerebellum	11.84 [11.63, 12.03]	11.99 [11.82, 12.16]	-0.002 [-0.004, 0.001]	0.29
Whole Hippocampus	4.04 [4.00, 4.08]	3.98 [3.93, 4.03]	0.06 [0.01, 0.12]	0.11
Anterior Hippocampus	1.40 [1.38, 1.42]	1.48 [1.46, 1.51]	0.09 [0.06, 0.12]	3.74×10^{-6}
Posterior Hippocampus	2.64 [2.61, 2.67]	2.50 [2.45, 2.54]	0.14 [0.09, 0.20]	2.23×10^{-5}

Table 2-2. Regional volumes for male and female C57BL/6 mice normalized to male and female mean whole brain volume respectively. All reported p-values are FDR-corrected for multiple comparisons. 95% confidence interval in brackets. (n = 30 males, 30 females)

Region	Relevant behaviors	This study	Mouse literature	Human literature
Cerebral cortex	Cognition, sensory functions, motor functions (Parent and Carpenter, 1996)	Larger in males	Some regions larger in males, some larger in females (Spring et al., 2007)	Larger in males (Giedd et al., 1997; Goldstein et al., 2001)
Bed nucleus of the stria terminalis	Fear (Fendt and Fanselow, 1999)	Larger in males	Larger in gonadal males (Corre et al., 2014)	Larger in males (Allen and Gorski, 1990)
Posterior hypothalamus	Hormone production and release (Parent and Carpenter, 1996) Sexual stimulation (Caggiula and Hoebel, 1966)	Larger in males	Larger in gonadal males (Corre et al., 2014) Larger in females (Spring et al., 2007)	Whole hypothalamus larger in males (Goldstein et al., 2001; Swaab et al., 1985)
Anterior hippocampus	Spatial memory (Jacobs et al., 1990) Fear conditioning (Gupta et al., 2001)	Larger in females	Larger in females (Spring et al., 2007)	Whole hippocampus larger in females (Giedd et al., 1996; Goldstein et al., 2001)
Ventral caudoputamen	Motivation, reward, impulse control (Becker and Hu, 2008; Bobzean et al., 2014)	Larger in males	Difference in shape (Spring et al., 2007) Several nuclei larger in chromosomal males (Corre et al., 2014)	Putamen larger in males (Goldstein et al., 2001) Caudate larger in females (Filipek et al., 1994; Goldstein et al., 2001; Murphy et al., 1996)
Dorsal caudoputamen	Motivation, reward, impulse control (Becker and Hu, 2008; Bobzean et al., 2014)	Larger in females	Difference in shape (Spring et al., 2007) Several nuclei larger in gonadal females (Corre et al., 2014)	Putamen larger in males (Goldstein et al., 2001) Caudate larger in females (Filipek et al., 1994; Goldstein et al., 2001; Murphy et al., 1996)
Medial cerebellar cortex (including lobules II-IX)	Sensorimotor functions (Allen et al., 1997; Stoodley and Schmahmann, 2009; Stoodley et al., 2012) Proximal limb and trunk coordination (Ivry et al., 1988)	Larger in males	Larger in males (Spring et al., 2007)	Larger in males (Fan et al., 2010)
Lateral cerebellar cortex (including paraflocculus and paramedian lobule)	Language tasks (Stoodley and Schmahmann, 2009; Stoodley et al., 2012) Motor planning for extremities (Ivry et al., 1988)	Larger in females	Larger in females (Spring et al., 2007)	Larger in females (Fan et al., 2010)
Basolateral amygdala	Pheromone processing, Anxiety, Aggression (Akhmadeev et al., 2016)	Larger in females	Larger in females (Spring et al., 2007)	Whole amygdala larger in males (Giedd et al., 1996; Goldstein et al., 2001)
Medial amygdala	Reproductive behavior (Newman, 1999) Social Recognition (Ferguson et al., 2001) Aggression (Wang et al., 2013)	Larger in males	Larger in gonadal males (Corre et al., 2014)	Whole amygdala larger in males (Giedd et al., 1996; Goldstein et al., 2001)

Table 2-3. Prominent regions displaying sexual dimorphism in this study compared to mouse and human literature.

2.7 References

Akhmadeev, A.V., Galieva, L.F., Kalimullina, L.B., 2016. The Basolateral Nucleus in the System of Reproductive Centers in the Amygdaloid Body of the Brain. Neuroscience and Behavioral Physiology 46, 652-658.

Allen, G., Buxton, R.B., Wong, E.C., Courchesne, E., 1997. Attentional activation of the cerebellum independent of motor involvement. Science 275, 1940-1943.

Allen, L.S., Gorski, R.A., 1990. Sex difference in the bed nucleus of the stria terminalis of the human brain. J Comp Neurol 302, 697-706.

Andreano, J.M., Cahill, L., 2009. Sex influences on the neurobiology of learning and memory. Learn Mem 16, 248-266.

Arnold, A.P., 2004. Sex chromosomes and brain gender. Nat Rev Neurosci 5, 701-708.

Arnold, A.P., 2009a. Mouse models for evaluating sex chromosome effects that cause sex differences in non-gonadal tissues. J Neuroendocrinol 21, 377-386.

Arnold, A.P., 2009b. The organizational-activational hypothesis as the foundation for a unified theory of sexual differentiation of all mammalian tissues. Horm Behav 55, 570-578.

Arnold, A.P., 2010. Promoting the understanding of sex differences to enhance equity and excellence in biomedical science. Biology of Sex Differences 1, 1.

Arnold, A.P., Chen, X., 2009. What does the "four core genotypes" mouse model tell us about sex differences in the brain and other tissues? Front Neuroendocrinol 30, 1-9.

Ashburner, J., 2007. A fast diffeomorphic image registration algorithm. Neuroimage 38, 95-113.

Ashburner, J., Friston, K.J., 2000. Voxel-based morphometry--the methods. Neuroimage 11, 805-821.

Ashburner, J., Friston, K.J., 2001. Why voxel-based morphometry should be used. Neuroimage

14, 1238-1243.

Ashburner, J., Friston, K.J., 2005. Unified segmentation. Neuroimage 26, 839-851.

Barnes, L.L., Wilson, R.S., Bienias, J.L., Schneider, J.A., Evans, D.A., Bennett, D.A., 2005. SEx differences in the clinical manifestations of alzheimer disease pathology. Archives of General Psychiatry 62, 685-691.

Becker, J.B., Hu, M., 2008. Sex Differences in Drug Abuse. Front Neuroendocrinol 29, 36-47.

Beery, A.K., Zucker, I., 2011. Sex Bias in Neuroscience and Biomedical Research. Neuroscience and biobehavioral reviews 35, 565-572.

Berkley, K.J., 1997. Sex differences in pain. Behav Brain Sci 20, 371-380; discussion 435-513.

Blatter, D.D., Bigler, E.D., Gale, S.D., Johnson, S.C., Anderson, C.V., Burnett, B.M., Parker, N., Kurth, S., Horn, S.D., 1995. Quantitative volumetric analysis of brain MR: normative database spanning 5 decades of life. Ajnr. American Journal of Neuroradiology 16, 241-251.

Bobzean, S.A., DeNobrega, A.K., Perrotti, L.I., 2014. Sex differences in the neurobiology of drug addiction. Exp Neurol 259, 64-74.

Caggiula, A.R., Hoebel, B.G., 1966. "Copulation-reward site" in the posterior hypothalamus. Science 153, 1284-1285.

Cahill, L., 2006. Why sex matters for neuroscience. Nat Rev Neurosci 7, 477-484.

Castle, D.J., Murray, R.M., 1991. The neurodevelopmental basis of sex differences in schizophrenia. Psychol Med 21, 565-575.

Champagne, F.A., 2008. Epigenetic Mechanisms and the Transgenerational Effects of Maternal Care. Frontiers in neuroendocrinology 29, 386-397.

Chua, E.F., Schacter, D.L., Rand-Giovannetti, E., Sperling, R.A., 2007. Evidence for a specific role of the anterior hippocampal region in successful associative encoding. Hippocampus 17, 1071-1080.

Chung, K., Wallace, J., Kim, S.Y., Kalyanasundaram, S., Andalman, A.S., Davidson, T.J., Mirzabekov, J.J., Zalocusky, K.A., Mattis, J., Denisin, A.K., Pak, S., Bernstein, H., Ramakrishnan, C., Grosenick, L., Gradinaru, V., Deisseroth, K., 2013. Structural and molecular interrogation of intact biological systems. Nature 497, 332-337.

Clayton, J.A., Collins, F.S., 2014. Policy: NIH to balance sex in cell and animal studies. Nature 509, 282-283.

Corre, C., Friedel, M., Vousden, D.A., Metcalf, A., Spring, S., Qiu, L.R., Lerch, J.P., Palmert, M.R., 2014. Separate effects of sex hormones and sex chromosomes on brain structure and function revealed by high-resolution magnetic resonance imaging and spatial navigation assessment of the Four Core Genotype mouse model. Brain Struct Funct.

Dorr, A.E., Lerch, J.P., Spring, S., Kabani, N., Henkelman, R.M., 2008. High resolution three-dimensional brain atlas using an average magnetic resonance image of 40 adult C57Bl/6J mice. Neuroimage 42, 60-69.

Fan, L., Tang, Y., Sun, B., Gong, G., Chen, Z.J., Lin, X., Yu, T., Li, Z., Evans, A.C., Liu, S., 2010. Sexual dimorphism and asymmetry in human cerebellum: An MRI-based morphometric study. Brain Research 1353, 60-73.

Fendt, M., Fanselow, M.S., 1999. The neuroanatomical and neurochemical basis of conditioned fear. Neuroscience and biobehavioral reviews 23, 743-760.

Ferguson, J.N., Aldag, J.M., Insel, T.R., Young, L.J., 2001. Oxytocin in the Medial Amygdala is Essential for Social Recognition in the Mouse. The Journal of Neuroscience 21, 8278-8285.

Filipek, P.A., Richelme, C., Kennedy, D.N., Caviness, V.S., Jr., 1994. The young adult human brain: an MRI-based morphometric analysis. Cereb Cortex 4, 344-360.

Fombonne, E., 2005. Epidemiology of Autistic Disorder and Other Pervasive Developmental Disorders. The Journal of Clinical Psychiatry 66, 3-8.

Giedd, J.N., Castellanos, F.X., Rajapakse, J.C., Vaituzis, A.C., Rapoport, J.L., 1997. Sexual

dimorphism of the developing human brain. Prog Neuropsychopharmacol Biol Psychiatry 21, 1185-1201.

Giedd, J.N., Snell, J.W., Lange, N., Rajapakse, J.C., Casey, B.J., Kozuch, P.L., Vaituzis, A.C., Vauss, Y.C., Hamburger, S.D., Kaysen, D., Rapoport, J.L., 1996. Quantitative magnetic resonance imaging of human brain development: ages 4-18. Cereb Cortex 6, 551-560.

Gioiosa, L., Chen, X., Watkins, R., Umeda, E.A., Arnold, A.P., 2008. Sex chromosome complement affects nociception and analgesia in newborn mice. J Pain 9, 962-969.

Goldstein, J.M., Seidman, L.J., Horton, N.J., Makris, N., Kennedy, D.N., Caviness, V.S., Jr., Faraone, S.V., Tsuang, M.T., 2001. Normal sexual dimorphism of the adult human brain assessed by in vivo magnetic resonance imaging. Cerebral Cortex 11, 490-497.

Gonthier, M., Lyon, M.A., 2004. Childhood-onset schizophrenia: An overview. Psychology in the Schools 41, 803-811.

Good, C.D., Johnsrude, I., Ashburner, J., Henson, R.N., Friston, K.J., Frackowiak, R.S., 2001. Cerebral asymmetry and the effects of sex and handedness on brain structure: a voxel-based morphometric analysis of 465 normal adult human brains. Neuroimage 14, 685-700.

Gupta, R.R., Sen, S., Diepenhorst, L.L., Rudick, C.N., Maren, S., 2001. Estrogen modulates sexually dimorphic contextual fear conditioning and hippocampal long-term potentiation (LTP) in rats1. Brain Research 888, 356-365.

Gur, R.C., Turetsky, B.I., Matsui, M., Yan, M., Bilker, W., Hughett, P., Gur, R.E., 1999. Sex differences in brain gray and white matter in healthy young adults: correlations with cognitive performance. Journal of Neuroscience 19, 4065-4072.

Hebert, L.E., Weuve, J., Scherr, P.A., Evans, D.A., 2013. Alzheimer disease in the United States (2010–2050) estimated using the 2010 census. Neurology 80, 1778-1783.

Hines, M., Allen, L.S., Gorski, R.A., 1992. Sex differences in subregions of the medial nucleus

of the amygdala and the bed nucleus of the stria terminalis of the rat. Brain Research 579, 321-326.

Hochberg, Y., Benjamini, Y., 1990. More powerful procedures for multiple significance testing. Stat Med 9, 811-818.

Isgor, C., Sengelaub, D.R., 1998. Prenatal Gonadal Steroids Affect Adult Spatial Behavior, CA1 and CA3 Pyramidal Cell Morphology in Rats. Hormones and Behavior 34, 183-198.

Ivry, R.B., Keele, S.W., Diener, H.C., 1988. Dissociation of the lateral and medial cerebellum in movement timing and movement execution. Exp Brain Res 73, 167-180.

Jacobs, L.F., Gaulin, S.J., Sherry, D.F., Hoffman, G.E., 1990. Evolution of spatial cognition: sex-specific patterns of spatial behavior predict hippocampal size. Proceedings of the National Academy of Sciences 87, 6349-6352.

Keifer, O.P., Jr., Hurt, R.C., Gutman, D.A., Keilholz, S.D., Gourley, S.L., Ressler, K.J., 2015. Voxel-based morphometry predicts shifts in dendritic spine density and morphology with auditory fear conditioning. Nat Commun 6, 7582.

Keller, A., Castellanos, F.X., Vaituzis, A.C., Jeffries, N.O., Giedd, J.N., Rapoport, J.L., 2003. Progressive loss of cerebellar volume in childhood-onset schizophrenia. Am J Psychiatry 160, 128-133.

Kovacevic, N., Henderson, J.T., Chan, E., Lifshitz, N., Bishop, J., Evans, A.C., Henkelman, R.M., Chen, X.J., 2005. A three-dimensional MRI atlas of the mouse brain with estimates of the average and variability. Cerebral Cortex 15, 639-645.

Krebs-Kraft, D.L., Hill, M.N., Hillard, C.J., McCarthy, M.M., 2010. Sex difference in cell proliferation in developing rat amygdala mediated by endocannabinoids has implications for social behavior. Proceedings of the National Academy of Sciences of the United States of America 107, 20535-20540.

Kurth, F., MacKenzie-Graham, A., Toga, A.W., Luders, E., 2015. Shifting brain asymmetry: the

link between meditation and structural lateralization. Soc Cogn Affect Neurosci, pp. 55-61.

Lebron-Milad, K., Abbs, B., Milad, M.R., Linnman, C., Rougemount-Bücking, A., Zeidan, M.A., Holt, D.J., Goldstein, J.M., 2012. Sex differences in the neurobiology of fear conditioning and extinction: a preliminary fMRI study of shared sex differences with stress-arousal circuitry. Biol Mood Anxiety Disord, p. 7.

Lejbak, L., Crossley, M., Vrbancic, M., 2011. A male advantage for spatial and object but not verbal working memory using the n-back task. Brain Cogn 76, 191-196.

Leonard, C.M., Towler, S., Welcome, S., Halderman, L.K., Otto, R., Eckert, M.A., Chiarello, C., 2008. Size matters: cerebral volume influences sex differences in neuroanatomy. Cerebral Cortex 18, 2920-2931.

Lerch, J.R., Sled, J.G., Henkelman, R.M., 2011. MRI Phenotyping of Genetically Altered Mice. Magnetic Resonance Neuroimaging: Methods and Protocols 711, 349-361.

Lin, L.-C., Lewis, D.A., Sibille, E., 2011. A human-mouse conserved sex bias in amygdala gene expression related to circadian clock and energy metabolism. Molecular Brain 4, 18.

Luders, E., Gaser, C., Jancke, L., Schlaug, G., 2004. A voxel-based approach to gray matter asymmetries. Neuroimage 22, 656-664.

Luders, E., Gaser, C., Narr, K.L., Toga, A.W., 2009. Why sex matters: brain size independent differences in gray matter distributions between men and women. Journal of Neuroscience 29, 14265-14270.

Luders, E., Narr, K.L., Thompson, P.M., Woods, R.P., Rex, D.E., Jancke, L., Steinmetz, H., Toga, A.W., 2005. Mapping cortical gray matter in the young adult brain: effects of gender. Neuroimage 26, 493-501.

Luders, E., Steinmetz, H., Jancke, L., 2002. Brain size and grey matter volume in the healthy human brain. Neuroreport 13, 2371-2374.

Luders, E., Toga, A.W., 2010. Sex differences in brain anatomy. Prog Brain Res 186, 3-12.

MacKenzie-Graham, A., Rinek, G.A., Avedisian, A., Gold, S.M., Frew, A.J., Aguilar, C., Lin, D.R., Umeda, E., Voskuhl, R.R., Alger, J.R., 2012. Cortical atrophy in experimental autoimmune encephalomyelitis: in vivo imaging. Neuroimage 60, 95-104.

MacKenzie-Graham, A., Tiwari-Woodruff, S.K., Sharma, G., Aguilar, C., Vo, K.T., Strickland, L.V., Morales, L., Fubara, B., Martin, M., Jacobs, R.E., Johnson, G.A., Toga, A.W., Voskuhl, R.R., 2009. Purkinje cell loss in experimental autoimmune encephalomyelitis. Neuroimage 48, 637-651.

McCarthy, M.M., Arnold, A.P., 2011. Reframing sexual differentiation of the brain. Nature neuroscience 14, 677-683.

McEwen, B.S., Woolley, C.S., 1994. Estradiol and progesterone regulate neuronal structure and synaptic connectivity in adult as well as developing brain. Experimental Gerontology 29, 431-436.

Morris, J.A., Jordan, C.L., Breedlove, S.M., 2004. Sexual differentiation of the vertebrate nervous system. Nature Neuroscience 7, 1034-1039.

Murphy, D.M., DeCarli, C., McLntosh, A.R., et al., 1996. Sex differences in human brain morphometry and metabolism: An in vivo quantitative magnetic resonance imaging and positron emission tomography study on the effect of aging. Archives of General Psychiatry 53, 585-594.

Newman, S.W., 1999. The Medial Extended Amygdala in Male Reproductive Behavior A Node in the Mammalian Social Behavior Network. Annals of the New York Academy of Sciences 877, 242-257.

Norman, M.A., Evans, J.D., Miller, W.S., Heaton, R.K., 2000. Demographically corrected norms for the California Verbal Learning Test. J Clin Exp Neuropsychol 22, 80-94.

Parent, A., Carpenter, M.B., 1996. Carpenter's human neuroanatomy, 9th ed. Williams & Wilkins, Baltimore.

Persson, J., Spreng, R.N., Turner, G., Herlitz, A., Morell, A., Stening, E., Wahlund, L.-O.,

Wikström, J., Söderlund, H., 2014. Sex differences in volume and structural covariance of the anterior and posterior hippocampus. Neuroimage 99, 215-225.

Phoenix, C.H., Goy, R.W., Gerall, A.A., Young, W.C., 1959. Organizing action of prenatally administered testosterone propionate on the tissues mediating mating behavior in the female guinea pig. Endocrinology 65, 369-382.

Piccinelli, M., Wilkinson, G., 2000. Gender differences in depression. The British Journal of Psychiatry 177, 486-492.

Raznahan, A., Probst, F., Palmert, M.R., Giedd, J.N., Lerch, J.P., 2013. High resolution whole brain imaging of anatomical variation in XO, XX, and XY mice. Neuroimage 83, 962-968.

Roof, R.L., Havens, M.D., 1992. Testosterone improves maze performance and induces development of a male hippocampus in females. Brain Research 572, 310-313.

Ruigrok, A.N.V., Salimi-Khorshidi, G., Lai, M.-C., Baron-Cohen, S., Lombardo, M.V., Tait, R.J., Suckling, J., 2014. A meta-analysis of sex differences in human brain structure. Neuroscience & Biobehavioral Reviews 39, 34-50.

Sasaki, K., Sumiyoshi, A., Nonaka, H., Kasahara, Y., Ikeda, K., Hall, F.S., Uhl, G.R., Watanabe, M., Kawashima, R., Sora, I., 2015. Specific regions display altered grey matter volume in mu-opioid receptor knockout mice: MRI voxel-based morphometry. Br J Pharmacol 172, 654-667.

Sawiak, S.J., Wood, N.I., Williams, G.B., Morton, A.J., Carpenter, T.A., 2009. Voxel-based morphometry in the R6/2 transgenic mouse reveals differences between genotypes not seen with manual 2D morphometry. Neurobiol Dis 33, 20-27.

Sawiak, S.J., Wood, N.I., Williams, G.B., Morton, A.J., Carpenter, T.A., 2013. Voxel-based morphometry with templates and validation in a mouse model of Huntington's disease. Magn Reson Imaging 31, 1522-1531.

Schlaepfer, T.E., Harris, G.J., Tien, A.Y., Peng, L., Lee, S., Pearlson, G.D., 1995. Structural

differences in the cerebral cortex of healthy female and male subjects: a magnetic resonance imaging study. Psychiatry Res 61, 129-135.

Shah, N.M., Pisapia, D.J., Maniatis, S., Mendelsohn, M.M., Nemes, A., Axel, R., 2004. Visualizing Sexual Dimorphism in the Brain. Neuron 43, 313-319.

Shattuck, D.W., Leahy, R.M., 2002. BrainSuite: an automated cortical surface identification tool. Med Image Anal 6, 129-142.

Shulman, L.M., Bhat, V., 2006. Gender disparities in Parkinson's disease. Expert Rev Neurother 6, 407-416.

Siegmund, D.O., Worsley, K.J., 1995. Testing for a Signal with Unknown Location and Scale in a Stationary Gaussian Random-Field. Annals of Statistics 23, 608-639.

Spence, R.D., Kurth, F., Itoh, N., Mongerson, C.R.L., Wailes, S.H., Peng, M.S., MacKenzie-Graham, A.J., 2014. Bringing CLARITY to Gray Matter Atrophy. Neuroimage 101, 625-632.

Spring, S., Lerch, J.P., Henkelman, R.M., 2007. Sexual dimorphism revealed in the structure of the mouse brain using three-dimensional magnetic resonance imaging. Neuroimage 35, 1424-1433.

Stoodley, C.J., Schmahmann, J.D., 2009. Functional topography in the human cerebellum: A meta-analysis of neuroimaging studies. 44, 489–501.

Stoodley, C.J., Valera, E.M., Schmahmann, J.D., 2012. Functional topography of the cerebellum for motor and cognitive tasks: an fMRI study. Neuroimage 59, 1560-1570.

Swaab, D.F., Fliers, E., Partiman, T.S., 1985. The suprachiasmatic nucleus of the human brain in relation to sex, age and senile dementia. Brain Res 342, 37-44.

Tottenham, L.S., Saucier, D., Elias, L., Gutwin, C., 2003. Female advantage for spatial location memory in both static and dynamic environments. Brain Cogn 53, 381-383.

Voyer, D., Postma, A., Brake, B., Imperato-McGinley, J., 2007. Gender differences in object location memory: a meta-analysis. Psychon Bull Rev 14, 23-38.

Voyer, D., Voyer, S., Bryden, M.P., 1995. Magnitude of sex differences in spatial abilities: a meta-analysis and consideration of critical variables. Psychol Bull 117, 250-270.

Wang, S.S.H., Kloth, A.D., Badura, A., 2014. The Cerebellum, Sensitive Periods, and Autism. Neuron 83, 518-532.

Wang, Y., He, Z., Zhao, C., Li, L., 2013. Medial amygdala lesions modify aggressive behavior and immediate early gene expression in oxytocin and vasopressin neurons during intermale exposure. Behavioural Brain Research 245, 42-49.

Webber, K.M., Casadesus, G., Perry, G., Atwood, C.S., Bowen, R., Smith, M.A., 2005. Gender differences in Alzheimer disease: the role of luteinizing hormone in disease pathogenesis. Alzheimer Dis Assoc Disord 19, 95-99.

Weiss, E.M., Ragland, J.D., Brensinger, C.M., Bilker, W.B., Deisenhammer, E.A., Delazer, M., 2006. Sex differences in clustering and switching in verbal fluency tasks. J Int Neuropsychol Soc 12, 502-509.

Whitacre, C.C., Reingold, S.C., O'Looney, P.A., 1999. A gender gap in autoimmunity. Science 283, 1277-1278.

Wong, J.E., Cao, J., Dorris, D.M., Meitzen, J., 2015. Genetic sex and the volumes of the caudate-putamen, nucleus accumbens core and shell: original data and a review. Brain Struct Funct.

Yoest, K.E., Cummings, J.A., Becker, J.B., 2014. Estradiol, Dopamine and Motivation. Cent Nerv Syst Agents Med Chem 14, 83-89.

Zhao, L., Mao, Z., Woody, S.K., Brinton, R.D., 2016. Sex differences in metabolic aging of the brain: insights into female susceptibility to Alzheimer's disease. Neurobiology of Aging 42, 69-79.

Chapter 3

Axonal damage in spinal cord is associated with gray matter atrophy in sensorimotor cortex in experimental autoimmune encephalomyelitis

3.1 Abstract

Background: Gray matter (GM) atrophy in brain is one of the best predictors of long-term disability in multiple sclerosis (MS) and recent findings have revealed that localized GM atrophy is associated with clinical disabilities. GM atrophy associated with each disability mapped to a distinct brain region; revealing a disability-specific atlas (DSA) of GM loss.

Objective: To uncover the mechanisms underlying the development of localized GM atrophy.

Methods: We used voxel-based morphometry (VBM) to evaluate localized GM atrophy and Clear Lipid-exchanged Acrylamide-hybridized Rigid Imaging-compatible Tissue-hYdrogel (CLARITY) to evaluate specific pathologies in mice with experimental autoimmune encephalomyelitis (EAE).

Results: We observed extensive GM atrophy throughout the cerebral cortex, with additional foci in the thalamus and caudoputamen, in mice with EAE compared to normal controls. Next, we generated pathology-specific atlases, voxelwise mappings of the correlation between specific pathologies and localized GM atrophy. Interestingly, axonal damage (end-bulbs and ovoids) in the spinal cord strongly correlated with GM atrophy in the sensorimotor cortex of the brain.

Conclusions: The combination of VBM with CLARITY in EAE can localize GM atrophy in brain that is associated with a specific pathology in spinal cord; revealing a pathology-specific atlas (PSA) of GM loss.

3.2 Introduction

Multiple sclerosis is an autoimmune-mediated disease of the central nervous system characterized by demyelination, axonal damage, and synaptic loss.(Dendrou et al., 2015) While MS has long been regarded as a disease of white matter (WM), gray matter (GM) atrophy has a direct relationship with clinical outcomes.(Fisniku et al., 2008; Kuceyeski et al., 2015; MacKenzie-Graham et al., 2016)

Voxel-based morphometry (VBM) is an effective method of analyzing localized GM atrophy in a biology-driven manner, as opposed to focusing on a priori selected structures. In VBM, statistical analyses are conducted throughout the entire brain on a voxelwise basis,(Ashburner and Friston, 2000) permitting localization of volume changes across neuroanatomical structures. Voxelwise analyses have been conducted extensively in MS and have provided valuable insights into the pattern and progression of GM atrophy.(Ceccarelli et al., 2008; Datta et al., 2015; Kuceyeski et al., 2015; Prinster et al., 2010) VBM is particularly well-suited in MS because GM atrophy is not homogenously distributed throughout the brain. For example, atrophy within sensorimotor cortex was shown to correlate with worse scores on the Expanded Disability Status Scale (EDSS), a composite heavily weighted by walking disability.(Prinster et al., 2010) Furthermore, our group has used VBM to generate disability-specific atlases (DSAs), voxelwise mappings of GM atrophy in the cerebral cortex that are associated with specific disabilities. We showed that GM atrophy in distinct, clinically-eloquent cortical regions correlated with distinct disabilities, such as atrophy in the primary auditory cortex with poorer performance on the paced auditory serial addition test (PASAT).(MacKenzie-Graham et al., 2016) These studies illustrate the need to further understand the mechanisms contributing to regional GM atrophy. Investigating these mechanisms is challenging in humans, but they can readily be addressed through the use of animal models, such as experimental autoimmune encephalomyelitis (EAE).

Clear Lipid-exchanged Acrylamide-hybridized Rigid Imaging-compatible Tissue-hYdrogel (CLARITY) is an optical clearing technology that permits intact imaging of the entire brain and spinal cord.(Chung et al., 2013) This approach is well-suited to visualizing neurons and axons in three dimensions, in both brain and spinal cord, in both normal and pathological conditions,(Chung et al., 2013; Lerner et al., 2015) such as in EAE.(Spence et al., 2014) Thus, CLARITY can be utilized to visualize pathological mechanisms across the neuraxis that may lead to GM atrophy. In fact, different cellular pathologies may be responsible for atrophy in

different brain regions. This may explain the difficulty in uncovering the underlying mechanism of whole GM atrophy – there is not one mechanism, but many.

Here, we will focus on an important candidate mechanism, axonal damage in the spinal cord. In order to visualize the relationship between GM atrophy and axonal damage, a voxelwise regression analysis was conducted and a mapping of GM atrophy in the cerebral cortex that was associated with axonal damage in the spinal cord was created – a pathology-specific atlas (PSA).

3.3 Materials and Methods

Mice

18 female Thy1-YFP^{+} C57BL/6J mice with EAE and 17 female age-matched, healthy controls (Jackson Laboratories, Bar Harbor ME) ranging from 11 to 15 weeks of age were used for this study. All procedures were performed in accordance to the guidelines of the National Institutes of Health and the Chancellor's Animal Research Committee of the University of California, Los Angeles Office for the Protection of Research Subjects.

Experimental Autoimmune Encephalomyelitis

EAE was induced as described.(Spence et al., 2014) Briefly, mice were immunized subcutaneously with MOG peptide 35–55 (300 µg) and Mycobacterium tuberculosis (500 µg) emulsified in complete Freund's adjuvant, in a volume of 0.1 ml over the right draining inguinal and axillary lymph nodes. One week later, a booster immunization was delivered subcutaneously over the contralateral lymph nodes. Pertussis toxin (500 ng; List Biological Laboratories, Campbell, CA) was injected intraperitoneally on days 0 and 2.(Suen et al., 1997) EAE was graded on a scale of 0–5, as described.(Pettinelli and McFarlin, 1981)

Magnetic Resonance Imaging

All animals were scanned *in vivo* 20 days after EAE induction at the Ahmanson-Lovelace Brain Mapping Center at UCLA on a 7T imaging spectrometer (Bruker Instruments, Billerica, MA), as described.(Meyer et al., 2017)

Voxel-based Morphometry

VBM analyses were performed with Statistical Parametric Mapping (SPM) 8 software (Welcome Trust Center for Neuroimaging, London, United Kingdom; http://www.fil.ion.ucl.ac.uk/spm) and SPMMouse (SPMMouse, http://www.spmmouse.org) (Sawiak et al., 2009) within MATLAB version 2013a (Mathworks, Natick, MA). MR images were manually registered to tissue probability maps (TPMs) generated from 60 C57BL/6J mice (Meyer et al., 2017) using 6-parameter linear transformations. The images were bias corrected and segmented into GM, WM, and cerebrospinal fluid (CSF) using the unified segmentation algorithm.(Ashburner and Friston, 2005) The resulting segments were used to create a Diffeomorphic Anatomical Registration using Exponentiated Lie algebra (DARTEL) template (Ashburner, 2007) and the individual GM segments were warped to this template and modulated. Finally, the normalized and modulated GM segments were smoothed with a 600 μm FWHM Gaussian kernel and used as the input for the statistical analysis.

Cross-sectional differences in local GM volume between EAE and control mice were examined with a general linear model. Whole brain volume was included as a covariate to account for the variance associated with brain size and to prevent potential effects due to differences in brain size. Within this model, significant differences in local GM volume between groups were determined via student's t-tests. All findings were corrected for multiple comparisons by controlling the false discovery rate (FDR) (Hochberg and Benjamini, 1990) and all significance maps were thresholded at $q \leq 0.05$. All analyses were performed bi-directionally.

Associations of voxelwise GM volumes with axonal end-bulbs and ovoids using voxelwise regression analyses were assessed within the general linear model. Whole brain size

was included as a variable of no interest. All significant findings were corrected for multiple comparisons by controlling the FDR.

Bias-corrected images were skull-stripped, warped to the DARTEL template, and averaged to create a mean template for visualization.

Atlas-based Morphometry

A minimum deformation atlas (MDA) was created using the MR images from all subjects and anatomical structures were manually labelled on the MDA using BrainSuite 16a (Shattuck and Leahy, 2002) (http://brainsuite.org) as described.(MacKenzie-Graham et al., 2012) The labels were then warped out to the individual images and manually corrected by an investigator blind to each treatment group.

CLARITY

The brains from a subset (9 EAE mice and 10 normal controls) and spinal cords from all of the animals were optically cleared using the CLARITY protocol modified for “passive clearing” as described.(Spence et al., 2014)

Immunohistochemistry

The brains of a subset of animals (5 EAE mice and 5 normal controls) were stained using immunohistochemistry (IHC) as described.(MacKenzie-Graham et al., 2012) Tissues were stained for either NeuroTrace (Invitrogen), myelin basic protein (MBP) (Aves), major histocompatibility complex II (MHC-II) (BioLegend), and/or ionized calcium-binding adapter molecule 1 (Iba1) (Wako).

Microscopy

Laser scanning confocal microscopy was performed at the California NanoSystems Institute (CNSI) Advanced Light Microscopy/Spectroscopy Shared Resource Facility at UCLA as described.(MacKenzie-Graham et al., 2012; Spence et al., 2014)

CLARITY Analysis

Automated cell counting in Imaris (Bitplane, Belfast, United Kingdom) was used to analyze the number of cortical layer V pyramidal neurons in the sensorimotor cortex. Spinal cord images were visualized and processed using FIJI (https://fiji.sc) as described.(Spence et al., 2014)

Statistical Analyses

ABM, CLARITY, and immunohistochemistry data were analyzed in R (https://www.r-project.org). Two-group comparisons were conducted using a student's t-test (two-tailed). Regression analyses are reported as Spearman correlation coefficients. All reported *p* values are corrected for multiple comparisons by controlling for the FDR. 95% confidence intervals for mean values are reported in brackets and were found by resampling (10,000 bootstraps).

3.4 Results

Gray matter atrophy

In vivo MRI scans were collected from 18 female mice with EAE and 17 female, age-matched normal controls 20 days after disease induction (Fig. 3-1). VBM was conducted to identify regions of significant GM volume change in mice with EAE ($p < 0.05$). A statistical parametric map (SPM) indicated substantial GM atrophy in the brains of mice with EAE compared to controls (Fig. 3-2A). Atrophy was observed primarily in the cerebral cortex with smaller clusters in the caudoputamen, cerebellum, and thalamus (Fig. 3-2B).

As a complementary approach, volumes were measured for whole brain, GM, WM, CSF, caudoputamen, cerebral cortex, cerebellum, and thalamus (Table 3-1). Mice with EAE demonstrated a decrease of 7.45% ($p = 0.0016$) in cerebral cortex volume, 3.15% ($p = 0.0052$) in caudoputamen volume, 2.32% ($p = 0.034$) in thalamus volume, and 2.27% ($p = 0.028$) in cerebellum volume compared to normal controls. Thus, this complementary approach corroborated our new findings of localized GM atrophy demonstrated by VBM (Fig. 3-2A & B). Further, EAE mice exhibited a 6.01% decrease in mean whole brain GM volume compared to controls ($p = 0.0020$). An analysis of whole brain WM and the corpus callosum volume revealed no significant difference between EAE mice and normal controls, consistent with our previous findings in the cerebellum. (MacKenzie-Graham et al., 2009)

Axonal damage in the spinal cord

We then addressed whether an important candidate pathology, remote injury in spinal cord, was associated with localized GM atrophy in the cerebral cortex. We evaluated axonal transection (end-bulbs) and axonal injury (ovoids) in the spinal cord. Whole spinal cords were optically cleared, imaged, and analyzed (Fig. 3-2C & D). Mice with EAE exhibited a 5.3-fold increase in axonal end-bulbs compared to control mice ($p = 0.0063$) (Fig. 3-2E). Additionally, EAE mice also exhibited a 5-fold increase in axonal ovoids compared to controls ($p = 1.3 \times 10^{-9}$) (Fig. 3-2F).

We had previously created disability-specific atlases using MRI scans from MS patients in order to highlight the relationship between voxelwise GM atrophy and specific disabilities.(MacKenzie-Graham et al., 2016) This biology-driven approach demonstrated that distinct disabilities were associated with GM atrophy in distinct, clinically-eloquent regions. Here, we created pathology-specific atlases using MRI scans in EAE mice to demonstrate the relationship between voxelwise GM atrophy and axonal damage in the spinal cord.

The spinal cord axonal-transection (end-bulbs) PSA showed a significant relationship with GM atrophy mainly within the primary and secondary motor cortex and much of the primary and supplemental somatosensory cortex (peak p = 0.0036, FDR corrected) (Fig. 3-2 G & H).(Franklin and Paxinos, 2008) The total volume of this PSA was 11.2 mm^3. This result demonstrated that worse axonal transection in spinal cord correlates with worse GM atrophy in the sensorimotor cortex.

The spinal cord axonal-injury (ovoids) PSA exhibited a pattern very similar to the axonal-transection PSA, albeit smaller (6.64 mm^3), yet still significant (peak p = 0.0093, FDR corrected) (Fig. 3-2 I & J). The similarity between the axonal-transection PSA and the axonal-injury PSA was expected, given that there was a strong correlation between axonal end-bulbs and ovoids (R = 0.754, p = 0.0016).

Notably, each pathology-specific atlas (axonal transection, Figure 3-2 G & H, and axonal injury, Figure 3-2 I & J) was distinctly less widespread than overall voxelwise GM atrophy in mice with EAE (Figure 3-2 A & B), together demonstrating that GM atrophy associated with axonal damage in the spinal cord represents a subset of overall GM atrophy in the brain during EAE.

Neuronal loss in sensorimotor cortex

The neuroanatomic correlation between axonal transection in spinal cord and GM atrophy in sensorimotor cortex prompted investigation into cellular pathology in the sensorimotor cortex of mice with EAE. Thy1-YFP^+ mice express yellow fluorescent protein in a subset of their cortical layer V pyramidal neurons (Fig. 3-3A & B).(Feng et al., 2000; Porrero et al., 2010) Mice with EAE demonstrated a 44.7% reduction in cortical layer V pyramidal neurons in the sensorimotor cortex compared to controls (p = 0.00028) (Fig. 3-3C). As a complementary approach, we quantified NeuroTrace-labeled cells (all neurons) in the sensorimotor cortex in

single tissue sections. We observed that mice with EAE showed a 13.7% reduction in cells labeled with NeuroTrace compared to controls ($p = 0.0063$) (Fig. 3-3C).

More loss of Thy1-YFP$^+$ neurons than NeuroTrace-labeled neurons in cerebral cortex is consistent with greater vulnerability of Thy1-YFP$^+$ neurons, since they are the source of Thy1-YFP$^+$ axons in spinal cord.(Porrero et al., 2010) Indeed, there was a strong inverse correlation between the number of cortical layer V pyramidal neurons and the number of end-bulb positive axons ($R = -0.785$, $p = 0.028$), indicating a strong relationship between axonal transection in spinal cord and neuronal loss in sensorimotor cortex.

Demyelination and microglial activation in sensorimotor cortex

We evaluated demyelination within the sensorimotor cortex by immunohistochemistry (Fig. 3-4A & B). Mice with EAE exhibited a 32% reduction in MBP-staining compared to controls ($p = 0.00030$) (Fig. 3-4C).

There was a strong correlation between neuronal loss and myelin loss in the sensorimotor cortex ($R = 0.758$, $p = 0.028$), indicating that neuronal loss and myelin loss are closely related. Nevertheless, there wasn't a statistically significant correlation between end-bulb positive axons in the spinal cord and myelin loss in the sensorimotor cortex.

We assessed differences in activated microglia within the sensorimotor cortex in Iba1/MHC-II double-stained confocal images using morphology (Fig. 3-5A). We observed that mice with EAE exhibited a 3.5-fold increase in activated microglia compared to controls ($p = 0.017$) (Fig. 3-5B).

There was a strong direct correlation between the percentage of activated microglia and end-bulb positive axons ($R = 0.714$, $p = 0.042$), indicating a strong relationship between microglial activation in sensorimotor cortex and axonal transection in spinal cord. We also observed a strong indirect correlation between the percentage of activated microglia and neuronal numbers, both within sensorimotor cortex ($R = -0.733$, $p = 0.042$).

3.5 Discussion

It has been suggested that axonal damage is associated with whole GM atrophy in the brains of MS patients,(Mahad et al., 2015) but localization of each has remained unclear. In this study, we used a biology-driven approach in the MS model, EAE, to reveal that axonal transection in spinal cord correlates strongly with GM atrophy in sensorimotor cortex. While we previously demonstrated that axonal transection in spinal cord correlated with atrophy of the whole cerebral cortex using atlas-based morphometry,(Spence et al., 2014) whether there were specific regions within the cerebral cortex that were associated with axonal transection in spinal cord was unknown. Here, we have developed a novel approach, pathology-specific atlases, mapping the relationship between localized GM atrophy and specific pathology, in effect localizing the impact of a specific pathology on GM in the brain.

These results extend previous studies from our lab demonstrating GM atrophy in discrete anatomical structures and neuronal loss in EAE.(MacKenzie-Graham et al., 2012; MacKenzie-Graham et al., 2009; Spence et al., 2014) In this study, we observed that axonal transection correlated strongly with Thy1-YFP$^+$ neuronal loss in the sensorimotor cortex. Together, our results suggest potential mechanisms underlying GM atrophy in EAE. Cortical layer V neurons in the sensorimotor cortex directly innervate the spinal cord through the corticospinal tract.(Kuang and Kalil, 1990; Steward et al., 2004) The Thy1-YFP$^+$ axons that we analyzed in the spinal cord are projections from the Thy1-YFP$^+$ cortical layer V neurons in sensorimotor cortex.(Porrero et al., 2010) We hypothesize that these long projections make them highly vulnerable to axonal injury and transection induced by inflammatory lesions along the length of the spinal cord, and that axonal injury and transection eventually lead to retrograde degeneration and cell death. Interestingly, in a mouse spinal cord injury model, axonal transection did not lead to Thy1-YFP$^+$ cortical layer V neuron loss in sensorimotor

cortex,(Ghosh et al., 2012) suggesting that processes specific to EAE are responsible for neuronal loss. The remarkable specificity of the axonal-transection PSA suggests that distal axonal damage plays a key role in the development of GM atrophy in the sensorimotor cortex during EAE.

Notably, although the axonal-transection PSA was within the area of overall GM atrophy observed in EAE mice compared to normal controls (Figure 3-2 A & B), there were also large regions of GM atrophy that were not within this PSA (Figure 3-2 G & H). This suggests that while axonal transection in spinal cord correlates with atrophy within sensorimotor cortex, additional pathologies may also contribute to overall GM atrophy in EAE. Interestingly, GM atrophy in sensorimotor cortex after axonal transection in spinal cord injury models is controversial,(Chen et al., 2017) again suggesting that processes specific to autoimmune-mediated disease may be responsible for GM atrophy in EAE.

MS has GM atrophy in cerebral cortex and cortical lesions characterized by focal demyelination. However, the relationship between cortical lesions and atrophy of normal-appearing gray matter (NAGM) in cerebral cortex is unclear. We do not observe cortical lesions in EAE, but we do observe cortical GM atrophy, demonstrating that cortical GM atrophy need not be limited only to areas affected by cortical lesions.(Kutzelnigg et al., 2007; Kutzelnigg and Lassmann, 2014)

Consistent with the development of GM atrophy in NAGM of the cerebral cortex, our VBM analysis in EAE also identified localized atrophy in several deep GM structures including the anterior caudoputamen and the thalamus (Fig. 3-2). Voxelwise analyses have previously shown thalamus, caudate, and putamen atrophy in MS, particularly in the early stages.(Ceccarelli et al., 2008; Datta et al., 2015; Houtchens et al., 2007; Schoonheim et al., 2012; Sepulcre et al., 2006) Here, we are the first to show thalamic atrophy in EAE, suggesting that EAE may be a useful model to further investigate deep GM vulnerability to degeneration early in MS. Notably, although Tambalo et al. (Tambalo et al., 2015) detected atrophy in the

caudoputamen in EAE in rats, they did not observe atrophy in thalamus. This difference may be due to the fact that Tambalo et al. used a relapsing-remitting EAE rat model, while we used a chronic EAE mouse model, although we cannot rule out technical differences.

The sensitive analyses used in this study allow us to detect atrophy and pathology earlier than has previously been observed, providing insight into the mechanisms responsible for early GM loss. It is likely that the processes contributing to GM atrophy will worsen as disease progresses and analyses at later timepoints would reveal greater atrophy in not only the cortical and deep GM structure highlighted in this study, but also in additional structures. For example, although we observed a 2.27% decrease in cerebellar volume, we anticipate greater cerebellar atrophy later in disease, as we have previously shown. (MacKenzie-Graham et al., 2012; MacKenzie-Graham et al., 2009) Longitudinal studies will be useful for investigating the rate of progression of GM atrophy.

While our results are intriguing, our study has some limitations. Our voxelwise regression analyses are indicative of a strong relationship, but they are not necessarily causal. Future investigations of treatments to reverse individual pathologies and then determine the effect on their respective gray matter PSAs will reveal causality.

In summary, the combination of VBM with CLARITY has the potential to be an important tool in illuminating the underlying pathogenesis of GM atrophy in EAE and other neurodegenerative disease models. PSAs map the effects of specific pathologies on localized GM atrophy, acting as *in vivo* biomarkers for those pathologies by visualizing localized GM changes associated with each pathology. This approach can also be used to investigate neuroprotective treatments aimed at reducing axonal damage and neuronal loss early in disease to prevent GM atrophy within neurological pathways.

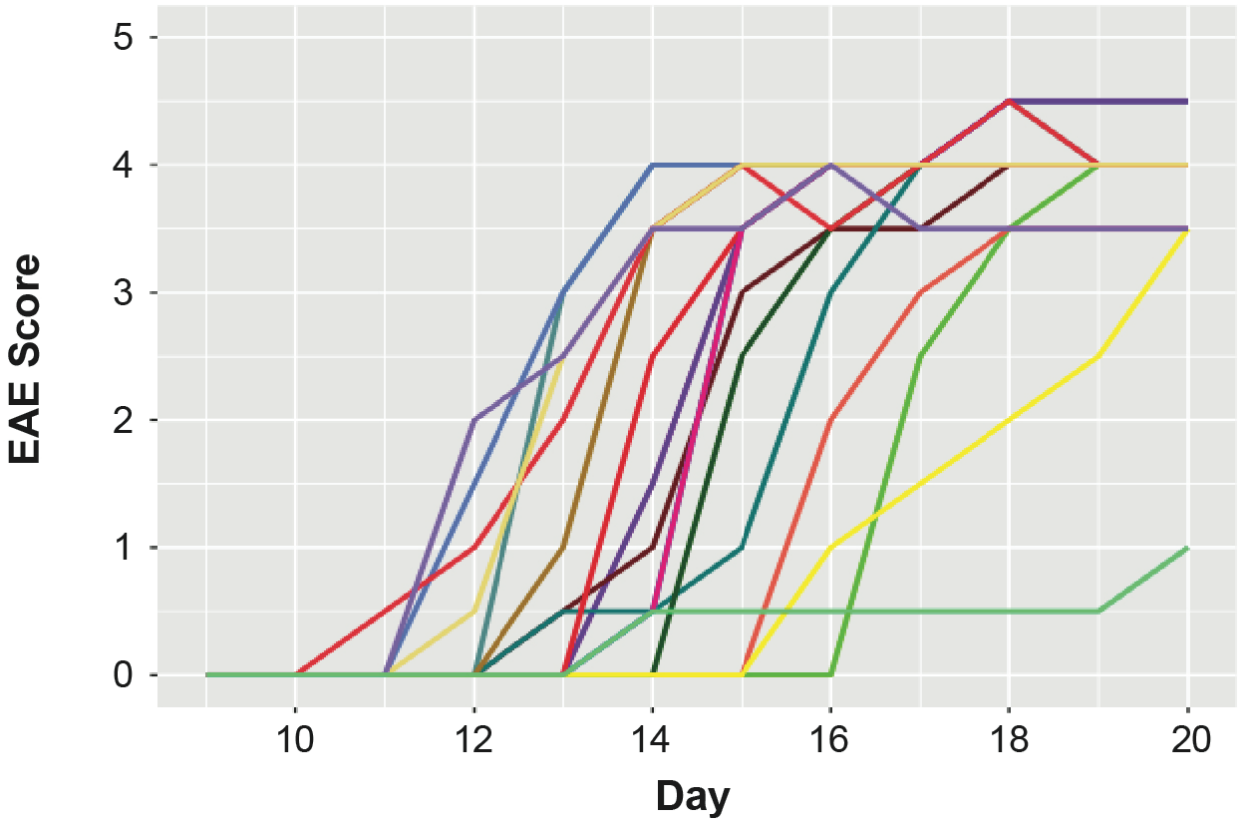

Figure 3-1. EAE clinical scores. Mice with EAE (n = 17) demonstrated typical chronic disease using standard EAE scoring while normal control mice (n = 18) displayed no signs of disease. EAE scores for each individual animal are plotted from day 9-20.

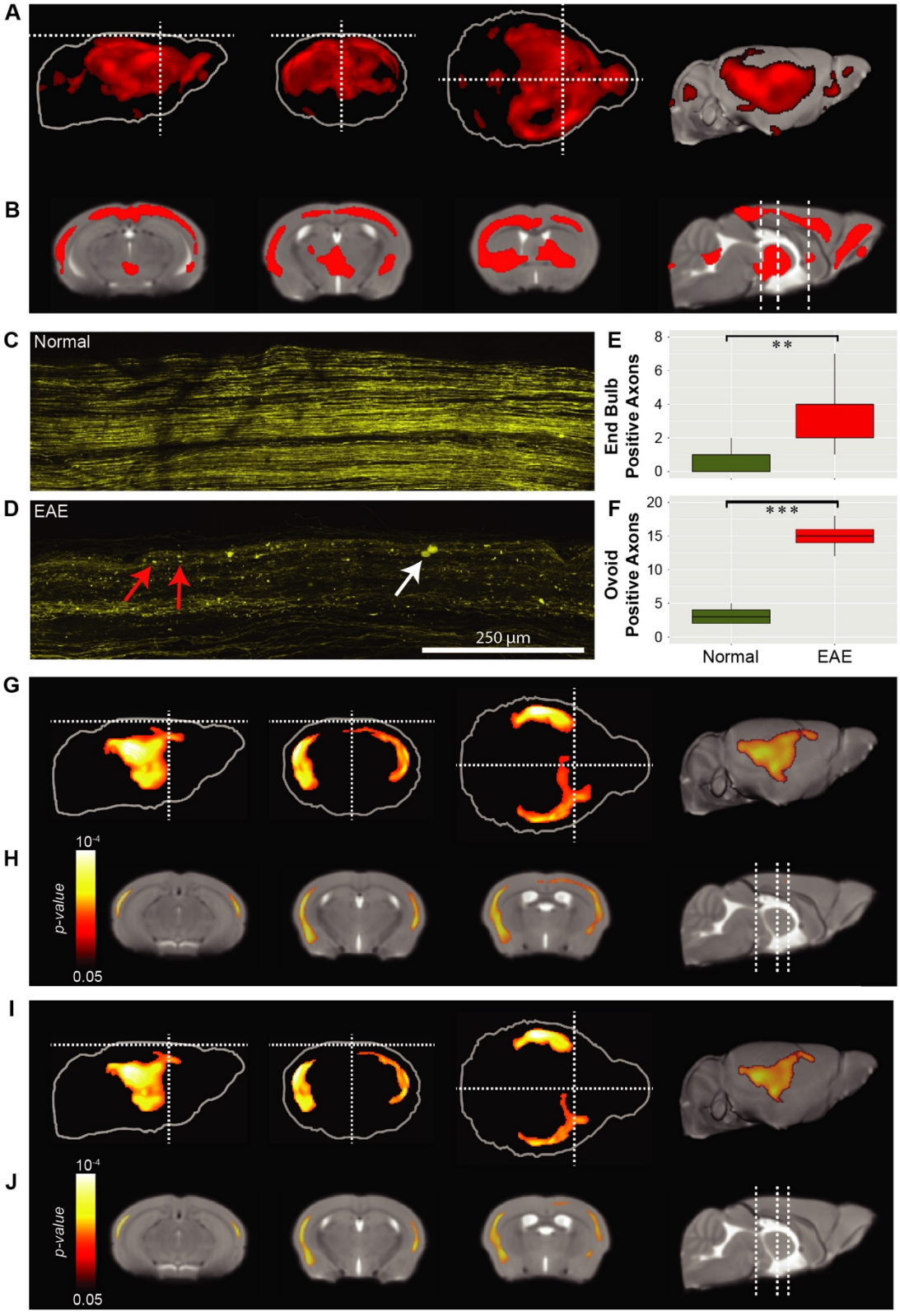

Figure 3- 2. Axonal transection in the spinal cord correlates with GM atrophy in sensorimotor cortex. A) Maximum intensity projections of GM atrophy in mice with EAE when

compared to normal controls ($p < 0.05$, FDR corrected) overlaid on the mean glass brain. The dotted line represents bregma. B) The statistical parametric map indicating GM atrophy in mice with EAE overlaid onto the mean template. The dashed lines represent the location of the representative coronal sections shown from left to right respectively. (n = 18 EAE, 17 normal). C & D) Spinal cords were optically cleared using CLARITY and imaged at 10X magnification. Representative maximum intensity projection images are shown for normal (C) and EAE (D) mice. Scale bar represents 250 μm. E) EAE mice (n = 9) show a significantly larger number of end bulb positive axons than normal mice (n = 9) **($p = 0.0063$). F) EAE mice (n = 9) show a significantly larger number of ovoid positive axons than normal mice (n = 9) ***($p = 1.3 \times 10^{-9}$). G) Maximum intensity projections of the axonal-transection PSA overlaid on the mean glass brain. The colormap indicates regions where axonal transection (end bulbs) in the spinal cord correlated with GM atrophy in the brain ($p < 0.05$, FDR corrected). H) The axonal-transection PSA overlaid on the mean template. (n = 9 EAE, 9 normal). I) Maximum intensity projections of the axonal-injury PSA overlaid on the mean glass brain. The colormap indicates regions where axonal injury (ovoids) in the spinal cord correlated with GM atrophy in the brain ($p < 0.05$, FDR corrected). J) The axonal-injury PSA overlaid on the mean template. (n = 9 EAE, 9 normal).

Region	Mean Volume (mm^3)		Effect Size (mm^3)	*P* value
	Normal	EAE		
Whole brain	435.05 [430.06, 439.89]	425.79 [415.88, 433.74]	n.s.	n.s.
Gray matter	252.96 [248.73, 257.24]	237.77 [231.64, 243.81]	15.20 [7.63, 22.57]	0.00205
White matter	139.87 [137.03, 142.81]	142.67 [139.24, 145.77]	n.s.	n.s.
Cerebrospinal fluid	42.22 [39.79, 44.66]	45.35 [41.91, 48.98]	n.s.	n.s.
Caudoputamen	15.85 [15.68, 16.03]	15.35 [15.14, 15.56]	0.50 [0.22, 0.78]	0.00523
Cerebellum	53.70 [52.99, 54.54]	52.49 [52.02, 52.95]	1.22 [0.34, 2.15]	0.0284
Cerebral cortex	45.39 [44.19, 46.65]	42.01 [40.97, 43.00]	3.38 [1.84, 5.00]	0.00161
Corpus callosum	2.56 [2.47, 2.64]	2.52 [2.48, 2.57]	n.s.	n.s.
Thalamus	13.38 [13.24, 13.52]	13.08 [12.88, 13.26]	0.31 [0.07, 0.55]	0.0342

Table 3-1. Volume comparisons for mice with EAE as compared to normal controls. All reported p-values are FDR-corrected for multiple comparisons. (n = 18 normal, 17 EAE). n.s. indicates not significant.

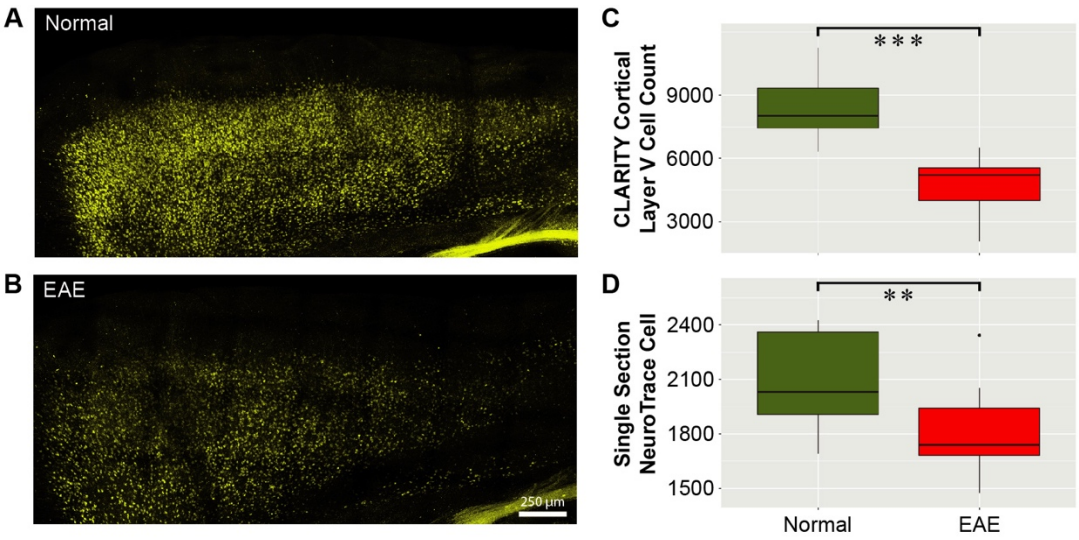

Figure 3-3. Reduced cortical layer V neuronal number in sensorimotor cortex during EAE. Brains were optically cleared using CLARITY and imaged at 10X magnification. Representative maximum intensity projection images are shown for normal (A) and EAE (B) mice. Scale bar represents 250 µm. C) Analysis of YFP CLARITY images demonstrated that normal mice (n = 9) have significantly more cortical layer V pyramidal neurons than EAE mice (n = 9) ***(p = 0.00028). D) Normal mice (n = 5) also had significantly more NeuroTrace-positive neurons in serial tissue sections than EAE mice (n = 5) **(p = 0.0063).

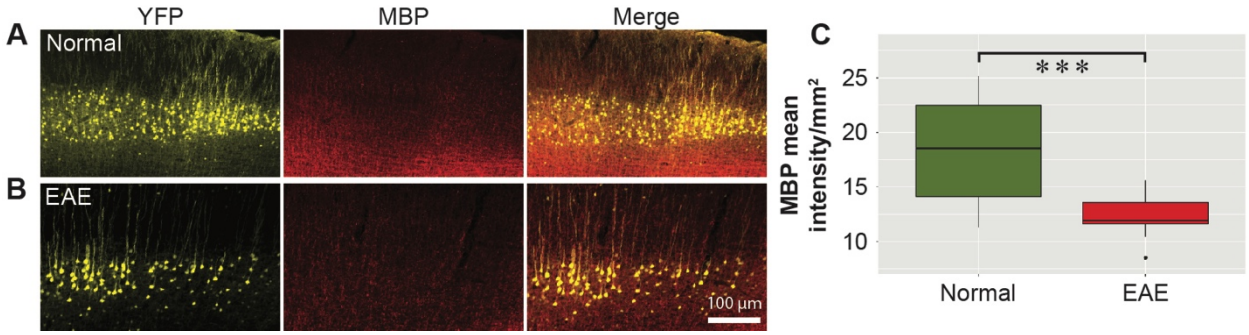

Figure 3-4. Demyelination in sensorimotor cortex during EAE. Cortical layer V pyramidal neurons and myelin in the sensorimotor cortex were imaged at 10X in normal (A) and EAE (B) mice. Scale bar represents 100 µm. C) Normal mice (n = 5) demonstrate significantly greater mean MBP staining intensity than mice with EAE (n = 5) (p = 0.00030).

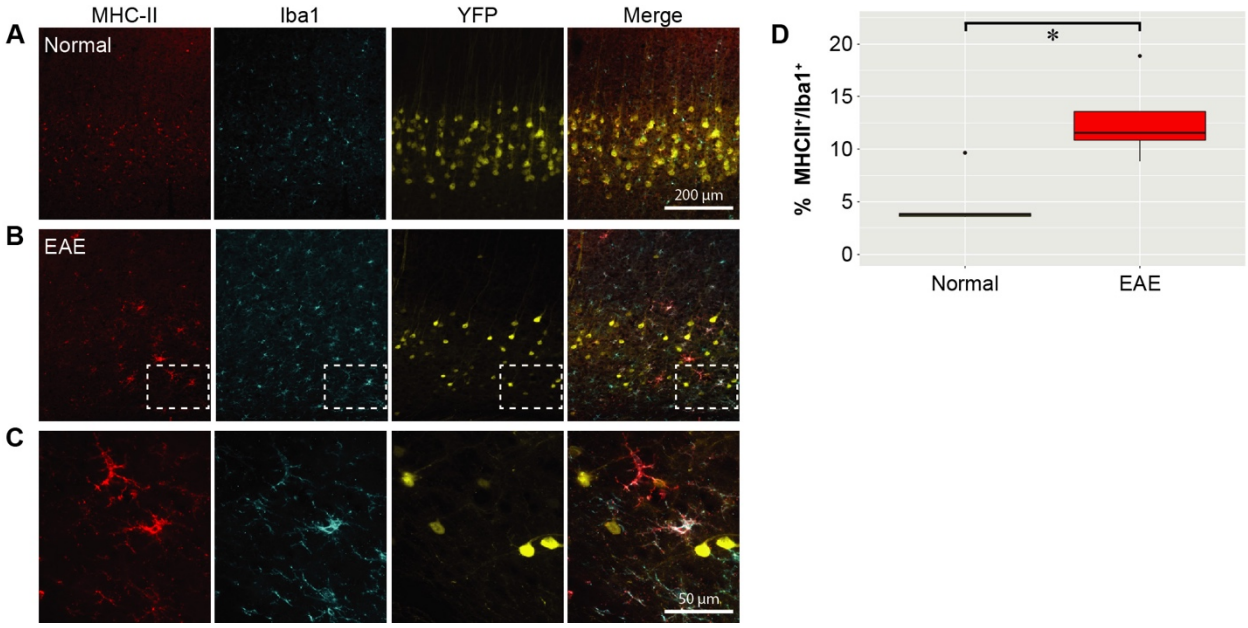

Figure 3-5. Activated microglia in sensorimotor cortex in EAE. Iba1 (red), MHC-II (cyan), and cortical layer V pyramidal neurons (yellow) in the sensorimotor cortex were imaged at 10X in normal (A) and EAE (B) mice. Scale bar represents 200 µm. C) 40X image of the area outlined in the EAE images. Scale bar represents 50 µm. D) Normal mice (n = 5) demonstrate significantly less activated microglia than mice with EAE (n = 5) (p = 0.017).

3.6 References

Ashburner, J., 2007. A fast diffeomorphic image registration algorithm. Neuroimage 38, 95-113.

Ashburner, J., Friston, K.J., 2000. Voxel-based morphometry--the methods. Neuroimage 11, 805-821.

Ashburner, J., Friston, K.J., 2005. Unified segmentation. Neuroimage 26, 839-851.

Ceccarelli, A., Rocca, M.A., Pagani, E., Colombo, B., Martinelli, V., Comi, G., Filippi, M., 2008. A voxel-based morphometry study of grey matter loss in MS patients with different clinical phenotypes. Neuroimage 42, 315-322.

Chen, Q., Zheng, W., Chen, X., Wan, L., Qin, W., Qi, Z., Chen, N., Li, K., 2017. Brain Gray Matter Atrophy after Spinal Cord Injury: A Voxel-Based Morphometry Study. Front Hum Neurosci 11, 211.

Chung, K., Wallace, J., Kim, S.Y., Kalyanasundaram, S., Andalman, A.S., Davidson, T.J., Mirzabekov, J.J., Zalocusky, K.A., Mattis, J., Denisin, A.K., Pak, S., Bernstein, H., Ramakrishnan, C., Grosenick, L., Gradinaru, V., Deisseroth, K., 2013. Structural and molecular interrogation of intact biological systems. Nature 497, 332-337.

Datta, S., Staewen, T.D., Cofield, S.S., Cutter, G.R., Lublin, F.D., Wolinsky, J.S., Narayana, P.A., 2015. Regional gray matter atrophy in relapsing remitting multiple sclerosis: baseline analysis of multi-center data. Mult Scler Relat Disord 4, 124-136.

Dendrou, C.A., Fugger, L., Friese, M.A., 2015. Immunopathology of multiple sclerosis. Nat Rev Immunol 15, 545-558.

Feng, G., Mellor, R.H., Bernstein, M., Keller-Peck, C., Nguyen, Q.T., Wallace, M., Nerbonne, J.M., Lichtman, J.W., Sanes, J.R., 2000. Imaging neuronal subsets in transgenic mice expressing multiple spectral variants of GFP. Neuron 28, 41-51.

Fisniku, L.K., Chard, D.T., Jackson, J.S., Anderson, V.M., Altmann, D.R., Miszkiel, K.A., Thompson, A.J., Miller, D.H., 2008. Gray matter atrophy is related to long-term disability in multiple sclerosis. Ann Neurol 64, 247-254.

Franklin, K.B.J., Paxinos, G., 2008. The Mouse Brain in Stereotaxic Coordinates, 3rd ed. Academic Press, New York.

Ghosh, A., Peduzzi, S., Snyder, M., Schneider, R., Starkey, M., Schwab, M.E., 2012. Heterogeneous spine loss in layer 5 cortical neurons after spinal cord injury. Cerebral Cortex 22, 1309-1317.

Hochberg, Y., Benjamini, Y., 1990. More powerful procedures for multiple significance testing. Stat Med 9, 811-818.

Houtchens, M.K., Benedict, R.H., Killiany, R., Sharma, J., Jaisani, Z., Singh, B., Weinstock-Guttman, B., Guttmann, C.R., Bakshi, R., 2007. Thalamic atrophy and cognition in multiple sclerosis. Neurology 69, 1213-1223.

Kuang, R.Z., Kalil, K., 1990. Specificity of corticospinal axon arbors sprouting into denervated contralateral spinal cord. J Comp Neurol 302, 461-472.

Kuceyeski, A.F., Vargas, W., Dayan, M., Monohan, E., Blackwell, C., Raj, A., Fujimoto, K., Gauthier, S.A., 2015. Modeling the relationship among gray matter atrophy, abnormalities in connecting white matter, and cognitive performance in early multiple sclerosis. Ajnr. American Journal of Neuroradiology 36, 702-709.

Kutzelnigg, A., Faber-Rod, J.C., Bauer, J., Lucchinetti, C.F., Sorensen, P.S., Laursen, H., Stadelmann, C., Bruck, W., Rauschka, H., Schmidbauer, M., Lassmann, H., 2007. Widespread demyelination in the cerebellar cortex in multiple sclerosis. Brain Pathol 17, 38-44.

Kutzelnigg, A., Lassmann, H., 2014. Pathology of multiple sclerosis and related inflammatory demyelinating diseases. Handb Clin Neurol 122, 15-58.

Lerner, T.N., Shilyansky, C., Davidson, T.J., Evans, K.E., Beier, K.T., Zalocusky, K.A., Crow, A.K., Malenka, R.C., Luo, L., Tomer, R., Deisseroth, K., 2015. Intact-Brain Analyses Reveal Distinct Information Carried by SNc Dopamine Subcircuits. Cell 162, 635-647.

MacKenzie-Graham, A., Kurth, F., Itoh, Y., Wang, H.J., Montag, M.J., Elashoff, R., Voskuhl,

R.R., 2016. Disability-Specific Atlases of Gray Matter Loss in Relapsing-Remitting Multiple Sclerosis. JAMA Neurology 73, 944-953.

MacKenzie-Graham, A., Rinek, G.A., Avedisian, A., Gold, S.M., Frew, A.J., Aguilar, C., Lin, D.R., Umeda, E., Voskuhl, R.R., Alger, J.R., 2012. Cortical atrophy in experimental autoimmune encephalomyelitis: in vivo imaging. Neuroimage 60, 95-104.

MacKenzie-Graham, A., Tiwari-Woodruff, S.K., Sharma, G., Aguilar, C., Vo, K.T., Strickland, L.V., Morales, L., Fubara, B., Martin, M., Jacobs, R.E., Johnson, G.A., Toga, A.W., Voskuhl, R.R., 2009. Purkinje cell loss in experimental autoimmune encephalomyelitis. Neuroimage 48, 637-651.

Mahad, D.H., Trapp, B.D., Lassmann, H., 2015. Pathological mechanisms in progressive multiple sclerosis. Lancet Neurol 14, 183-193.

Meyer, C.E., Kurth, F., Lepore, S., Gao, J.L., Johnsonbaugh, H., Oberoi, M.R., Sawiak, S.J., MacKenzie-Graham, A., 2017. In vivo magnetic resonance images reveal neuroanatomical sex differences through the application of voxel-based morphometry in C57BL/6 mice. Neuroimage 163, 197-205.

Pettinelli, C.B., McFarlin, D.E., 1981. Adoptive transfer of experimental allergic encephalomyelitis in SJL/J mice after in vitro activation of lymph node cells by myelin basic protein: requirement for Lyt 1+ 2- T lymphocytes. J Immunol 127, 1420-1423.

Porrero, C., Rubio-Garrido, P., Avendano, C., Clasca, F., 2010. Mapping of fluorescent protein-expressing neurons and axon pathways in adult and developing Thy1-eYFP-H transgenic mice. Brain Res 1345, 59-72.

Prinster, A., Quarantelli, M., Lanzillo, R., Orefice, G., Vacca, G., Carotenuto, B., Alfano, B., Brunetti, A., Morra, V.B., Salvatore, M., 2010. A voxel-based morphometry study of disease severity correlates in relapsing-- remitting multiple sclerosis. Mult Scler 16, 45-54.

Sawiak, S.J., Wood, N.I., Williams, G.B., Morton, A.J., Carpenter, T.A., 2009. Voxel-based

morphometry in the R6/2 transgenic mouse reveals differences between genotypes not seen with manual 2D morphometry. Neurobiol Dis 33, 20-27.

Schoonheim, M.M., Popescu, V., Rueda Lopes, F.C., Wiebenga, O.T., Vrenken, H., Douw, L., Polman, C.H., Geurts, J.J., Barkhof, F., 2012. Subcortical atrophy and cognition: sex effects in multiple sclerosis. Neurology 79, 1754-1761.

Sepulcre, J., Sastre-Garriga, J., Cercignani, M., Ingle, G.T., Miller, D.H., Thompson, A.J., 2006. Regional gray matter atrophy in early primary progressive multiple sclerosis: a voxel-based morphometry study. Arch Neurol 63, 1175-1180.

Shattuck, D.W., Leahy, R.M., 2002. BrainSuite: an automated cortical surface identification tool. Med Image Anal 6, 129-142.

Spence, R.D., Kurth, F., Itoh, N., Mongerson, C.R., Wailes, S.H., Peng, M.S., MacKenzie-Graham, A.J., 2014. Bringing CLARITY to gray matter atrophy. Neuroimage 101, 625-632.

Steward, O., Zheng, B., Ho, C., Anderson, K., Tessier-Lavigne, M., 2004. The dorsolateral corticospinal tract in mice: an alternative route for corticospinal input to caudal segments following dorsal column lesions. J Comp Neurol 472, 463-477.

Suen, W.E., Bergman, C.M., Hjelmstrom, P., Ruddle, N.H., 1997. A critical role for lymphotoxin in experimental allergic encephalomyelitis. J Exp Med 186, 1233-1240.

Tambalo, S., Peruzzotti-Jametti, L., Rigolio, R., Fiorini, S., Bontempi, P., Mallucci, G., Balzarotti, B., Marmiroli, P., Sbarbati, A., Cavaletti, G., Pluchino, S., Marzola, P., 2015. Functional Magnetic Resonance Imaging of Rats with Experimental Autoimmune Encephalomyelitis Reveals Brain Cortex Remodeling. Journal of Neuroscience 35, 10088-10100.

Chapter 4

Neuroprotective mechanisms underlying mitigation of cerebral cortex atrophy by estriol treatment

4.1 Abstract

Gray matter (GM) atrophy, particularly cortical GM atrophy, associates with multiple sclerosis (MS) disability. Immunomodulatory treatments in MS have had modest success at preventing GM atrophy and disability progression. Treatment with estriol, an estrogen produced during pregnancy, mitigates disease in the widely used mouse model for MS, experimental autoimmune encephalomyelitis (EAE). In MS patients, estriol treatment induced cortical GM preservation which correlated with cognitive improvement. We sought to investigate mechanisms underlying estriol-mediated mitigation of cerebral cortex atrophy in EAE. We treated EAE mice with estriol therapeutically after disease onset. *In vivo* magnetic resonance imaging (MRI) and Clear Lipid-exchanged Acrylamide-hybridized Rigid Imaging-compatible Tissue-hYdrogel (CLARITY) were used to examine changes in cortical GM volume and underlying neuropathology. Mice expressing green fluorescent protein (GFP) in newly formed remyelinating oligodendrocytes were used to assess remyelination in cerebral cortex. Estriol treatment decreased cortical GM atrophy by MRI and reduced cerebral cortex demyelination, microglial activation, synapse loss, dendritic spine loss, and cortical layer V neuronal loss. Mechanistically, ligation of estrogen receptor beta induced remyelination, reduced microglial activation, and preserved synapses in the cerebral cortex. Together, this demonstrates that therapeutic estriol treatment is neuroprotective in EAE by preventing cortical GM atrophy and attenuating its underlying pathology.

4.2 Introduction

Gray matter (GM) atrophy is a strong indicator of disability progression in multiple sclerosis (MS) (Fisniku et al., 2008), an autoimmune-mediated neurodegenerative disease of the central nervous system. It is well established that GM atrophy in MS is closely tied to clinical

disability (Fisniku et al., 2008; MacKenzie-Graham et al., 2016). In fact, GM atrophy is better than either white matter atrophy or white matter lesion load at predicting motor disability (Fisniku et al., 2008; Roosendaal et al., 2011). Thus, identifying neurodegenerative mechanisms that lead to GM atrophy is an important step in developing targeted therapies that can prevent irreversible disability.

The most widely used mouse model for MS, experimental autoimmune encephalomyelitis (EAE), is a valuable tool for investigating neurodegenerative mechanisms underlying GM pathology. GM atrophy occurs during chronic EAE in C57BL/6 mice in conjunction with key GM pathologies, namely demyelination, microglial activation, synaptic loss, axonal damage, and neuronal loss (MacKenzie-Graham et al., 2012a; Meyer et al., 2019; Spence et al., 2014). Here, we use cross modality investigation to determine how intervention with a neuroprotective treatment alters GM pathology in the cerebral cortex to prevent cortical GM atrophy as quantified by *in vivo* MRI.

Estriol, a hormone produced by the fetoplacental unit during pregnancy, is a promising neuroprotective treatment demonstrating beneficial disease-modifying effects in MS and EAE. Pregnancy is protective in MS and leads to a reduction in relapses, with the greatest reduction seen in the third trimester when estriol levels are highest (Confavreux et al., 1998). Estriol is an attractive therapeutic option because it preferentially binds to estrogen receptor beta (ERβ) over estrogen receptor alpha (ERα)(2:1) (Kuiper et al., 1997). In contrast, estradiol, which binds preferentially to ERα, is associated with an increase in breast cancer risk and other off-target side effects (Rossouw et al., 2002), which have not been observed during estriol treatment, likely due to its preferential binding to ERβ (Head, 1998; Voskuhl et al., 2016b). Studies in EAE show that estriol treatment ameliorates motor disability and has a beneficial immunomodulatory effect in the peripheral immune system (Kim et al., 1999; Palaszynski et al., 2004). Further, estriol pre-treatment (prior to disease onset) was shown to provide neuroprotection by preventing CA1 atrophy and reducing synaptic loss in the hippocampus of mice with EAE (Ziehn

et al., 2012). In phase 2 clinical trials, estriol treatment in MS reduced gadolinium-enhancing lesions, was immunomodulatory in the peripheral immune system (Sicotte et al., 2002; Soldan et al., 2003), and reduced relapses (Krysko et al., 2020; Voskuhl and Momtazee, 2017; Voskuhl et al., 2016a; Voskuhl et al., 2016b). Regarding neuroprotection, estriol treatment in MS induced GM sparing in the cerebral cortex which was correlated with improvement in cognitive testing performance (Krysko et al., 2020; MacKenzie-Graham et al., 2018; Voskuhl and Momtazee, 2017; Voskuhl et al., 2016b). Mechanisms underlying these neuroprotective effects in cerebral cortex remain unknown.

Here, estriol treatment was given therapeutically after disease onset in EAE. We combined the use of MRI, CLARITY, and immunohistochemistry to determine the neuroprotective mechanism of estriol in the cerebral cortex during EAE. We further pursued a candidate mechanism of GM preservation by investigating whether ligation of ERβ could induce remyelination in the cerebral cortex. For the first time, we demonstrate that therapeutic estriol treatment (after disease onset) can prevent cortical GM atrophy and ERβ ligation can induce cortical remyelination during EAE.

4.3 Materials and Methods

Animals: All mice (8-16 weeks old) used in this study were from the C57BL/6J background, originally ordered from Jackson Labs (Bar Harbor, ME), and bred within our facilities. 20 female Thy1-YFP^{+} C57BL/6J mice were used in the therapeutic estriol treatment study. 21 female wild-type C57BL/6J mice were used in the experiment assessing the effect of ERβ-ligand on cortical pathology. 19 Cspg4-CreERT2/Mapt-mGFP mice were used in the experiment investigating cortical remyelination with ERβ-ligand treatment in EAE. Cspg4-CreERT2/Mapt-mGFP mice were obtained by crossing B6.Cg-Tg(Cspg4-cre/Esr1*)BAkik/J with B6;129P2-Mapt<tm2Arbr>/J

mice (Mei et al., 2016; Voskuhl et al., 2019). 28 female Thy1-YFP^{+} C57BL/6J mice were used in the estriol pre-treatment study (*supplemental*).

All procedures were done in accordance with the guidelines of the National Institutes of Health and the Chancellor's Animal Research Committee of the University of California, Los Angeles Office for the Protection of Research Subjects.

EAE induction and experimental treatment: EAE was induced as described (Meyer et al., 2019). EAE was scored a scale of 0–5, as described (Kim et al., 2018).

In the therapeutic estriol treatment experiment, either a 90-day release pellet of estriol at 5 mg dose or a placebo pellet (Innovative Research of America, Sarasota, FL) was implanted as described(Kim et al., 1999) when the mice first started showing symptoms of EAE. In the pre-treatment experiment (*supplemental*) either an estriol or placebo pellet was similarly implanted one week prior to EAE induction.

For ERβ-ligand treatment, diarylpropionitrile (DPN; Tocris, Minneapolis, MN) was administered as described (Kim et al., 2018; Voskuhl et al., 2019). For Cspg4-CreERT2/Mapt-mGFP transgenic mice, Tamoxifen (Sigma-Aldrich, St. Louis, MO) was administered subcutaneously two weeks prior ERβ-ligand treatment for 5 consecutive days as described (Kim et al., 2018; Voskuhl et al., 2019).

Magnetic resonance imaging: All animals were scanned *in vivo* at the Ahmanson-Lovelace Brain Mapping Center at UCLA on a 7T Bruker imaging spectrometer (Bruker Instruments, Billerica, MA) as described (Meyer et al., 2019).

Atlas-based morphometry (ABM): A minimum deformation atlas (MDA) was created using the MR images from all subjects. The cerebral cortex was manually labeled on the MDA using BrainSuite 18a (Shattuck and Leahy, 2002) (http://brainsuite.org) as described (MacKenzie-Graham et al., 2012a). The labels were warped out to the individual images and manually corrected by an investigator blind to disease and treatment group.

Clear Lipid-exchanged Acrylamide-hybridized Rigid Imaging-compatible Tissue-hYdrogel: The brains and spinal cords from the pre-treatment experiment and the spinal cords from the therapeutic treatment experiment were optically cleared using the CLARITY protocol modified for “passive clearing” as described (Spence et al., 2014).

Immunohistochemistry: Sagittal brain sections from a subset of animals were stained using immunohistochemistry as described (Meyer et al., 2019). Tissues were stained for postsynaptic density protein 95 (PSD95; Millipore, Darmstadt, Germany), myelin basic protein (MBP; Aves, Davis, CA), green fluorescent protein (GFP; Abcam, Cambridge, MA), Glutathione S-transferase pi (GSTπ; Enzo Life Sciences, Farmingdale, NY), major histocompatibility complex II (MHC-II; BioLegend, San Diego, CA), or ionized calcium-binding adapter molecule 1 (Iba1; Wako, Richmond, VA).

Microscopy: Laser scanning confocal microscopy for CLARITY analysis was performed at the California NanoSystems Institute (CNSI) Advanced Light Microscopy/Spectroscopy Shared Resource Facility at UCLA as described (Spence et al., 2014). Immunostained sections were imaged using Olympus BX51 fluorescence microscope with a DP50 digital camera (MacKenzie-Graham et al., 2012a). ImageJ (https://fiji.sc) was used for analysis of images. In all analyses, the investigator was blind to treatment group.

Statistical analyses: ABM, CLARITY, and immunohistochemistry data were analyzed in R (https://www.r-project.org). Two-group comparisons were conducted using a Student’s t-test (two-tailed). Regression analyses are reported as Pearson correlation coefficients. All reported p-values are corrected for multiple comparisons by controlling for the false discovery rate (FDR) (Benjamini and Hochberg, 1995).

4.4 Results

Therapeutic estriol treatment spares cortical GM atrophy during EAE

We used *in vivo* MRI to investigate whether therapeutic estriol treatment (initiated after disease onset) could prevent GM atrophy in the cerebral cortex during chronic EAE. Placebo-treated EAE mice, estriol-treated EAE mice, and placebo-treated healthy control mice were imaged and sacrificed 45 days after disease induction. Therapeutic estriol treatment reduced clinical EAE severity scores (Figure 4-1), as previously observed (Kim et al., 1999). Regarding MRI outcomes, we observed a 9.3% reduction in cerebral cortex volume in placebo-treated EAE mice compared to placebo-treated healthy controls ($p = 0.0024$), consistent with previous findings (Meyer et al., 2019; Spence et al., 2014). Importantly, we discovered that estriol-treated EAE mice exhibited only a 5.9% reduction in GM volume in the cerebral cortex, which was significantly different than placebo-treated EAE mice ($p = 0.0027$) (Figure 4-2,A-B).

To complement our observed results using therapeutic estriol treatment (initiated after disease onset), we performed another experiment where estriol treatment was initiated one week prior to disease induction. Estriol pre-treatment almost completely prevented clinical signs of disease (Figure 4-7A) and led to complete GM preservation in the cerebral cortex (Figure 4-7B).

Estriol-mediated neuroprotective effects

Next, we investigated whether estriol-mediated preservation of cortical GM volume by MRI was associated with neuroprotection at the cellular level. In the same mice used for *in vivo* MRI analysis, we quantified cortical layer V pyramidal neurons. The mice used were Thy1-YFP^{+} and expressed yellow fluorescent protein in cortical layer V pyramidal neurons and projections(Porrero et al., 2010). Mice with EAE demonstrated a 16.1% decrease in cortical layer V neurons compared to healthy mice ($p = 0.0098$). Interestingly, cortical layer V neurons were preserved in estriol-treated EAE mice compared to placebo-treated EAE mice ($p = 0.0031$) and indeed were not significantly different than healthy controls (Figure 4-2,C-D). We next examined synaptic integrity in cerebral cortex since synapse loss is known to occur in

MS(Werneburg et al., 2020) and EAE (Hammond et al., 2020; Ziehn et al., 2012). Dendritic spine density on the apical dendrites of cortical layer V pyramidal neurons showed a reduction in EAE mice versus healthy controls ($p = 0.0027$). Conversely, estriol-treated EAE mice demonstrated sparing of spine density compared to placebo-treated EAE mice ($p = 0.034$) (Figure 4-2,E-F) and were not significantly different from healthy controls. In a complementary approach, we examined PSD95 staining, a marker for postsynaptic density, in the cerebral cortex and observed that estriol-treated EAE mice exhibited more PSD95 synaptic staining compared to placebo-treated EAE mice ($p = 0.0058$) (Figure 4-2G) and were not significantly different than healthy controls.

We previously identified an intimate relationship between axonal damage in the spinal cord and GM volume loss in the cerebral cortex during EAE (Meyer et al., 2019) and others have suggested that axonal damage plays a key role in neurodegeneration and GM volume loss (Nikic et al., 2011; Trapp et al., 1998). Thus, we performed CLARITY on spinal cords and quantified axonal damage (ovoids) and axonal transection (end bulbs) along YFP^+ axons. An increase in axonal damage and axonal transection were observed in placebo-treated EAE mice compared to healthy controls ($p = 0.0058$ and $p = 0.00073$, respectively). Remarkably, we found that estriol treatment led to reduced axonal damage and less axonal transection when compared to placebo-treated EAE mice ($p = 0.018$ and $p = 0.0024$, respectively) (Figure 4-2,H-J). When estriol treatment was given prior to EAE induction, there was complete protection against cortical GM atrophy and pathology including neuronal loss and synapse loss. (Figure 4-7,C-G).

Estriol treatment reduces pathology in cerebral cortex during EAE

We then investigated how estriol treatment altered non-neuronal pathology in the cerebral cortex during EAE. Microglial activation was increased in mice with EAE compared to healthy controls ($p = 0.00021$). Estriol treatment in EAE reduced microglial activation in cerebral

cortex compared to placebo-treated EAE mice ($p = 0.0058$) (Figure 4-3,A-B). In contrast, we did not observe a significant difference in astrocyte activation between any of the three groups in the cerebral cortex (*data not shown*).

We quantified myelin integrity and observed a 26.4% reduction in myelin in placebo-treated EAE mice compared to healthy controls ($p = 0.0011$). Estriol treatment in EAE preserved myelin in the cerebral cortex compared to placebo-treated EAE ($p = 0.0015$) (Figure 4-3,C-D).

Estriol pre-treatment during EAE led to complete prevention of microglial activation and preservation of myelin in the cerebral cortex (Figure 4-7,H-I). Together, these data show that therapeutic estriol treatment ameliorates the pathologies within the cerebral cortex previously correlated with GM atrophy in EAE (Meyer et al., 2019) and documented to occur in MS(Trapp et al., 1998; Werneburg et al., 2020), including synaptic and neuronal loss, microglial activation, and demyelination.

Estriol treatment abrogates the relationship between cerebral cortex volume loss and neuropathology

To understand how estriol treatment affects the relationship between cortical GM atrophy by MRI and cerebral cortex neuropathology, we examined correlations in Thy1-YFP$^+$ mice that had undergone *in vivo* MRI. We observed strong relationships between cortical volume loss by MRI and cortical pathologies by immunohistochemistry (Table 4-1, Figure 4-4 left). Less cortical GM volume was correlated with less cortical layer V neurons ($r = 0.87$, $p = 0.0018$) and less cortical MBP intensity ($r = 0.72$, $p = 0.017$), and more microglial activation ($r = -0.73$, $p = 0.017$) in the cerebral cortex. Less MBP intensity in the cerebral cortex was correlated with less cortical layer V neurons ($r = 0.68$, $p = 0.024$) and with activated microglia in the cerebral cortex ($r = -0.84$, $p = 0.0018$). Most importantly, therapeutic treatment with estriol disrupted this neuropathologic network, (Table 4-1, Figure 4-4 right).

ERβ-ligand treatment is neuroprotective in cerebral cortex

Together, the above results show for the first time that cerebral cortex atrophy by MRI is associated with a network of pathologies that include demyelination and microglia activation. Since estriol treatment disrupted this network and binds principally to ERβ (Kuiper et al., 1997; Rossouw et al., 2002), we next pursued ERβ ligation as a mechanism for preventing demyelination and reducing microglial activation in the cerebral cortex. We treated EAE mice with either ERβ-ligand or placebo (Figure 4-5A). We observed that ERβ-ligand treatment reduced disease severity (Figure 4-5B), consistent with previous findings (Itoh et al., 2016; Kim et al., 2018; MacKenzie-Graham et al., 2012b; Voskuhl et al., 2019). Interestingly, we found that ERβ-ligand treatment prevented demyelination in the cerebral cortex during EAE ($p = 0.00037$) (Figure 4-5C). ERβ-ligand treatment also decreased microglial activation ($p = 0.034$) (Figure 4-5D) and preserved synapses in cerebral cortex ($p = 0.0082$) (Figure 4-5E).

ERβ-ligand treatment induces remyelination in cerebral cortex

Lastly, we distinguished between the possibility of treatment-mediated reduction in demyelination versus treatment-mediated induction in remyelination in the cerebral cortex of EAE mice. The Cspg4-CreERT2/Mapt-mGFP mouse line provides an ideal model to address this question as these mice express green fluorescent protein (GFP) in newly formed remyelinating oligodendrocytes (Mei et al., 2016). We induced EAE in Cspg4-CreERT2/Mapt-mGFP mice and initiated either placebo or ERβ-ligand treatment (Figure 4-6A). The cerebral cortices of ERβ-ligand treated EAE mice demonstrated both increased myelin ($p = 0.029$) (Figure 4-6B) and increased GFP % area ($p = 0.0015$) (Figure 4-6,C-D) compared to placebo-treated EAE mice. Thus, ERβ-ligand treatment facilitates the maturation of oligodendrocyte progenitor cells and induces cortical remyelination during EAE.

4.5 Discussion

GM atrophy as measured by MRI is associated with disability progression in MS, yet there is currently no directly neuroprotective treatment designed to prevent it. Recent evidence suggests that estriol treatment can prevent cortical GM atrophy in patients with MS (Krysko et al., 2020; MacKenzie-Graham et al., 2018; Voskuhl and Momtazee, 2017; Voskuhl et al., 2016b), but the neuroprotective mechanism remains unclear. In this study, we utilized EAE to explore an important candidate mechanism of neuroprotection, namely remyelination in cortical GM. We show direct evidence that therapeutic estriol treatment can mitigate cerebral cortex GM atrophy during EAE. Our results demonstrate that estriol-mediated cortical GM sparing occurs alongside preservation of synapses and cortical layer V neurons in the cerebral cortex and preservation of their axonal integrity in the spinal cord. We further show that estriol can work through ERβ to induce remyelination in cortical GM. This warrants further investigation of estriol and ERβ-ligand treatment to prevent cortical GM atrophy in MS.

Cortical pathology has been described in both MS (Klaver et al., 2015) and EAE (MacKenzie-Graham et al., 2012a; Meyer et al., 2019; Spence et al., 2014). Here, we observe strong associations among cortical pathologies as measured by immunohistochemistry or CLARITY and cortical GM atrophy as measured by *in vivo* MRI. In particular, we observed a strong correlation between cortical volume loss and layer V pyramidal neuronal loss in the cortex and between cortical volume loss and axonal transection in the spinal cord in EAE, consistent with previous observations in MS (Meyer et al., 2019; Trapp et al., 1998). Interestingly, we further observed correlations across the neuraxis between cortical pathology and axonal damage in the spinal cord. This demonstrates a complex and interrelated network of pathology that contributes to cortical GM atrophy. Estriol treatment disrupted this network and reduced cortical GM atrophy and its underlying neuropathology. Our lab previously demonstrated that estrogen treatment before disease induction preserved GM volume in the

cerebellum during EAE using *ex vivo* MRI (MacKenzie-Graham et al., 2012b). This study demonstrates that estriol treatment can preserve cerebral cortex GM volume on *in vivo* MRI and decrease pathology in the cerebral cortex, even when treatment is initiated after disease onset.

We also investigated ERβ as a mechanism through which estriol could prevent cortical GM atrophy. We found that ERβ-ligand treatment promotes neuroprotection in the cerebral cortex by preserving synapses, consistent with previous literature(Itoh et al., 2016). Oligodendrocytes and microglia have been identified as the cellular targets for ERβ-ligand treatment mediated neuroprotection in white matter during EAE (Kim et al., 2018; Voskuhl et al., 2019), whereas ERβ-ligand treatment did not act directly on astrocytes or neurons (Spence et al., 2013). Remyelination occurs naturally in the CNS after injury to some degree in adults, however in MS and EAE it is thought that the inflammatory microenvironment impedes that process (Mei et al., 2016). A recent study found that ERβ-ligand treatment upregulates cholesterol synthesis genes in oligodendrocyte progenitor cells (OPCs) during remyelination (Voskuhl et al., 2019). Combined with findings herein, we hypothesize that estriol acts on ERβ on OPCs to upregulate cholesterol synthesis genes to enhance remyelination in both white and gray matter. Increased remyelination in the cortex provides trophic support to axons, thereby preserving axons, neurons, and synapses, the pathologies underlying cortical GM atrophy.

In addition, we showed that estriol treatment in EAE suppresses microglial activation. Increased microglial activation has been observed in the hippocampus(Ziehn et al., 2012) and cerebral cortex (Meyer et al., 2019) during EAE. Activated microglia produce nitric oxide and reactive oxygen species which induce axonal damage and oligodendrocyte apoptosis (Howell et al., 2010; Nikic et al., 2011). In the cerebral cortex, activated microglia have also been found to be involved in complement-related synaptic loss in MS and EAE (Hammond et al., 2020; Werneburg et al., 2020). We found that both estriol and ERβ-ligand treatment reduced microglia/macrophage activation in the cerebral cortex. Previously, ERβ-ligand treatment was shown to act directly on $CD11c^+$ microglia/macrophages to promote neuroprotection in white

matter of spinal cord in EAE(Kim et al., 2018). Together, these observations suggest that estriol can also act through ERβ to reduce microglial activation in the cerebral cortex. Less microglial activation mitigates neuronal damage and synaptic loss, while providing an environment more conducive to the maturation of OPCs. We posit that estriol's ability to facilitate remyelination and reduce microglial activation initiates a neuroprotective cascade that results in reduced cortical neurodegeneration by pathology and reduced GM atrophy by MRI.

We focused on investigation of cortical remyelination through ERβ as a possible mechanism of estriol-mediated prevention of cerebral cortex atrophy during EAE. However, it is possible that estriol treatment initiates additional neuroprotective mechanisms.

In conclusion, we are the first to show that therapeutic estriol treatment mitigates neuropathology associated with cortical GM atrophy during EAE. We demonstrated that ligation of ERβ can induce remyelination, reduce microglial activation, and preserve synapses in cortical GM, which are important therapeutic goals in MS.

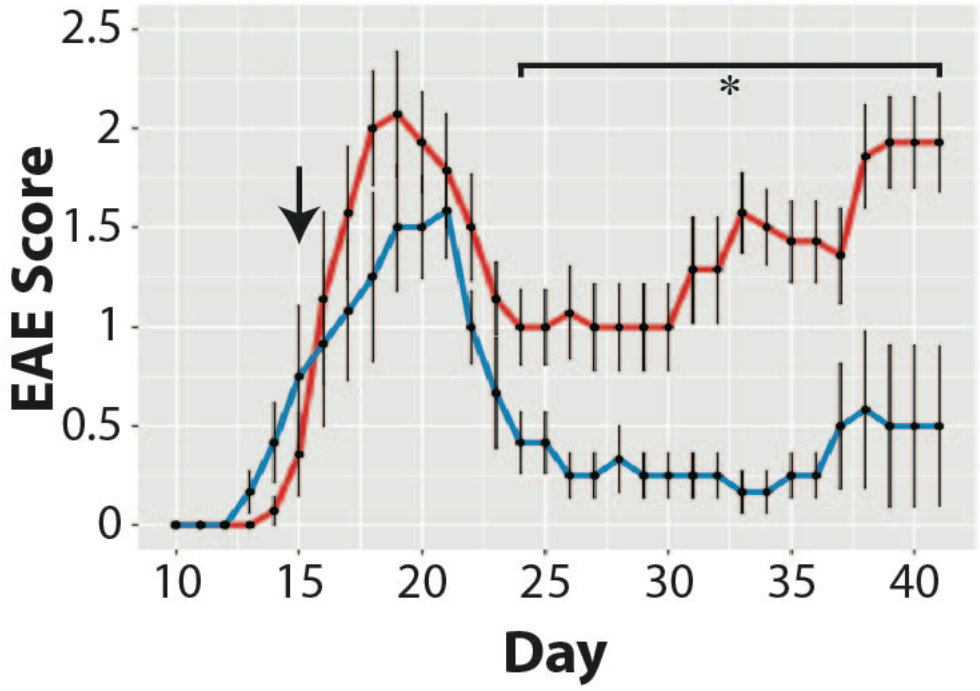

Figure 4-1: Therapeutic estriol treatment reduces EAE scores. Estriol (n = 7; blue) or placebo pellets (n = 6; red) were implanted in each animal at first sign of disease. The average day of onset was 15 days after disease induction (arrow). Estriol-treated mice demonstrated significantly reduced EAE severity compared to placebo-treated mice after 23 days after disease induction. The ameliorative effect continued through 45 days after disease induction when the animals were sacrificed. The asterisk indicates a significant difference ($p < 0.05$, FDR corrected) in EAE score between placebo-treated and estriol-treated EAE.

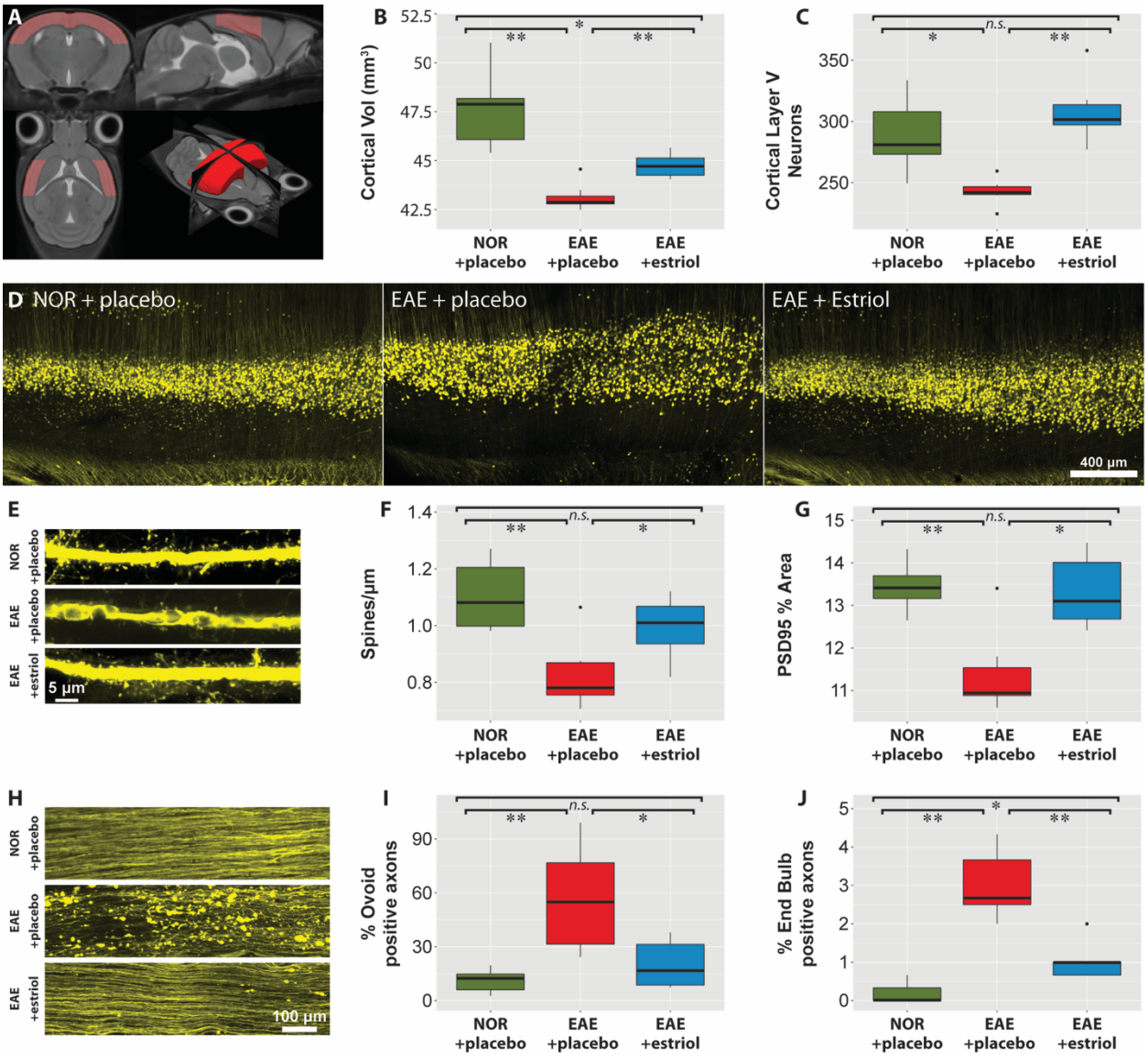

Figure 4-2: Estriol treatment reduces cortical gray matter atrophy and mitigates underlying neurodegeneration in cerebral cortex during EAE. *In vivo* MRI was collected at d45 from Thy1-YFP^{+} mice with EAE treated with placebo (EAE + placebo, n = 6), with EAE and treated with estriol (EAE + estriol, n = 7) healthy controls treated with placebo (NOR + placebo, n = 7) for pathological analysis. A) A minimum deformation atlas (MDA) was constructed from all the images in the dataset and a cerebral cortex was delineated on the MDA and warped out to the constituent images. B) Significant atrophy was observed in placebo-treated EAE mice when compared to placebo-treated healthy control mice. Estriol-treated EAE mice showed reduced

atrophy when compared to placebo-treated EAE mice. C) Placebo-treated EAE mice demonstrated loss of YFP^+ cortical layer V pyramidal neurons in cerebral cortex compared to healthy controls. This loss was prevented by estriol treatment. D) Representative 10X images of YFP^+ neurons in cerebral cortex are shown for each treatment group. E) Representative 63X images of YFP^+ dendritic spines on the apical dendrites of cortical layer V neurons in the cerebral cortex for each treatment group. F) Reduced dendritic spine density was observed during EAE and was prevented with estriol treatment. G) Estriol treatment protected against loss of synapses in mice with EAE indicated by preservation of PSD95 % area compared to placebo-treated mice with EAE. H) Representative 10X images of axonal damage (ovoids, red arrows) and axonal transection (end bulbs, white arrows) in the spinal cord are shown for each treatment group. Quantification of % of axons with ovoids (I) and % of axons with end bulbs (J) reveals preservation of axonal integrity with estriol treatment during EAE. $*p < 0.05$, $**p < 0.01$, $***p < 0.001$; *t* test, FDR corrected.

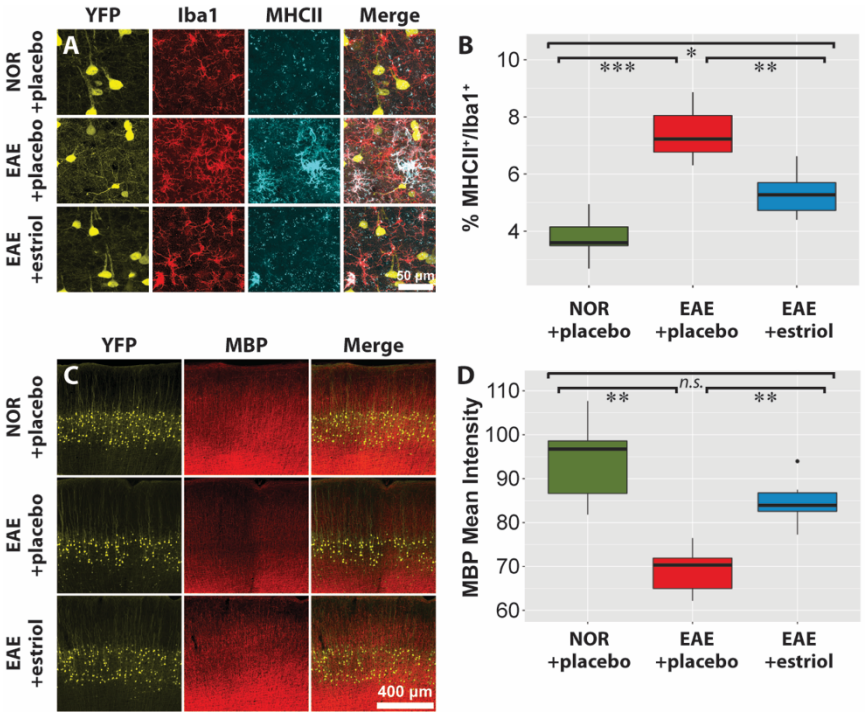

Figure 4-3: Estriol treatment reduces microglial activation and preserves myelin in cerebral cortex during EAE. Thy1-YFP^{+} mice with EAE treated with placebo (EAE + placebo, n = 6), with EAE and treated with estriol (EAE + estriol, n = 7), and healthy controls treated with placebo (NOR + placebo, n = 7) were sacrificed 45 days after disease induction for pathological analysis. A) Representative 40X images of microglial activation in the cerebral cortex for each treatment group. B) Increased microglial activation in the cerebral cortex was observed during EAE as compared to healthy controls. This was reduced with estriol treatment. C) Representative images of MBP staining in the cerebral cortex are shown for each treatment group. D) Quantification of MBP mean intensity demonstrates preservation of myelin in the cerebral cortex in estriol-treated EAE mice compared to placebo-treated EAE mice. *$p < 0.05$, **$p < 0.01$, ***$p < 0.001$; *t* test, FDR corrected.

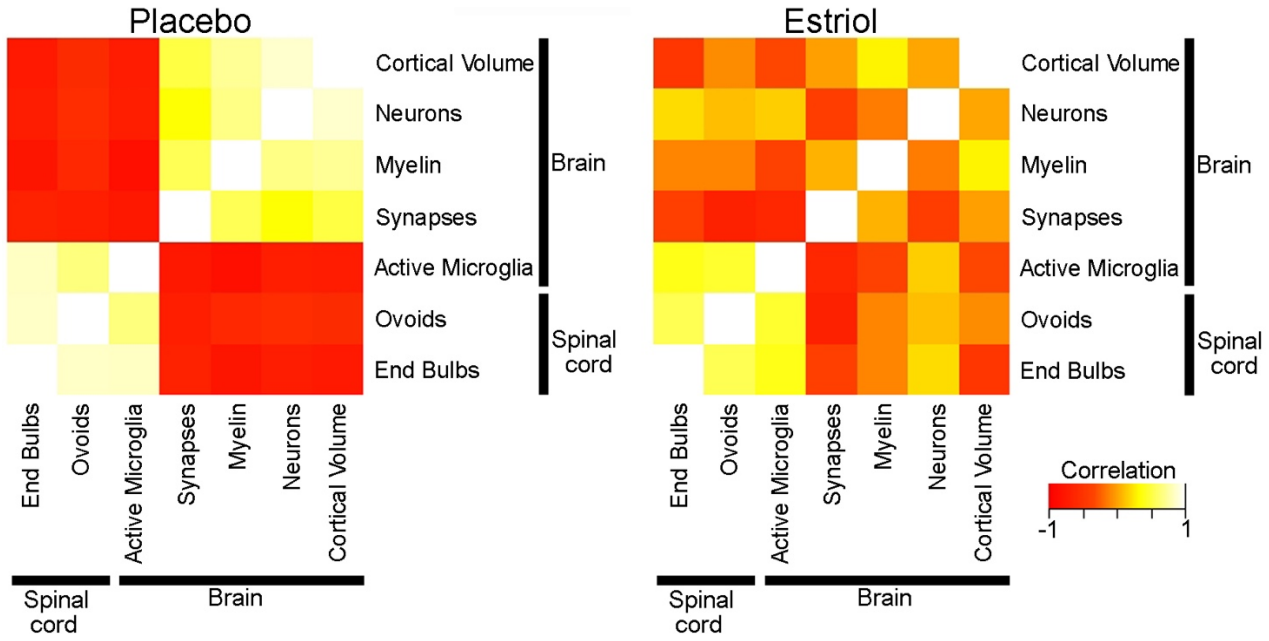

Figure 4-4: Estriol treatment abrogates associations between cortical GM atrophy and underlying neuropathology during EAE. A heat map demonstrates Pearson correlations in placebo-treated EAE mice and placebo-treated healthy controls (left) compared to estriol-treated EAE mice and placebo-treated healthy controls (right). Positive (yellow) and negative (red) correlations are clustered in the placebo group and healthy group, but this clustering was not observed in the estriol and healthy group. Strong pathological relationships are observed in the placebo group and healthy group comparison. These relationships are much weaker in the estriol group and healthy group comparison.

Pearson Correlation	Placebo		Estriol	
	r value	p value	r value	p value
Cortical Volume vs YFP^+ Neuronal Count	0.8681	0.001802	0.01976	0.9971
Cortical Volume vs Ovoids (Spinal Cord)	-0.5781	0.07084	-0.08103	0.9245
Cortical Volume vs End Bulbs (Spinal Cord)	-0.7554	0.01069	-0.4740	0.1858
Cortical Volume vs Synaptic Density	0.5080	0.1216	-0.008183	0.9971
Cortical Volume vs MBP Intensity	0.7217	0.01664	0.2970	0.4867
Cortical Volume vs Microglial Activation	-0.7250	0.01664	-0.3025	0.6905
YFP^+ Neuronal Count vs Ovoids (Spinal Cord)	-0.5547	0.08296	0.09954	0.8977
YFP^+ Neuronal Count vs End Bulbs (Spinal Cord)	-0.7953	0.01676	0.2099	0.6878
YFP^+ Neuronal Count vs Synaptic Density	0.3419	0.3601	-0.4036	0.2880
YFP^+ Neuronal Count vs MBP Intensity	0.6791	0.02401	-0.1326	0.8739
YFP^+ Neuronal Count vs Microglial Activation	-0.6965	0.01977	-0.3758	0.5881
Ovoids (Spinal Cord) vs End Bulbs (Spinal Cord)	0.8504	0.001802	0.5472	0.1058
Ovoids (Spinal Cord) vs Synaptic Density	-0.7027	0.01933	-0.6792	0.02803
Ovoids (Spinal Cord) vs MBP Intensity	-0.6116	0.04967	-0.09882	0.8977
Ovoids (Spinal Cord) vs Microglial Activation	0.6605	0.02804	-0.1095	0.9254
End Bulbs (Spinal Cord) vs Synaptic Density	-0.6756	0.02401	-0.3810	0.3142
End Bulbs (Spinal Cord) vs MBP Intensity	-0.7965	0.005475	-0.1007	0.8977
End Bulbs (Spinal Cord) vs Microglial Activation	0.8460	0.001802	-0.01162	0.9971
Synaptic Density vs MBP Intensity	0.5552	0.08296	0.05788	0.9406
Synaptic Density vs Microglial Activation	-0.7669	0.009602	0.0017	0.9971
MBP Intensity vs Microglial Activation	-0.8397	0.001802	-0.6603	0.1863

Table 4-1: Pearson correlation coefficients and FDR corrected p values for relationships between different pathological measures. Correlation coefficients were calculated in two separate analyses: placebo-treated EAE mice (Placebo; n = 6) combined with placebo-treated healthy controls (NL; n = 7) and estriol-treated EAE mice (Estriol; n = 7) combined with placebo-treated healthy controls (NL; n = 7). Cortical volume = volume of the cerebral cortex, YFP^+ neuronal count = Cortical layer V neurons expressing YFP, Ovoids = axonal damage in spinal

cord, End bulbs = axonal transection in spinal cord, Synaptic density = dendritic spine density on apical dendrites of cortical layer V pyramidal neurons, MBP intensity = myelination, Microglial activation = MHCII and Iba1 colocalized area as a percentage of total Iba1 area. All pathology was measured in the cerebral cortex except ovoids and end bulbs which were measured in the spinal cord (labeled).

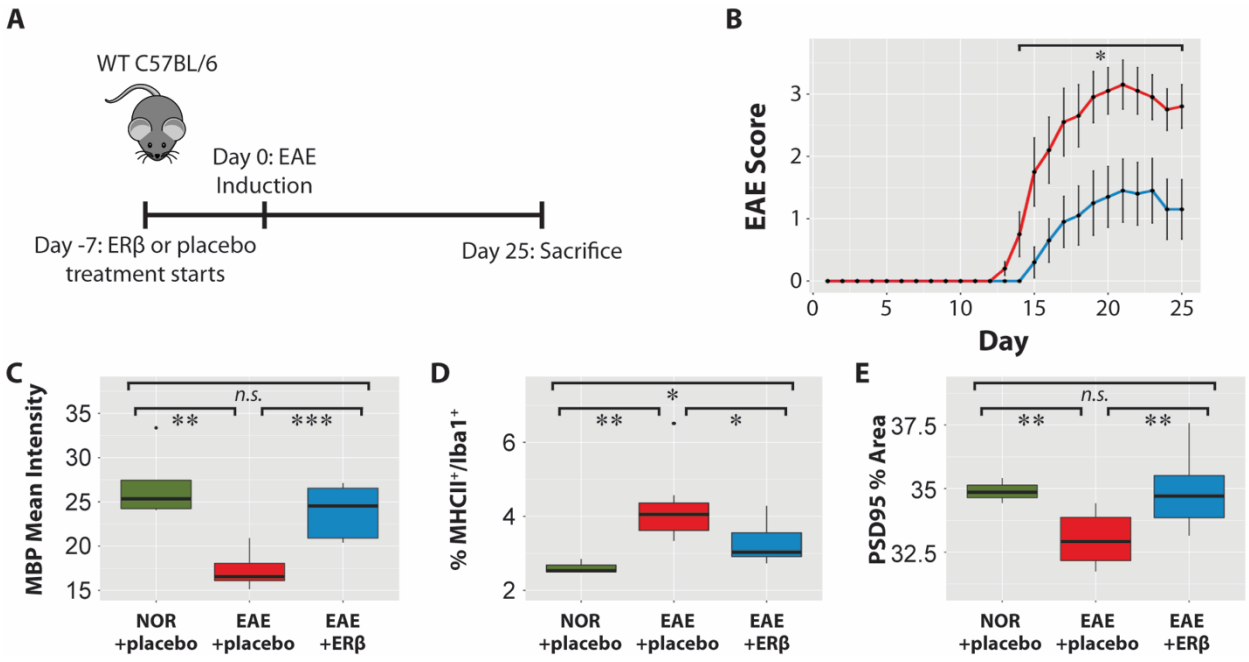

Figure 4-5: ERβ-ligand treatment is neuroprotective in the cerebral cortex during EAE. A) Experiment schematic. Wild-type C57BL/6 mice were treated either with ERβ-ligand (EAE + ERβ, n = 9) or placebo injections (EAE + placebo, n = 9) one week prior to EAE induction. Animals were sacrificed alongside placebo-treated healthy controls (NOR + placebo, n = 10) at 25 days after disease induction. B) ERβ-ligand treated EAE mice (blue) demonstrated a less severe disease course compared to placebo-treated EAE mice (red). Asterisks indicate a significant difference ($p < 0.05$) in EAE score between placebo-treated and ERβ-treated EAE mice. C) ERβ-ligand treatment preserves MBP intensity in cerebral cortex compared to placebo-treated EAE mice. D) ERβ-ligand treatment reduces microglial activation in cerebral cortex compared to placebo-treated EAE mice. E) ERβ-ligand treatment preserves PSD95-stained synapses compared to placebo-treated EAE mice. *$p < 0.05$, **$p < 0.01$, ***$p < 0.001$; *t* test, FDR corrected.

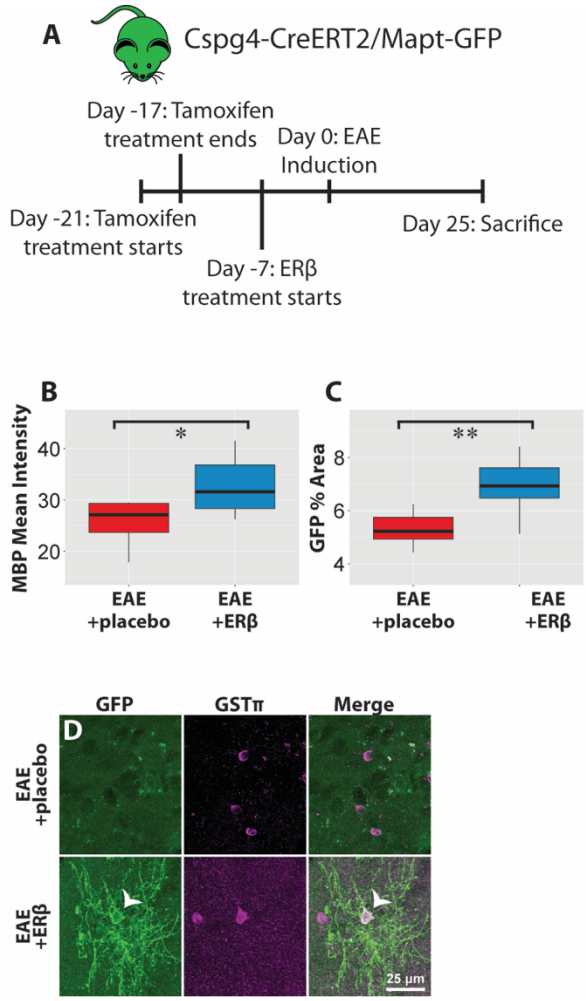

Figure 4-6: ERβ-ligand treatment promotes remyelination in the cerebral cortex during EAE. A) Experiment schematic. Tamoxifen was given to Cspg4-CreERT2/Mapt-mGFP mice for 5 consecutive days, 2 weeks prior to ERβ-ligand treatment. Mice were treated either with ERβ-ligand (EAE + ERβ, n = 10) or placebo injections (EAE + placebo, n = 9) one week prior to EAE induction. Animals were sacrificed at 25 days after disease induction. B) ERβ-ligand treatment preserves MBP intensity in cerebral cortex compared to placebo-treated EAE mice. C) ERβ-ligand treatment increases GFP expression in cerebral cortex compared to placebo-treated EAE mice. D) Representative 40X images of GFP expression in the cerebral cortex are shown for each treatment group. The arrowhead identifies a mature, remyelinating oligodendrocyte

expressing GFP, colocalized with GSTΠ, a marker for mature oligodendrocytes, in an ERβ-ligand treated mouse. *p < 0.05, **p < 0.01, ***p < 0.001; *t* test, FDR corrected

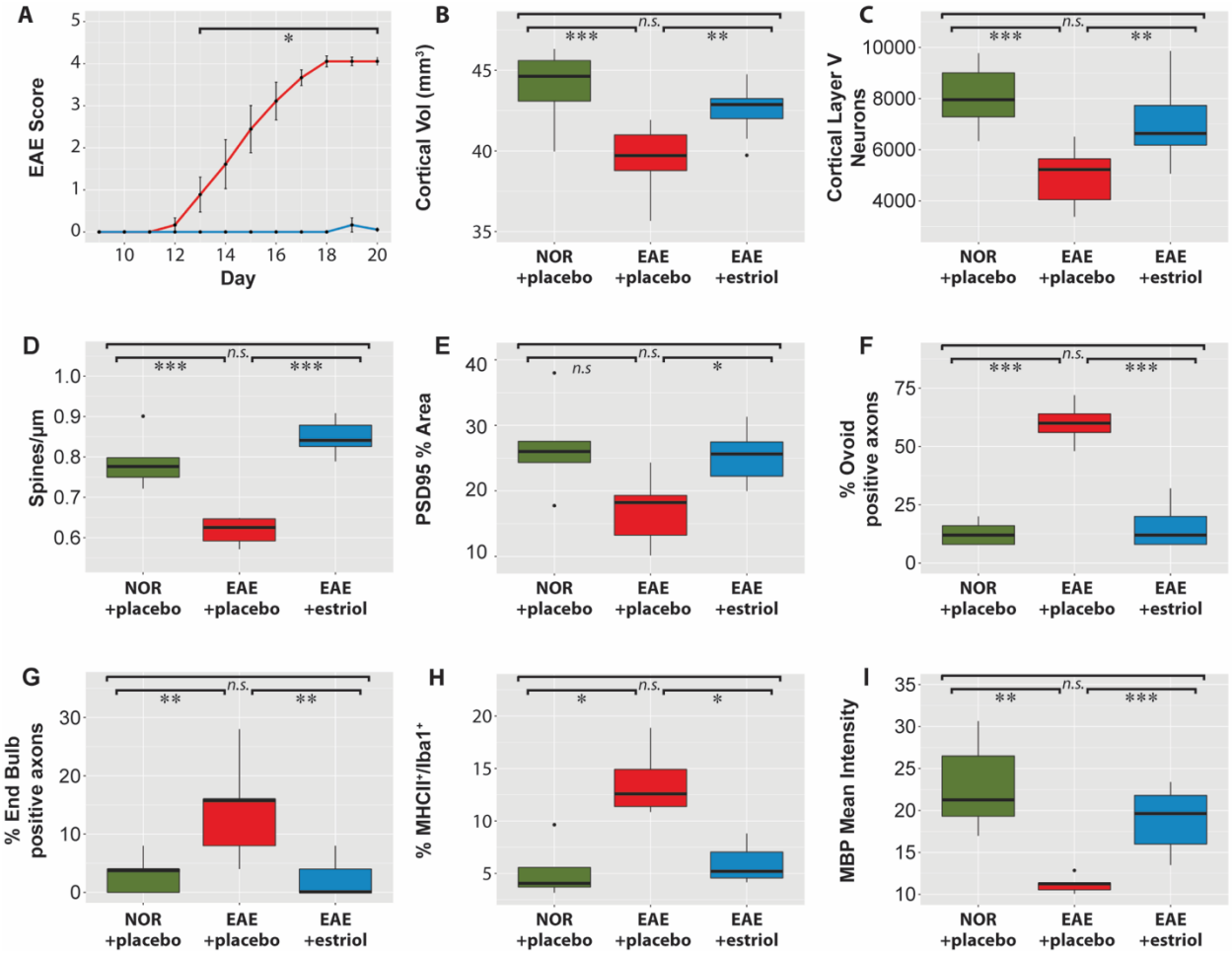

Figure 4-7: Estriol pre-treatment prevents gray matter atrophy and induces neuroprotection in EAE. Thy1-YFP^{+} mice with EAE were pre-treated one week prior to disease induction with either an estriol pellet (EAE + estriol, n = 9) or placebo pellet (EAE + placebo, n = 9). *In vivo* images were collected at 20 days after disease induction, along with placebo-treated healthy controls (NOR + placebo = 10), and the mice were subsequently sacrificed for pathological analyses. A) Estriol pre-treatment (blue) almost completely prevented clinical signs of disease compared to placebo-treated EAE mice (red). Asterisk indicates a significant difference ($p < 0.05$) in EAE scores between placebo-treated and estriol-treated EAE. B) Estriol pre-treated EAE mice showed complete preservation of cortical volume compared to placebo-treated EAE mice. C) Estriol pre-treatment prevented loss of cortical layer V neurons in

cerebral cortex during EAE. D) Estriol pre-treatment in EAE prevented loss of dendritic spines on the apical dendrites of cortical layer V pyramidal neurons in cerebral cortex. E) Estriol pre-treatment also protected against loss of synapses in mice with EAE indicated by preservation of PSD95 % area. F-G) Estriol pre-treated EAE mice showed almost no axonal damage in the spinal cord when % of axons with ovoids (F) and % of axons with end bulbs (G) were quantified. H) Estriol pre-treatment prevented microglial activation in cerebral cortex during EAE. I) Estriol pre-treatment preserved MBP intensity in the cerebral cortex during EAE. *$p < 0.05$, **$p < 0.01$, ***$p < 0.001$; *t* test, FDR corrected.

4.6 References

Benjamini, Y., Hochberg, Y., 1995. Controlling the False Discovery Rate: A Practical and Powerful Approach to Multiple Testing. Journal of the Royal Statistical Society Series B … 57, 289-300.

Confavreux, C., Hutchinson, M., Hours, M.M., Cortinovis-Tourniaire, P., Moreau, T., 1998. Rate of pregnancy-related relapse in multiple sclerosis. Pregnancy in Multiple Sclerosis Group [see comments]. New England Journal of Medicine 339, 285-291.

Fisniku, L.K., Chard, D.T., Jackson, J.S., Anderson, V.M., Altmann, D.R., Miszkiel, K.A., Thompson, A.J., Miller, D.H., 2008. Gray matter atrophy is related to long-term disability in multiple sclerosis. Ann Neurol 64, 247-254.

Hammond, J.W., Bellizzi, M.J., Ware, C., Qiu, W.Q., Saminathan, P., Li, H., Luo, S., Ma, S.A., Li, Y., Gelbard, H.A., 2020. Complement-dependent synapse loss and microgliosis in a mouse model of multiple sclerosis. Brain Behav Immun.

Head, K.A., 1998. Estriol: safety and efficacy. Altern Med Rev 3, 101-113.

Howell, O.W., Rundle, J.L., Garg, A., Komada, M., Brophy, P.J., Reynolds, R., 2010. Activated microglia mediate axoglial disruption that contributes to axonal injury in multiple sclerosis. J Neuropathol Exp Neurol 69, 1017-1033.

Itoh, N., Kim, R., Peng, M., DiFilippo, E., Johnsonbaugh, H., MacKenzie-Graham, A., Voskuhl, R.R., 2016. Bedside to bench to bedside research: Estrogen receptor beta ligand as a candidate neuroprotective treatment for multiple sclerosis. J Neuroimmunol.

Kim, R.Y., Mangu, D., Hoffman, A.S., Kavosh, R., Jung, E., Itoh, N., Voskuhl, R., 2018. Oestrogen receptor β ligand acts on CD11c+ cells to mediate protection in experimental autoimmune encephalomyelitis. Brain 141, 132-147.

Kim, S., Liva, S.M., Dalal, M.A., Verity, M.A., Voskuhl, R.R., 1999. Estriol ameliorates autoimmune demyelinating disease: implications for multiple sclerosis. Neurology 52, 1230-1238.

Klaver, R., Popescu, V., Voorn, P., Galis-de Graaf, Y., van der Valk, P., de Vries, H.E., Schenk, G.J., Geurts, J.J., 2015. Neuronal and axonal loss in normal-appearing gray matter and subpial lesions in multiple sclerosis. J Neuropathol Exp Neurol 74, 453-458.

Krysko, K., Graves, J., Dobson, R., Altintas, A., Amato, M., Bernard, J., Bonavita, S., Bove, R., Cavalla, P., Clerico, M., Corona, T., Doshi, A., Fragoso, Y., Jacobs, D., Jokubaitis, V., Landi, D., Llamosa, G., Longbrake, E., Maillart, E., Marta, M., Midaglia, L., Shah, S., Tintore, M., van der Walt, A., Voskuhl, R., Wang, Y., Zabad, R., Zeydan, B., Houtchens, M., Hellwig, K., 2020. Sex effects across the lifespan in women with multiple sclerosis. Therapeutic advances in neurological disorders 13.

Kuiper, G.G., Carlsson, B., Grandien, K., Enmark, E., Haggblad, J., Nilsson, S., Gustafsson, J.A., 1997. Comparison of the ligand binding specificity and transcript tissue distribution of estrogen receptors alpha and beta. Endocrinology 138, 863-870.

MacKenzie-Graham, A., Brook, J., Kurth, F., Itoh, Y., Meyer, C., Montag, M.J., Wang, H.J., Elashoff, R., Voskuhl, R.R., 2018. Estriol-mediated neuroprotection in multiple sclerosis l ocalized by voxel-based morphometry. Brain Behav, e01086.

MacKenzie-Graham, A., Kurth, F., Itoh, Y., Wang, H.J., Montag, M.J., Elashoff, R., Voskuhl, R.R., 2016. Disability-Specific Atlases of Gray Matter Loss in Relapsing-Remitting Multiple Sclerosis. JAMA Neurology 73, 944-953.

MacKenzie-Graham, A., Rinek, G.A., Avedisian, A., Gold, S.M., Frew, A.J., Aguilar, C., Lin, D.R., Umeda, E., Voskuhl, R.R., Alger, J.R., 2012a. Cortical atrophy in experimental autoimmune encephalomyelitis: in vivo imaging. Neuroimage 60, 95-104.

MacKenzie-Graham, A.J., Rinek, G.A., Avedisian, A., Morales, L.B., Umeda, E., Boulat, B., Jacobs, R.E., Toga, A.W., Voskuhl, R.R., 2012b. Estrogen treatment prevents gray matter atrophy in experimental autoimmune encephalomyelitis. Journal of Neuroscience Research 90, 1310-1323.

Mei, F., Lehmann-Horn, K., Shen, Y.A., Rankin, K.A., Stebbins, K.J., Lorrain, D.S., Pekarek, K.,

S, A.S., Xiao, L., Teuscher, C., von Budingen, H.C., Wess, J., Lawrence, J.J., Green, A.J., Fancy, S.P., Zamvil, S.S., Chan, J.R., 2016. Accelerated remyelination during inflammatory demyelination prevents axonal loss and improves functional recovery. Elife 5.

Meyer, C.E., Gao, J.L., Cheng, J.Y., Oberoi, M.R., Johnsonbaugh, H., Lepore, S., Kurth, F., Thurston, M.J., Itoh, N., Patel, K.R., Voskuhl, R.R., MacKenzie-Graham, A., 2019. Axonal damage in spinal cord is associated with gray matter atrophy in sensorimotor cortex in experimental autoimmune encephalomyelitis. Mult Scler, 1352458519830614.

Nikic, I., Merkler, D., Sorbara, C., Brinkoetter, M., Kreutzfeldt, M., Bareyre, F.M., Bruck, W., Bishop, D., Misgeld, T., Kerschensteiner, M., 2011. A reversible form of axon damage in experimental autoimmune encephalomyelitis and multiple sclerosis. Nat Med 17, 495-499.

Palaszynski, K.M., Liu, H., Loo, K.K., Voskuhl, R.R., 2004. Estriol treatment ameliorates disease in males with experimental autoimmune encephalomyelitis: implications for multiple sclerosis. J Neuroimmunol 149, 84-89.

Porrero, C., Rubio-Garrido, P., Avendano, C., Clasca, F., 2010. Mapping of fluorescent protein-expressing neurons and axon pathways in adult and developing Thy1-eYFP-H transgenic mice. Brain Res 1345, 59-72.

Roosendaal, S.D., Bendfeldt, K., Vrenken, H., Polman, C.H., Borgwardt, S., Radue, E.W., Kappos, L., Pelletier, D., Hauser, S.L., Matthews, P.M., Barkhof, F., Geurts, J.J., 2011. Grey matter volume in a large cohort of MS patients: relation to MRI parameters and disability. Mult Scler 17, 1098-1106.

Rossouw, J.E., Anderson, G.L., Prentice, R.L., LaCroix, A.Z., Kooperberg, C., Stefanick, M.L., Jackson, R.D., Beresford, S.A., Howard, B.V., Johnson, K.C., Kotchen, J.M., Ockene, J., 2002. Risks and benefits of estrogen plus progestin in healthy postmenopausal women: principal results From the Women's Health Initiative randomized controlled trial. JAMA

288, 321-333.

Shattuck, D.W., Leahy, R.M., 2002. BrainSuite: an automated cortical surface identification tool. Med Image Anal 6, 129-142.

Sicotte, N.L., Liva, S.M., Klutch, R., Pfeiffer, P., Bouvier, S., Odesa, S., Wu, T.C., Voskuhl, R.R., 2002. Treatment of multiple sclerosis with the pregnancy hormone estriol. Ann Neurol 52, 421-428.

Soldan, S.S., Alvarez Retuerto, A.I., Sicotte, N.L., Voskuhl, R.R., 2003. Immune modulation in multiple sclerosis patients treated with the pregnancy hormone estriol. J Immunol 171, 6267-6274.

Spence, R.D., Kurth, F., Itoh, N., Mongerson, C.R., Wailes, S.H., Peng, M.S., MacKenzie-Graham, A.J., 2014. Bringing CLARITY to gray matter atrophy. Neuroimage 101, 625-632.

Spence, R.D., Wisdom, A.J., Cao, Y., Hill, H.M., Mongerson, C.R., Stapornkul, B., Itoh, N., Sofroniew, M.V., Voskuhl, R.R., 2013. Estrogen mediates neuroprotection and anti-i nflammatory effects during EAE through ERalpha signaling on astrocytes but not through ERbeta signaling on astrocytes or neurons. Journal of Neuroscience 33, 10924-10933.

Trapp, B.D., Peterson, J., Ransohoff, R.M., Rudick, R., Mork, S., Bo, L., 1998. Axonal transection in the lesions of multiple sclerosis. N Engl J Med 338, 278-285.

Voskuhl, R., Momtazee, C., 2017. Pregnancy: Effect on Multiple Sclerosis, Treatment Considerations, and Breastfeeding. Neurotherapeutics : the journal of the American Society for Experimental NeuroTherapeutics 14.

Voskuhl, R., Wang, H., Elashoff, R., 2016a. Why use sex hormones in relapsing-remitting multiple sclerosis? - Authors' reply. The Lancet. Neurology 15.

Voskuhl, R.R., Itoh, N., Tassoni, A., Matsukawa, M.A., Ren, E., Tse, V., Jang, E., Suen, T.T., Itoh, Y., 2019. Gene expression in oligodendrocytes during remyelination reveals

cholesterol homeostasis as a therapeutic target in multiple sclerosis. Proceedings of the National Academy of Sciences of the United States of America 116, 10130-10139.

Voskuhl, R.R., Wang, H., Wu, T.C., Sicotte, N.L., Nakamura, K., Kurth, F., Itoh, N., Bardens, J., Bernard, J.T., Corboy, J.R., Cross, A.H., Dhib-Jalbut, S., Ford, C.C., Frohman, E.M., Giesser, B., Jacobs, D., Kasper, L.H., Lynch, S., Parry, G., Racke, M.K., Reder, A.T., Rose, J., Wingerchuk, D.M., MacKenzie-Graham, A.J., Arnold, D.L., Tseng, C.H., Elashoff, R., 2016b. Estriol combined with glatiramer acetate for women with relapsing-remitting multiple sclerosis: a randomised, placebo-controlled, phase 2 trial. Lancet Neurol 15, 35-46.

Werneburg, S., Jung, J., Kunjamma, R.B., Ha, S.K., Luciano, N.J., Willis, C.M., Gao, G., Biscola, N.P., Havton, L.A., Crocker, S.J., Popko, B., Reich, D.S., Schafer, D.P., 2020. Targeted Complement Inhibition at Synapses Prevents Microglial Synaptic Engulfment and Synapse Loss in Demyelinating Disease. Immunity 52, 167-182.e167.

Ziehn, M.O., Avedisian, A.A., Dervin, S.M., O'Dell, T.J., Voskuhl, R.R., 2012. Estriol preserves synaptic transmission in the hippocampus during autoimmune demyelinating disease. Lab Invest 92, 1234-1245.

Chapter 5

Increased neurodegeneration in male C57BL/6 mice with experimental autoimmune encephalomyelitis

5.1 Abstract

Women with multiple sclerosis (MS) show increased susceptibility to disease and increased inflammatory activity, while men demonstrate more severe disability progression and neurodegeneration. This indicates a role for sex-specific factors influencing neurodegenerative response in MS. Gray matter (GM) atrophy is associated with disability in MS. Particularly, GM atrophy in the cerebral cortex is highly predictive of both motor and cognitive dysfunction in MS patients. Males with MS show more GM atrophy than females. To better understand the mechanisms underlying this sexual dimorphism in neurodegeneration, we sought to investigate whether the most commonly used mouse model for multiple sclerosis, chronic experimental autoimmune encephalomyelitis (EAE), would also demonstrate sex differences in GM atrophy and associated pathology. We used voxel-based morphometry to identify localized GM atrophy by comparing males and females to their healthy controls. Clear Lipid-exchanged Acrylamide-hybridized Rigid Imaging-compatible Tissue-hYdrogel (CLARITY) and immunohistochemistry were used to identify sex differences in cerebral cortex and spinal cord pathology. We observed more extensive GM atrophy in EAE males compared to healthy males than in EAE females compared to healthy females. We further identified a sex-specific relationship between worse walking disability and worse GM atrophy in the somatosensory cortex in males. Males with EAE showed greater neuronal loss in the cerebral cortex and greater axonal transection in the spinal cord. Together, these results demonstrate increased neurodegeneration in male mice with chronic EAE, similar to increased neurodegeneration seen in males with MS.

5.2 Introduction

Sex differences in disease prevalence and progression are well-established in multiple sclerosis (MS), a putative autoimmune disease of the central nervous system characterized by inflammation, demyelination, and neurodegeneration. Females are more susceptible to MS by a factor of 3:1 (Koch-Henriksen and Sørensen, 2010; Wallin et al., 2012). This female

preponderance is common in other autoimmune diseases as well, in part due to a more robust immune response (Hewagama et al., 2009; Klein and Flanagan, 2016; Voskuhl, 2011). Conversely, males with MS demonstrate worse disease progression (Golden and Voskuhl, 2017), have worse long term disability outcomes (Benedict and Zivadinov, 2011; Confavreux et al., 2003), and progress from relapse-remitting MS to secondary progressive MS more quickly than females (Koch et al., 2010; Weinshenker et al., 1991). Males demonstrate a greater number of T1-hypointense lesions, which are thought to be more destructive than T2-hyperintense lesions and represent increased neurodegeneration (Pozzilli et al., 2003; van Walderveen et al., 2001). The accelerated disease course in males does not seem to be associated with inflammation and instead may be attributed to neurodegenerative factors within the central nervous system (CNS) (Voskuhl and Gold, 2012). The mechanisms underlying increased neurodegeneration in males with MS remain unclear.

Investigating sex differences can elucidate disease mechanisms and aid in identifying therapeutic targets. The most commonly used mouse model for MS, experimental autoimmune encephalomyelitis (EAE), provides a valuable method to investigate the mechanisms underlying sex differences in disease. The disease course and sex-specific effects of EAE differ depending on the strain of mouse suggesting that genetic background influences sex-specific variables. In the SJL strain, which demonstrates a relapse-remitting disease course, females are more susceptible to EAE (Voskuhl et al., 1996) and recent evidence suggests this may be due to a direct effect of the XX chromosome complement in the immune system (Golden et al., 2019; Smith-Bouvier et al., 2008). In the C57BL/6 strain, which demonstrates a chronic disease course, no sex differences in susceptibility or walking disability have been observed (Okuda et al., 2002; Palaszynski et al., 2004; Papenfuss et al., 2004). No previous study has rigorously investigated whether sex differences exist in neurodegeneration in wild-type C57BL/6 mice with chronic EAE.

Gray matter (GM) atrophy measured by magnetic resonance imaging (MRI) is a means of noninvasively evaluating neurodegeneration and is a strong indicator of disability progression in MS. It is known to occur early in disease and may become more aggressive with age (Fisher et al., 2008). GM atrophy is better associated with motor disability and cognitive dysfunction than either white matter lesion load or white matter atrophy (Eijlers et al., 2018; Fisniku et al., 2008; Rocca et al., 2021; Roosendaal et al., 2011). Interestingly, localized GM atrophy has been found to correlate with clinically relevant disabilities (MacKenzie-Graham et al., 2016). Males with MS demonstrate worse GM atrophy than females (Antulov et al., 2009; Jakimovski et al., 2020). Particularly, males show greater atrophy in the cortex, thalamus, caudate, and putamen (Schoonheim et al., 2012; Schoonheim et al., 2014; Voskuhl et al., 2020). Increased atrophy has been linked to worse cognitive outcomes in males with MS (Schoonheim et al., 2012; Voskuhl et al., 2020). GM atrophy is also known to occur during chronic EAE and is associated with neuropathology (MacKenzie-Graham et al., 2012a; Meyer et al., 2019; Spence et al., 2014). However, sex differences in brain neurodegeneration during EAE have been poorly characterized and no previous studies have examined sex differences in GM atrophy during EAE.

In this investigation, we use voxel-based morphometry (VBM) to analyze GM atrophy in mice with EAE. We show that males have worse GM atrophy in the C57BL/6 EAE mouse model, mimicking clinical observations in MS patients. We combine the use of CLARITY and immunohistochemistry to demonstrate worse neuronal loss in the cerebral cortex and worse axonal transection in the spinal cord of males with EAE. These results provide a critical step in understanding mechanisms underlying sex differences in neurodegeneration during MS.

5.3 Materials and Methods

Animals: All mice (12-20 weeks old) used in this study were from the C57BL/6J background. 120 Thy1-YFP-H C57BL/6J mice over three experiments, originally ordered from Jackson Labs

(www.jax.org) and bred within our facilities, were used in this study (29 healthy female, 29 EAE female, 31 healthy male, 31 EAE male).

Animals were maintained under standard conditions in a 12 h dark/12 h light cycle with access to food and water *ad libitum*. All procedures were done in accordance to the guidelines of the National Institutes of Health and the Chancellor's Animal Research Committee of the University of California, Los Angeles Office for the Protection of Research Subjects.

EAE induction: EAE was induced as described (Meyer et al., 2019). Briefly, mice were immunized subcutaneously with MOG peptide 35–55 (300 µg) and Mycobacterium tuberculosis (500 µg) emulsified in complete Freund's adjuvant, in a volume of 0.1 mL over the right draining inguinal and axillary lymph nodes. One week later, a booster immunization was delivered subcutaneously over the contralateral lymph nodes. Pertussis toxin (500 ng; List Biological Laboratories, Campbell, CA) was injected intraperitoneally on days 0 and 2. EAE was graded on a scale of 0–5, as described (Kim et al., 2018; Pettinelli and McFarlin, 1981).

Magnetic resonance imaging: All animals were scanned *in vivo* at the Ahmanson-Lovelace Brain Mapping Center at UCLA on a 7T Bruker imaging spectrometer with a micro-imaging gradient insert with a maximum gradient strength of 100 G/cm (Bruker Instruments, Billerica, MA). An actively decoupled quadrature surface coil array was used for signal reception and a 72-mm birdcage coil was used for transmission. For image acquisition, mice were anesthetized with isoflurane and their heads secured with bite and ear bars. All mice were given a 0.5 ml saline injection subcutaneously prior to being placed in the scanner and another 0.5 ml injection upon being removed from the scanner to prevent dehydration. Respiration rate was monitored and the mice were maintained at 37° C using a circulating water pump. Each animal was scanned using a rapid-acquisition with relaxation enhancement (RARE) sequence with the following parameters: TR/TE_{eff} 3500/32 ms, ETL 16, matrix: 256 × 192 × 100, voxel dimensions:

100 × 100 × 100 μm^3. Total imaging time was 93 minutes. Images were acquired and reconstructed using ParaVision 5.1 software.

Voxel-based morphometry (VBM): All MRI brain images were skull stripped using Brainsuite 19b (Shattuck and Leahy, 2002)(http://brainsuite.org). Images were then processed and examined with Statistical Parametric Mapping (SPM) 8 software (Welcome Trust Center for Neuroimaging, London, United Kingdom; http://www.fil.ion.ucl.ac.uk/spm) and SPMMouse (SPMMouse, http://www.spmmouse.org)(Sawiak et al., 2009) within MATLAB version 2013a (MathWorks, Natick, MA). Images were manually registered to tissue probability maps (TPMs) generated from 60 C57BL/6J mice (Meyer et al., 2017) using 6-parameter linear transformations. The images were bias corrected and segmented into GM, WM, and cerebrospinal fluid (CSF) using the unified segmentation algorithm (Ashburner and Friston, 2005). The resulting segments were used to create a Diffeomorphic Anatomical Registration using Exponentiated Lie algebra (DARTEL) template (Ashburner, 2007) and the individual GM segments were warped to this template and modulated. Finally, the normalized and modulated GM segments were smoothed with a 600 µm FWHM Gaussian kernel and used as the input for the statistical analysis.

Cross-sectional differences in local GM volume between EAE and control mice were examined with a general linear model. Whole brain volume was included as a covariate to account for the variance associated with brain size and to prevent potential effects due to differences in brain size. Within this model, significant differences in local GM volume between groups were determined via Student's *t*-tests. All findings were corrected for multiple comparisons by controlling the false discovery rate (FDR)(Benjamini and Hochberg, 1995) and all significance maps were thresholded at $q \leqslant 0.05$. All analyses were performed bi-directionally. Associations of voxelwise GM volumes with cumulative EAE scores and disease duration using voxelwise regression analyses were assessed within the general linear model. Whole brain size

was included as a variable of no interest. All significant findings were corrected for multiple comparisons by controlling the FDR.

Bias-corrected images were warped to the DARTEL template, and averaged to create a mean template for visualization.

Clear Lipid-exchanged Acrylamide-hybridized Rigid Imaging-compatible Tissue-hYdrogel: The spinal cords from a subset of the mice (19 healthy females 19, 12 healthy males, 19 EAE females, 19 EAE males) were optically cleared using the CLARITY protocol modified for "passive clearing" as described (Meyer et al., 2019; Roberts et al., 2016; Spence et al., 2014).

Immunohistochemistry: 40 μm sagittal brain sections from a subset of animals (19 healthy females, 12 healthy males, 19 EAE females, 19 EAE males) were stained using immunohistochemistry (IHC) as described (MacKenzie-Graham et al., 2012a). Tissues were stained for myelin basic protein (MBP; Aves, Davis, CA) and cluster of differentiation 45 (CD45, BD Pharmingen, San Diego, CA).

Microscopy: Laser scanning confocal microscopy for CLARITY analysis and all publication images was performed at the California NanoSystems Institute (CNSI) Advanced Light Microscopy/Spectroscopy Shared Resource Facility at UCLA as described (MacKenzie-Graham et al., 2012a; Spence et al., 2014). CLARITY samples were imaged in z-stacks with a Leica HCX PL FLUOTAR NA 0.3 10X objective in 11 μm z-steps (the limit of optical resolution). Stained 40 μm sections were examined and imaged using Olympus BX51 fluorescence microscope with a DP50 digital camera. All images were taken and processed using the integrated software program cellSens2.2 (Olympus Life Science, Tokyo, Japan). ImageJ

(https://fiji.sc) was used to perform integration and analysis of images. All analyses were done in a blinded fashion with regards to knowledge of experimental group.

Statistical analyses: CLARITY and IHC data were analyzed in R (https://www.r-project.org). All data were first analyzed with a 2-way ANOVA. Two-group comparisons were conducted using a Student's *t*-test (two-tailed). Regression analyses are reported as Pearson correlation coefficients. All reported p values are corrected for multiple comparisons by controlling for the FDR.

5.4 Results

Voxel-based morphometry reveals more extensive gray matter atrophy in males than females during EAE

We collected *in vivo* MRI and utilized VBM to investigate GM atrophy during EAE by comparing male and female mice with EAE to their sex and age-matched healthy controls. A one-way ANOVA revealed that there was not a statistically significant effect of sex on EAE score ($p = 0.509$)(Fig 5-1). Despite similar EAE scores, the statistical parametric map (SPM) indicating atrophy during EAE was larger in males (51.365 mm^3) than females (16.657 mm^3)(Fig 5-2A & B). Males particularly demonstrated more GM atrophy in the motor cortex, visual cortex, somatosensory cortex, hypothalamus, amygdala, and cerebellum.

Worse disability associated with worse gray matter atrophy in the somatosensory cortex in males but not females during EAE

Our group previously identified that males with MS demonstrated a relationship between worse performance on the 9-hole peg test and worse GM atrophy in the thalamus, while females with MS did not demonstrate this relationship (Voskuhl et al., 2020). To evaluate whether there would be a sex difference in the relationship between walking disability (as

measured by cumulative EAE scores over 45 days) and GM atrophy, we performed a voxel-wise regression analysis within each sex. This biology-driven approach identified that the somatosensory cortex was associated with cumulative EAE scores in males (SPM volume = 14.403 mm^3), while no relationship was found in females (Fig 5-3A). We further found that disease duration was associated with more GM atrophy in the somatosensory cortex in males only (SPM volume = 3.69 mm^3) (Fig 5-3B). No relationship was observed in females. These results suggest that more profound GM atrophy is associated with walking disability in males than in females with EAE.

Males show more neurodegeneration in cerebral cortex than females during EAE

The VBM results demonstrated increased GM atrophy in the cerebral cortex of male mice with EAE. We sought to investigate whether males would also show increased neuronal loss in the cerebral cortex. Thy1-YFP^+ mice express yellow fluorescent protein in a subset of their cortical layer V pyramidal neurons, the projection neurons of the cerebral cortex (Porrero et al., 2010). We analyzed the number of YFP^+ cortical layer V pyramidal neurons and found that females demonstrated a 8.44% loss ($p = 0.040$) compared to healthy control females. Interestingly, males showed 28.19% loss of cortical layer V neurons ($p = 4.35 \times 10^{-6}$) compared to healthy control males. There was a significant interaction between sex and EAE indicating that males demonstrated greater neuronal loss in the cerebral cortex than females ($p = 0.036$)(Fig. 5-4A & B).

Our group has previously demonstrated that axonal damage, particularly axonal transection, is strongly associated with GM atrophy in the cerebral cortex (Meyer et al., 2019; Spence et al., 2014). We evaluated axonal transection (end-bulbs) and axonal injury (ovoids) in the spinal cord (Fig 5-4C). Both females and males demonstrated a similar increase in axonal injury during EAE (196% increase in females and 234% increase in males; $p = 2.68 \times 10^{-6}$, $p = 3.79 \times 10^{-9}$, respectively)(Fig 5-4D). Interestingly, EAE males demonstrated a 3.9% increase in

end bulb positive axons ($p = 3.6 \times 10^{-5}$) compared to healthy control males while EAE females only demonstrated a 1.8% increase in end bulb positive axons compared to healthy control females ($p = 0.0014$). A 2-way ANOVA revealed a significant interaction between sex and EAE ($p = 0.025$) suggesting males demonstrated more axonal transection during EAE.

Cumulative EAE score is a measure of walking disability over time and primarily relies on spinal cord function. We therefore investigated whether cumulative EAE scores were associated with axonal damage in the spinal cord. Interestingly, we found that axonal damage was associated with cumulative EAE scores in a sex-specific manner. Female EAE mice showed a significant correlation between percentage of ovoid positive axons and cumulative EAE scores ($r = 0.52$, $p = 0.022$), whereas males did not. Conversely, males showed a significant correlation between percentage of end bulb positive axons and cumulative EAE scores ($r = 0.57$, $p = 0.011$), whereas females did not.

Males and females show similar immune cell infiltration and demyelination in the cerebral cortex during EAE

Inflammatory demyelination is a key feature of EAE that may contribute to neurodegeneration and disability. We next investigated whether $CD45^+$ immune cell infiltration and demyelination would reveal sex differences in the cerebral cortex. Analysis of $CD45^+$ T-cells in the cerebral cortex showed similar immune cell infiltration in EAE females and males when compared to their respective healthy controls (Figure 5-5A)($p = 0.026$, $p = 1.93 \times 10^{-4}$, respectively). Further, myelin staining in the cerebral cortex was decreased similarly during EAE in both females and males when compared to their respective healthy controls (Figure 5-5B) ($p = 0.049$, $p = 0.030$, respectively). This was confirmed in a separate experiment (Figure 5-6A & B). These results suggest that neither T-cell infiltration nor demyelination in the cerebral cortex is driving the increased neurodegeneration observed in males during EAE.

5.5 Discussion

Males with MS demonstrate faster disease progression and increased GM atrophy compared to females with MS (Golden and Voskuhl, 2017; Voskuhl et al., 2020). An accessible model that mimics this clinical observation would allow for the investigation of the underlying mechanisms contributing to sex differences in disease progression in MS. In this study we showed increased regional GM atrophy and increased neurodegeneration in C57BL/6 males with chronic EAE compared to females; a finding which may serve as a starting point for future investigations of sex differences in disease progression.

It is important to analyze sex differences in GM atrophy during EAE in a region-specific manner as EAE is highly heterogeneous, as is MS, and sex-specific factors may have differing effects in the brain depending on the region. For example, while we found increased neurodegeneration in the cerebral cortex of males compared to females, a previous study found greater retinal cell ganglion loss and greater axonal loss in optic nerves of female mice with EAE (Tassoni et al., 2019). This suggests that mechanisms of neurodegeneration may vary between region and sex. Whole brain or whole GM MRI analyses risk overlooking region-specific information that may provide valuable insight into disease progression within the sexes as we did not see a sex difference in whole GM volume.

We used a biology-driven approach, VBM, to identify localized GM atrophy in male and female mice with EAE. Males showed more extensive atrophy, particularly in areas linked to sensory and motor function including the motor cortex, somatosensory cortex, visual cortex, and cerebellum. This expands upon previous studies from our lab identifying atrophy in these regions in females with chronic EAE (Meyer et al., 2019). We previously found that females demonstrate atrophy particularly in the cerebral cortex. In this investigation we confirmed those results and found that males demonstrate more extensive cerebral cortex atrophy. The cerebral cortex, including the motor cortex, somatosensory cortex, and visual cortex demonstrate atrophy in MS (Calabrese et al., 2007) and is associated with disability (Charil et al., 2007;

Eijlers et al., 2019; Steenwijk et al., 2016). Increased cortical thinning was found in males with MS but not females (Voskuhl et al., 2020), consonant with our results in mice with chronic EAE.

Males with MS demonstrate worse cognitive impairment than their age-matched female counterparts (Beatty and Aupperle, 2002; Benedict and Zivadinov, 2011; Schoonheim et al., 2014). Our VBM results indicate worse atrophy in males in several regions associated with cognition. In addition to the cerebral cortex which is highly associated with cognitive deficits in MS patients (Eijlers et al., 2018; Eijlers et al., 2019), we identified GM atrophy in males, but not females, in the amygdala and entorhinal cortex. Atrophy of the amygdala has been found to predict worse social cognition in MS patients (Batista et al., 2017). Further, the entorhinal cortex, a region highly connected to the cortex and hippocampus, has shown atrophy in MS patients (Steenwijk et al., 2016) and is known to be involved in learning and memory (Coutureau and Di Scala, 2009). To date there is not evidence of sexual dimorphism in these regions in MS.

We also identified atrophy in the hypothalamus of males, but not females, with chronic EAE. The hypothalamus is a highly sexually dimorphic structure involved in many hormone-mediated behaviors including feeding, temperature control, stress, and sleep (Swaab et al., 2001). Lesions in the hypothalamus are associated with worse disease course (Huitinga et al., 2003) and there is some evidence that the hypothalamus atrophies during MS (Henry et al., 2008; Polacek et al., 2019), but its role in sex-specific disease progression remains unknown. Together, our results indicating regional GM atrophy demonstrate more extensive GM damage in males with chronic EAE compared to females and suggest regions of interest for further investigation into sex differences in underlying pathology.

Mapping disability to GM atrophy in specific brain regions can provide insight into mechanistic pathways related to disability. Our group has previously created disability specific atlases mapping specific disabilities to clinically eloquent brain regions in MS patients (MacKenzie-Graham et al., 2016). We used a similar approach and found that, in males, cumulative EAE scores and disease duration were associated with GM atrophy primarily in the

somatosensory cortex. This relationship was not observed in females. These results emphasize the importance of conducting comparisons within sex as disability may have a differing relationship to neurodegeneration depending on sex.

The VBM results and voxelwise-regression results highlighting the increased atrophy of the cerebral cortex in males, prompted us to investigate sex differences in pathology in the cerebral cortex. Healthy males had less YFP^+ cortical layer V neurons in the cerebral cortex than females, likely an effect of the Thy1-YFPH mouse strain. Though this effect has not previously been studied, there is some evidence that the Thy1 promotor is responsive to sex hormones (Li et al., 2012; Montanari et al., 2019). Sex-specific factors may therefore influence the expression of the Thy1 promoter in cortical layer V neurons. This again highlights the importance of conducting comparisons within each sex. We identified worse cortical layer V neuronal loss in the cerebral cortex of males compared to females using a two-way ANOVA. This suggests that worse GM atrophy in the cerebral cortex observed by VBM is accompanied by loss of functionally relevant neurons.

A previous investigation by our group had identified that GM atrophy in the somatosensory cortex was highly associated with axonal damage in the spinal cord (Meyer et al., 2019). We investigated sex differences in axonal damage in the spinal cords of Thy1-YFP^+ projections from cortical layer V neurons and found that axonal injury was similar in males and females. Interestingly, axonal transection was increased in males compared to females. This corroborates a recent study that found increased gliosis, demyelination, and axonal damage in the spinal cord of male mice with chronic EAE (Catuneanu et al., 2019). However, another study that found increased axonal damage and worse demyelination in the spinal cords of female mice with chronic EAE (Wiedrick et al., 2021). These observed differences may be due to timing as Wiedrick et al. looked earlier in disease at 20 days post induction.

Remarkably, we observed that axonal injury was directly correlated with cumulative EAE scores in females, but not males, while axonal transection was directly correlated with

cumulative EAE scores in males, but not females. This is despite similar cumulative EAE scores in males and females during EAE. Previous studies have similarly observed a lack of sex differences in EAE scores between males and females. (Okuda et al., 2002; Papenfuss et al., 2004). Cumulative EAE score is a very gross measure of walking disability and different mechanisms may contribute to similar levels of disability. Ovoids are thought to be precursors to end bulbs, suggesting that more advanced axonal damage is associated with disability in males. Together, our results imply that axonal damage leads to atrophy in the somatosensory cortex and contributes to irreversible motor disability, a relationship that is more pronounced in males than females, during EAE.

No sex differences were observed in immune cell infiltration or demyelination in the cerebral cortex. Future investigations should examine sex differences in reactive astrocytes and microglia to determine whether other forms of pathology may be contributing to the increased neurodegeneration in the cerebral cortex observed in males.

Sex differences can be due to sex hormones, sex chromosomes, environmental factors, or an interaction between them. While we cannot fully rule out the effect of environment, male and female mice in this study shared the same environment, making it is unlikely that any sex differences observed are influenced by environmental factors. Therefore, we are left with the possibility that sex hormones, sex chromosomes, or their interaction are influencing the observed sex differences. It is unlikely that endogenous testosterone levels are exacerbating GM atrophy since testosterone has been found to be protective in EAE (Palaszynski et al., 2004; Ziehn et al., 2012) and MS (Kurth et al., 2014). It is possible, however, that endogenous estrogen may be protecting against increased GM atrophy as estrogens are known to be neuroprotective (Christianson et al., 2015; MacKenzie-Graham et al., 2012b). Gonadectomy, thereby removing endogenous sex hormones, provides a method to determine if sex hormones are influencing the observed differences in disease. Gonadectomy has not been shown to have an effect on the EAE scores of male C57BL/6 mice (Palaszynski et al., 2004) or female SJL

mice (Palaszynski et al., 2004; Voskuhl and Palaszynski, 2001). An interesting area of future study will be to determine if gonadectomized mice show sex differences in neurodegeneration.

Sex chromosomes (XY vs XX) may also contribute to worse neurodegeneration in males. In the four core genotype model the testes determining gene (*Sry*) is removed from the Y chromosome and placed on an autosome. This allows for the creation of both XX and XY^- gonadal females as well as XX*Sry* and XY^-*Sry* gonadal males, decoupling the effect of sex hormones and sex chromosomes. The four core genotype model has revealed that sex chromosome complement influences neurodegeneration during EAE. In one study, it was observed that the presence of the Y chromosome in the CNS led to worse EAE progression and neurodegeneration in SJL mice and C57BL/6 mice, mimicking sex differences observed in humans with MS (Du et al., 2014). Sex chromosome compliment may work in concert with sex hormones to affect disease. Further study is needed to disentangle the contribution of both sex chromosome complement and sex hormones in producing the observed sex differences in neurodegeneration during EAE.

This study is limited in that it does not yet quantify sex differences in the GM atrophy of the brain regions of interest. Our study also does not rule out that differences in neurodegeneration may be due to qualitative differences in peripheral immune response between the sexes, as was described in a recent study (Wiedrick et al., 2021). It is possible that immune components may work in conjunction with components solely within the CNS, as described in Du et al. (2014). Further investigation is needed to determine whether the peripheral immune system interacts with the CNS to produce worse neurodegeneration in males.

Findings from this study present evidence of increased neurodegeneration in male mice compared to females in the C57BL/6/MOG EAE model. This suggests an increased neurodegenerative response to inflammatory demyelination in males with EAE, a phenomenon

that is also observed in men with MS. These results will aid in elucidating sex-specific mechanisms of increased neurodegeneration associated with GM atrophy in EAE and MS.

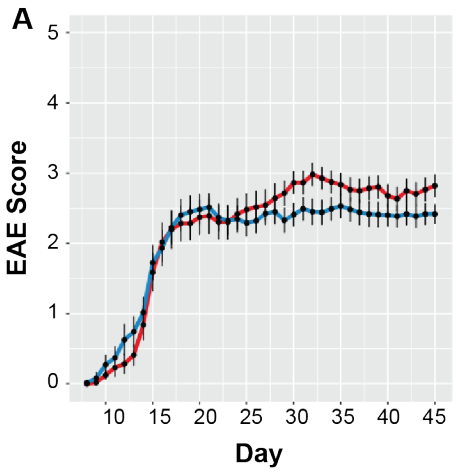

Figure 5-1: EAE scores. Male (blue, n = 31) and female (red, n = 29) EAE scores included in MRI analysis.

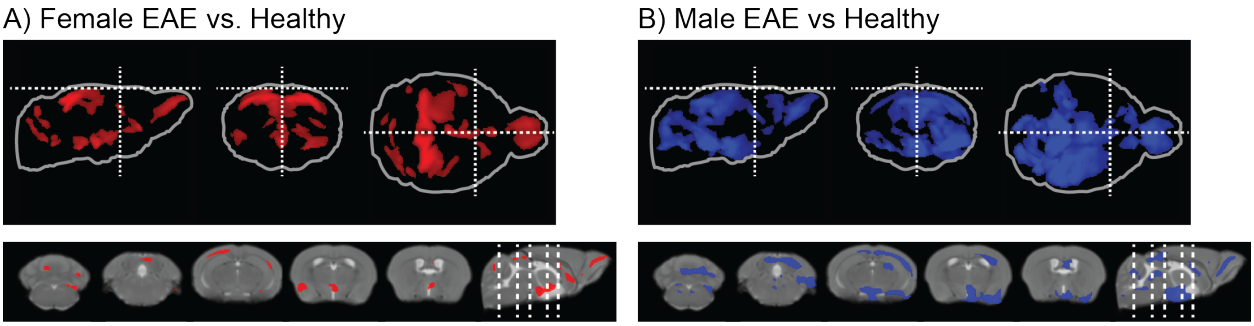

Figure 5-2: Voxel-based morphometry reveal more gray matter atrophy in males with EAE. *In vivo* MRI was collected at d45 from C57BL/6 male (n = 31) and female mice with EAE (n = 29) and were compared to age matched male (n = 31) and female (n = 29) healthy controls respectively. A-B) VBM revealed regions that demonstrate significant ($p \leq 0.05$, FDR corrected) atrophy in females (red) or males (blue). Maximum intensity projections are overlain on the Mortimer Space Atlas standard glass brains where the dotted line represents bregma, The female SPM volume was 16.657 mm^3 while the male SPM volume was 51.365 mm^3. Coronal sections demonstrate regions with more gray matter atrophy in males including the motor cortex, somatosensory cortex, visual cortex, hypothalamus, amygdala, entorhinal cortex, and cerebellum. Dotted lines on the sagittal section indicate the position of the coronal slices from left to right, respectively.

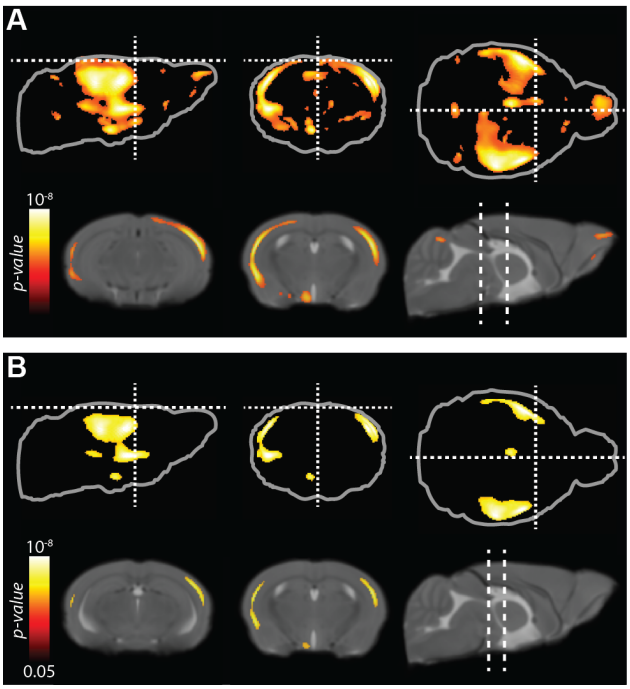

Figure 5-3: Worse disability correlates with gray matter atrophy in somatosensory cortex in males but not females. A) Worse cumulative EAE scores correlated with more gray matter atrophy in somatosensory cortex in males (n = 31) but not in females (n = 29). B) Disease duration (number of days sick) correlated with more gray matter atrophy in the somatosensory cortex of males but not females.

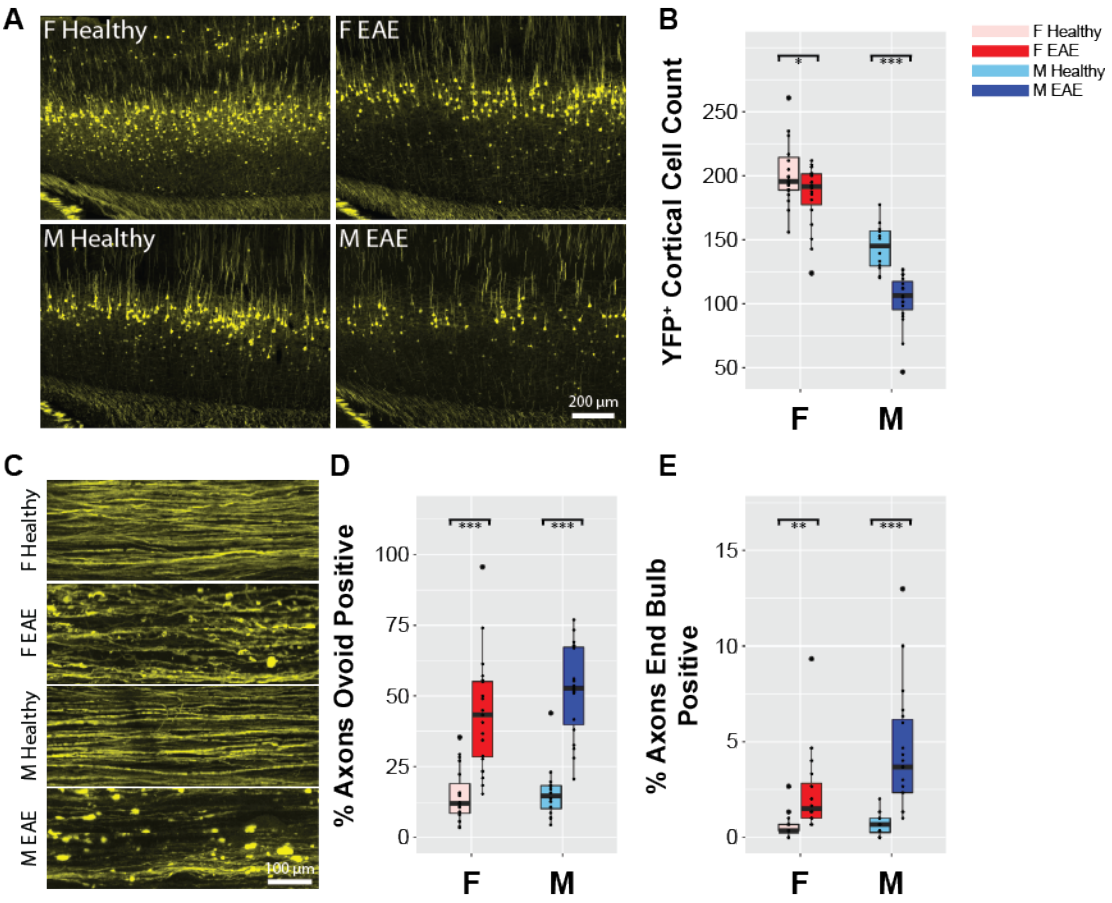

Figure 5-4: Male mice demonstrate worse neurodegeneration during EAE than females. A subset of the same mice used in MRI analysis that were Thy1-YFP^{+} were processed for analysis of neurodegeneration. (healthy females = 19, healthy males = 12, EAE females n =19, EAE males n = 19). A) Brains were sectioned at 40 µm and imaged at 10X magnification. Representative images are shown. B) Female and male EAE mice show cortical layer V cells loss compared to their healthy controls. A 2-way ANOVA indicated an interaction between sex and EAE ($p = 0.036$). C) Spinal cords were optically cleared using CLARITY and imaged at 10X magnification. Representative maximum intensity projection images are shown. D) Female and male EAE mice show an increased number of ovoid positive axons compared to their healthy controls. There was no interaction between sex and EAE. E) Female and male EAE mice show an increased number of end bulb positive axons compared to their healthy controls. A 2-way

ANOVA indicated an interaction between sex and EAE ($p = 0.025$). *$p < 0.05$, **$p < 0.01$, ***$p < 0.001$; *t* test.

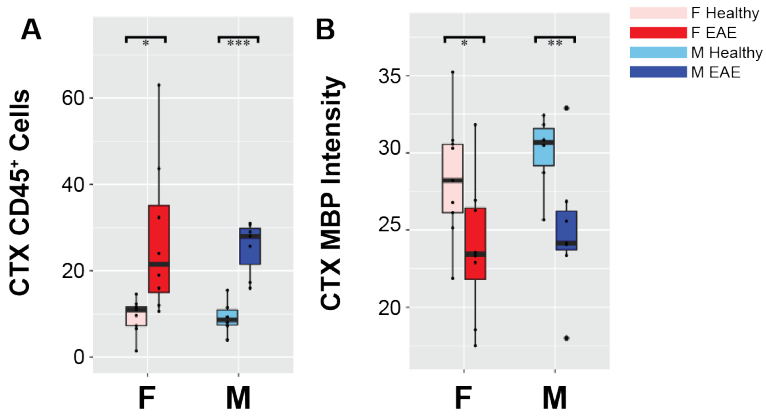

Figure 5-5: Male and female mice demonstrate similar inflammation and demyelination in the cerebral cortex during EAE. A subset of the same mice used in MRI analysis were processed for pathological analysis. (healthy females = 9, healthy males = 6, EAE females n =8, EAE males n = 7). A) Quantification of $CD45^+$ immune cells in cerebral cortex demonstrates an increase in inflammation in both male and female mice during EAE. There was no interaction between sex and EAE. B) . Quantification of MBP mean intensity in the cerebral cortex demonstrates demyelination in both male and female mice with EAE compared to their healthy controls. There was no interaction between sex and EAE. *p < 0.05, **p < 0.01, ***p < 0.001; *t* test.

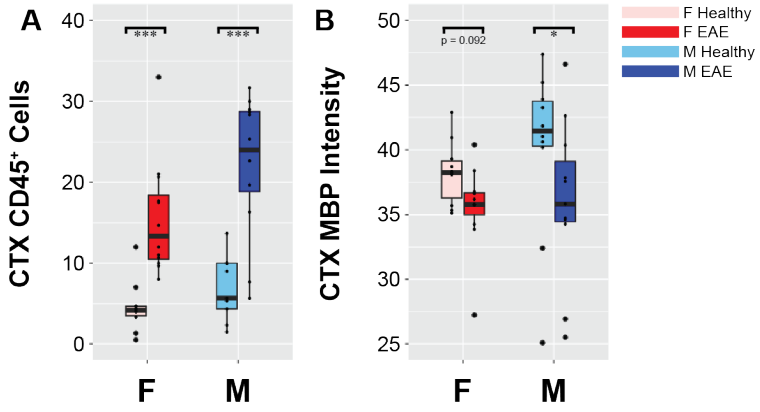

Figure 5-6: Supporting data. An additional subset of the same mice used in MRI analysis from a separate experiment were processed for pathological analysis to confirm our observed results. (healthy females = 10, healthy males = 6, EAE females n =12, EAE males n = 9). A) Quantification of $CD45^+$ immune cells in cerebral cortex demonstrates an increase in inflammation in both male and female mice during EAE. There was no interaction between sex and EAE. B) Quantification of MBP mean intensity in the cerebral cortex demonstrates demyelination in both male and female mice with EAE compared to their healthy controls. There was no interaction between sex and EAE. *p < 0.05, **p < 0.01, ***p < 0.001; *t* test.

5.6 References

Antulov, R., Weinstock-Guttman, B., Cox, J.L., Hussein, S., Durfee, J., Caiola, C., Dwyer, M.G., Bergsland, N., Abdelrahman, N., Stosic, M., Hojnacki, D., Munschauer, F.E., Miletic, D., Zivadinov, R., 2009. Gender-related differences in MS: a study of conventional and nonconventional MRI measures. Mult Scler 15, 345-354.

Ashburner, J., 2007. A fast diffeomorphic image registration algorithm. Neuroimage 38, 95-113.

Ashburner, J., Friston, K.J., 2005. Unified segmentation. Neuroimage 26, 839-851.

Batista, S., d'Almeida, O., Afonso, A., Freitas, S., Macário, C., Sousa, L., Castelo-Branco, M., Santana, I., Cunha, L., 2017. Impairment of social cognition in multiple sclerosis: Amygdala atrophy is the main predictor. Multiple sclerosis (Houndmills, Basingstoke, England) 23.

Beatty, W.W., Aupperle, R.L., 2002. Sex differences in cognitive impairment in multiple sclerosis. Clin Neuropsychol 16, 472-480.

Benedict, R.H., Zivadinov, R., 2011. Risk factors for and management of cognitive dysfunction in multiple sclerosis. Nat Rev Neurol 7, 332-342.

Benjamini, Y., Hochberg, Y., 1995. Controlling the False Discovery Rate: A Practical and Powerful Approach to Multiple Testing. Journal of the Royal Statistical Society Series B … 57, 289-300.

Calabrese, M., Atzori, M., Bernardi, V., Morra, A., Romualdi, C., Rinaldi, L., McAuliffe, M., Barachino, L., Perini, P., Fischl, B., Battistin, L., Gallo, P., 2007. Cortical atrophy is relevant in multiple sclerosis at clinical onset. J Neurol 254.

Catuneanu, A., Paylor, J., Winship, I., Colbourne, F., Kerr, B., 2019. Sex differences in central nervous system plasticity and pain in experimental autoimmune encephalomyelitis. Pain 160.

Charil, A., A, D., Lerch, J., Zijdenbos, A., Worsley, K., Evans, A., 2007. Focal cortical atrophy in multiple sclerosis: relation to lesion load and disability. Neuroimage 34.

Christianson, M.S., Mensah, V.A., Shen, W., 2015. Multiple sclerosis at menopause: Potential neuroprotective effects of estrogen. Maturitas 80, 133-139.

Cocozza, S., Petracca, M., Mormina, E., Buyukturkoglu, K., Podranski, K., Heinig, M., Pontillo, G., Russo, C., Tedeschi, E., Russo, C., Costabile, T., Lanzillo, R., Harel, A., Klineova, S., Miller, A., Brunetti, A., Morra, V., Lublin, F., Inglese, M., 2017. Cerebellar lobule atrophy and disability in progressive MS. Journal of neurology, neurosurgery, and psychiatry 88.

Confavreux, C., Vukusic, S., Adeleine, P., 2003. Early clinical predictors and progression of irreversible disability in multiple sclerosis: an amnesic process. Brain 126, 770-782.

Coutureau, E., Di Scala, G., 2009. Entorhinal cortex and cognition. Prog Neuropsychopharmacol Biol Psychiatry 33.

Damasceno, A., Damasceno, B., Cendes, F., 2014. The clinical impact of cerebellar grey matter pathology in multiple sclerosis. PLoS ONE 9.

Du, S., Itoh, N., Askarinam, S., Hill, H., Arnold, A.P., Voskuhl, R.R., 2014. XY sex chromosome complement, compared with XX, in the CNS confers greater neurodegeneration during experimental autoimmune encephalomyelitis. Proceedings of the National Academy of Sciences of the United States of America 111, 2806-2811.

Eijlers, A., van Geest, Q., Dekker, I., Steenwijk, M., Meijer, K., Hulst, H., Barkhof, F., Uitdehaag, B., Schoonheim, M., Geurts, J., 2018. Predicting cognitive decline in multiple sclerosis: a 5-year follow-up study. Brain : a journal of neurology 141.

Eijlers, A.J.C., Dekker, I., Steenwijk, M.D., Meijer, K.A., Hulst, H.E., Pouwels, P.J.W., Uitdehaag, B.M.J., Barkhof, F., Vrenken, H., Schoonheim, M.M., Geurts, J.J.G., 2019. Cortical atrophy accelerates as cognitive decline worsens in multiple sclerosis. Neurology 93, e1348-e1359.

Fisher, E., Lee, J.C., Nakamura, K., Rudick, R.A., 2008. Gray matter atrophy in multiple sclerosis: a longitudinal study. Ann Neurol 64, 255-265.

Fisniku, L.K., Chard, D.T., Jackson, J.S., Anderson, V.M., Altmann, D.R., Miszkiel, K.A., Thompson, A.J., Miller, D.H., 2008. Gray matter atrophy is related to long-term disability in multiple sclerosis. Ann Neurol 64, 247-254.

Golden, L., Itoh, Y., Itoh, N., Iyengar, S., Coit, P., Salama, Y., Arnold, A., Sawalha, A., Voskuhl, R., 2019. Parent-of-origin differences in DNA methylation of X chromosome genes in T lymphocytes. Proceedings of the National Academy of Sciences of the United States of America 116.

Golden, L.C., Voskuhl, R., 2017. The importance of studying sex differences in disease: The example of multiple sclerosis. Journal of Neuroscience Research 95, 633-643.

Henry, R., Shieh, M., Okuda, D., Evangelista, A., Gorno-Tempini, M., Pelletier, D., 2008. Regional grey matter atrophy in clinically isolated syndromes at presentation. Journal of neurology, neurosurgery, and psychiatry 79.

Hewagama, A., Patel, D., Yarlagadda, S., Strickland, F., Richardson, B., 2009. Stronger inflammatory/cytotoxic T-cell response in women identified by microarray analysis. Genes and immunity 10.

Huitinga, I., Erkut, Z., van Beurden, D., Swaab, D., 2003. The hypothalamo-pituitary-adrenal axis in multiple sclerosis. Annals of the New York Academy of Sciences 992.

Jakimovski, D., Zivadinov, R., Bergsland, N., Ramasamy, D., Hagemeier, J., Weinstock-Guttman, B., Kolb, C., Hojnacki, D., Dwyer, M., 2020. Sex-Specific Differences in Life Span Brain Volumes in Multiple Sclerosis. Journal of neuroimaging : official journal of the American Society of Neuroimaging 30.

Kim, R.Y., Mangu, D., Hoffman, A.S., Kavosh, R., Jung, E., Itoh, N., Voskuhl, R., 2018. Oestrogen receptor β ligand acts on CD11c+ cells to mediate protection in experimental autoimmune encephalomyelitis. Brain 141, 132-147.

Klein, S., Flanagan, K., 2016. Sex differences in immune responses. Nature reviews. Immunology 16.

Koch, M., Kingwell, E., Rieckmann, P., Tremlett, H., Neurologists, U.M.C., 2010. The natural history of secondary progressive multiple sclerosis. Journal of Neurology, Neurosurgery and Psychiatry 81, 1039-1043.

Koch-Henriksen, N., Sørensen, P., 2010. The changing demographic pattern of multiple sclerosis epidemiology. The Lancet. Neurology 9.

Kurth, F., Luders, E., Sicotte, N.L., Gaser, C., Giesser, B.S., Swerdloff, R.S., Montag, M.J., Voskuhl, R.R., Mackenzie-Graham, A., 2014. Neuroprotective effects of testosterone treatment in men with multiple sclerosis. Neuroimage Clin 4, 454-460.

Li, M., Masugi-Tokita, M., Takanami, K., Yamada, S., Kawata, M., 2012. Testosterone has sublayer-specific effects on dendritic spine maturation mediated by BDNF and PSD-95 in pyramidal neurons in the hippocampus CA1 area. Brain Research 1484.

MacKenzie-Graham, A., Kurth, F., Itoh, Y., Wang, H.J., Montag, M.J., Elashoff, R., Voskuhl, R.R., 2016. Disability-Specific Atlases of Gray Matter Loss in Relapsing-Remitting Multiple Sclerosis. JAMA Neurology 73, 944-953.

MacKenzie-Graham, A., Rinek, G.A., Avedisian, A., Gold, S.M., Frew, A.J., Aguilar, C., Lin, D.R., Umeda, E., Voskuhl, R.R., Alger, J.R., 2012a. Cortical atrophy in experimental autoimmune encephalomyelitis: in vivo imaging. Neuroimage 60, 95-104.

MacKenzie-Graham, A.J., Rinek, G.A., Avedisian, A., Morales, L.B., Umeda, E., Boulat, B., Jacobs, R.E., Toga, A.W., Voskuhl, R.R., 2012b. Estrogen treatment prevents gray matter atrophy in experimental autoimmune encephalomyelitis. Journal of Neuroscience Research 90, 1310-1323.

Meyer, C.E., Gao, J.L., Cheng, J.Y., Oberoi, M.R., Johnsonbaugh, H., Lepore, S., Kurth, F., Thurston, M.J., Itoh, N., Patel, K.R., Voskuhl, R.R., MacKenzie-Graham, A., 2019. Axonal damage in spinal cord is associated with gray matter atrophy in sensorimotor cortex in experimental autoimmune encephalomyelitis. Mult Scler, 1352458519830614.

Meyer, C.E., Kurth, F., Lepore, S., Gao, J.L., Johnsonbaugh, H., Oberoi, M.R., Sawiak, S.J.,

MacKenzie-Graham, A., 2017. In vivo magnetic resonance images reveal neuroanatomical sex differences through the application of voxel-based morphometry in C57BL/6 mice. Neuroimage 163, 197-205.

Montanari, M., Carbone, M., Coppola, L., Giuliano, M., Arpino, G., Lauria, R., Nardone, A., Leccia, F., Trivedi, M., Garbi, C., Bianco, R., Avvedimento, E., De Placido, S., Veneziani, B., 2019. Epigenetic Silencing of THY1 Tracks the Acquisition of the Notch1-EGFR Signaling in a Xenograft Model of CD44 +/CD24 low/CD90 + Myoepithelial Cells. Molecular cancer research : MCR 17.

Okuda, Y., Okuda, M., Bernard, C., 2002. Gender does not influence the susceptibility of C57BL/6 mice to develop chronic experimental autoimmune encephalomyelitis induced by myelin oligodendrocyte glycoprotein. Immunology letters 81.

Palaszynski, K.M., Loo, K.K., Ashouri, J.F., Liu, H., Voskuhl, R.R., 2004. Androgens are protective in experimental autoimmune encephalomyelitis: implications for multiple sclerosis. J Neuroimmunol 146, 144-152.

Papenfuss, T., Rogers, C., Gienapp, I., Yurrita, M., McClain, M., Damico, N., Valo, J., Song, F., Whitacre, C., 2004. Sex differences in experimental autoimmune encephalomyelitis in multiple murine strains. J Neuroimmunol 150.

Pettinelli, C.B., McFarlin, D.E., 1981. Adoptive transfer of experimental allergic encephalomyelitis in SJL/J mice after in vitro activation of lymph node cells by myelin basic protein: requirement for Lyt 1+ 2- T lymphocytes. J Immunol 127, 1420-1423.

Polacek, H., Kantorova, E., Hnilicova, P., Grendar, M., Zelenak, K., Kurca, E., 2019. Increased glutamate and deep brain atrophy can predict the severity of multiple sclerosis. Biomedical papers of the Medical Faculty of the University Palacky, Olomouc, Czechoslovakia 163.

Porrero, C., Rubio-Garrido, P., Avendano, C., Clasca, F., 2010. Mapping of fluorescent protein-

expressing neurons and axon pathways in adult and developing Thy1-eYFP-H transgenic mice. Brain Res 1345, 59-72.

Pozzilli, C., Tomassini, V., Marinelli, F., Paolillo, A., Gasperini, C., Bastianello, S., 2003. 'Gender gap' in multiple sclerosis: magnetic resonance imaging evidence. Eur J Neurol 10, 95-97.

Roberts, D.G., Johnsonbaugh, H.B., Spence, R.D., MacKenzie-Graham, A., 2016. Optical Clearing of the Mouse Central Nervous System Using Passive CLARITY. J Vis Exp.

Rocca, M., Valsasina, P., Meani, A., Gobbi, C., Zecca, C., Rovira, A., Sastre-Garriga, J., Kearney, H., Ciccarelli, O., Matthews, L., Palace, J., Gallo, A., Bisecco, A., Lukas, C., Bellenberg, B., Barkhof, F., Vrenken, H., Preziosa, P., Filippi, M., 2021. Association of Gray Matter Atrophy Patterns with Clinical Phenotype and Progression in Multiple Sclerosis. Neurology.

Roosendaal, S.D., Bendfeldt, K., Vrenken, H., Polman, C.H., Borgwardt, S., Radue, E.W., Kappos, L., Pelletier, D., Hauser, S.L., Matthews, P.M., Barkhof, F., Geurts, J.J., 2011. Grey matter volume in a large cohort of MS patients: relation to MRI parameters and disability. Mult Scler 17, 1098-1106.

Sawiak, S.J., Wood, N.I., Williams, G.B., Morton, A.J., Carpenter, T.A., 2009. Voxel-based morphometry in the R6/2 transgenic mouse reveals differences between genotypes not seen with manual 2D morphometry. Neurobiol Dis 33, 20-27.

Schoonheim, M.M., Popescu, V., Rueda Lopes, F.C., Wiebenga, O.T., Vrenken, H., Douw, L., Polman, C.H., Geurts, J.J., Barkhof, F., 2012. Subcortical atrophy and cognition: sex effects in multiple sclerosis. Neurology 79, 1754-1761.

Schoonheim, M.M., Vigeveno, R.M., Rueda Lopes, F.C., Pouwels, P.J., Polman, C.H., Barkhof, F., Geurts, J.J., 2014. Sex-specific extent and severity of white matter damage in multiple sclerosis: implications for cognitive decline. Hum Brain Mapp 35, 2348-2358.

Shattuck, D.W., Leahy, R.M., 2002. BrainSuite: an automated cortical surface identification tool.

Med Image Anal 6, 129-142.

Smith-Bouvier, D.L., Divekar, A.A., Sasidhar, M., Du, S., Tiwari-Woodruff, S.K., King, J.K., Arnold, A.P., Singh, R.R., Voskuhl, R.R., 2008. A role for sex chromosome complement in the female bias in autoimmune disease. J Exp Med 205, 1099-1108.

Spence, R.D., Kurth, F., Itoh, N., Mongerson, C.R., Wailes, S.H., Peng, M.S., MacKenzie-Graham, A.J., 2014. Bringing CLARITY to gray matter atrophy. Neuroimage 101, 625-632.

Steenwijk, M., Geurts, J., Daams, M., Tijms, B., Wink, A., Balk, L., Tewarie, P., Uitdehaag, B., Barkhof, F., Vrenken, H., Pouwels, P., 2016. Cortical atrophy patterns in multiple sclerosis are non-random and clinically relevant. Brain : a journal of neurology 139.

Swaab, D., Chung, W., Kruijver, F., Hofman, M., Ishunina, T., 2001. Structural and functional sex differences in the human hypothalamus. Hormones and Behavior 40.

Tassoni, A., Farkhondeh, V., Itoh, Y., Itoh, N., Sofroniew, M., Voskuhl, R., 2019. The astrocyte transcriptome in EAE optic neuritis shows complement activation and reveals a sex difference in astrocytic C3 expression. Scientific reports 9.

van Walderveen, M.A., Lycklama, A.N.G.J., Ader, H.J., Jongen, P.J., Polman, C.H., Castelijns, J.A., Barkhof, F., 2001. Hypointense lesions on T1-weighted spin-echo magnetic resonance imaging: relation to clinical characteristics in subgroups of patients with multiple sclerosis. Arch Neurol 58, 76-81.

Voskuhl, R., 2011. Sex differences in autoimmune diseases. Biol Sex Differ 2, 1.

Voskuhl, R., Patel, K., Paul, F., Gold, S., Scheel, M., Kuchling, J., Cooper, G., Asseyer, S., Chien, C., Brandt, A., Meyer, C., MacKenzie-Graham, A., 2020. Sex differences in brain atrophy in multiple sclerosis. Biology of sex differences 11.

Voskuhl, R.R., Gold, S.M., 2012. Sex-related factors in multiple sclerosis susceptibility and progression. Nat Rev Neurol 8, 255-263.

Voskuhl, R.R., Palaszynski, K., 2001. Sex hormones and experimental autoimmune

encephalomyelitis:Implications for multiple sclerosis. The Neuroscientist 7, 258-270.

Voskuhl, R.R., Pitchekian-Halabi, H., MacKenzie-Graham, A., McFarland, H.F., Raine, C.S., 1996. Gender differences in autoimmune demyelination in the mouse: implications for multiple sclerosis. Ann Neurol 39, 724-733.

Wallin, M., Culpepper, W., Coffman, P., Pulaski, S., Maloni, H., Mahan, C., Haselkorn, J., Kurtzke, J., 2012. The Gulf War era multiple sclerosis cohort: age and incidence rates by race, sex and service. Brain : a journal of neurology 135.

Weier, K., Penner, I., Magon, S., Amann, M., Naegelin, Y., Andelova, M., Derfuss, T., Stippich, C., Radue, E., Kappos, L., Sprenger, T., 2014. Cerebellar abnormalities contribute to disability including cognitive impairment in multiple sclerosis. PLoS ONE 9.

Weinshenker, B.G., Rice, G.P., Noseworthy, J.H., Carriere, W., Baskerville, J., Ebers, G.C., 1991. The natural history of multiple sclerosis: a geographically based study. 3. Multivariate analysis of predictive factors and models of outcome. Brain 114 (Pt 2), 1045-1056.

Wiedrick, J., Meza-Romero, R., Gerstner, G., Seifert, H., Chaudhary, P., Headrick, A., Kent, G., Maestas, A., Offner, H., Vandenbark, A., 2021. Sex differences in EAE reveal common and distinct cellular and molecular components. Cellular immunology 359.

Ziehn, M.O., Avedisian, A.A., Dervin, S.M., Umeda, E.A., O'Dell, T.J., Voskuhl, R.R., 2012. Therapeutic testosterone administration preserves excitatory synaptic transmission in the hippocampus during autoimmune demyelinating disease. Journal of Neuroscience 32, 12312-12324.

Chapter 6

Conclusions, limitations and future directions

Neurodegeneration in MS presents a unique investigatory challenge as it does not necessarily coincide with inflammation. A growing body of literature has indicated that GM atrophy is an effective biomarker for neurodegeneration (Dutta and Trapp, 2011) and is strongly associated with irreversible disability progression in MS (Fisher et al., 2008; Fisniku et al., 2008; Ghione et al., 2018). Unfortunately, the mechanisms underlying GM atrophy are poorly understood. Characterizing GM atrophy and associated pathology in the mouse model of MS, EAE, is an essential step in disentangling the neurodegenerative pathways in MS. The experiments in this volume progress towards utilizing *in vivo* MRI in mice to illustrate patterns of GM atrophy and its pathological correlates in EAE.

In chapter 2, I, for the first time, described the use of *in vivo* MRI and VBM to measure sex differences in the C57BL/6 mouse brain. Sex is an important factor to consider in the brain and is often overlooked in biomedical research (Beery and Zucker, 2011). Now, with the National Institute of Health mandate that researchers consider sex as a biological variable (Clayton and Collins, 2014), it is vital that we understand what sex differences exist in normal controls so we can incorporate that information into our interpretation of experimental results. By using VBM to compare 30 male and 30 female age-matched C57BL/6 mice, I identified several areas of interest. In particular, I found that males had a larger cortex, bed nucleus of the stria terminalis, posterior hypothalamus, ventral portion of caudoputamen, medial amygdala, and medial regions of the cerebellum. Females had a larger anterior hippocampus, basolateral amygdala, dorsal region of the caudoputamen, periaqueductal grey, and lateral portion of the cerebellar cortex. These results establish that sex differences in the brain are not negligible and can be measured utilizing VBM on *in vivo* MR images. This finding also emphasizes the importance of doing cross-sectional analyses within sex since there are baseline sex differences in the brain exist. For example, when analyzing sexual dimorphism in disease it is necessary that experimental males are compared to control males, while experimental females are compared to control females. If experimental males are compared to experimental females

without accounting for baseline sex differences, interpretations may be inaccurate. Lastly, many of the observed sex differences in this investigation were concordant with previous *ex vivo* mouse literature (Corre et al., 2014; Dorr et al., 2008; Spring et al., 2007) as well as human literature (Fan et al., 2010; Giedd et al., 1997; Goldstein et al., 2001), indicating these sex differences in brain are conserved in humans. This can provide insight into sex differences in behavior and disease.

An important limitation of this study is that we cannot make conclusions about the cellular or behavioral correlates of differences in brain volume. An interesting area of future research may be to perform molecular, genetic, or behavioral analyses and use voxelwise regression analyses to investigate the biological significance of baseline sex differences in brain volume.

Next, in chapter 3, I applied the use of *in vivo* MRI and VBM to the EAE disease model. The importance of studying regionalized GM atrophy has been increasingly recognized in MS literature, yet few studies have applied a voxelwise approach to investigate GM volume loss in EAE. To describe regionalized atrophy, I applied VBM and found substantial GM volume loss throughout the brain particularly within the cortex, caudoputamen, and thalamus, consistent with MS (Bergsland et al., 2012; Datta et al., 2015; Eshaghi et al., 2018). I further utilized VBM to create a pathology-specific atlas and define a relationship between axonal damage and GM atrophy in EAE. Interestingly, axonal damage in the spinal cord was correlated with GM atrophy in motor and sensorimotor regions of the cerebral cortex. Together, these results indicate that axonal damage plays a direct role in permanent GM atrophy. Conclusions drawn by identifying specific pathology related to atrophy can be used to inform our approach to treating GM atrophy and associated disabilities in MS. In particular, this investigation highlights the importance of preserving axonal integrity early in disease.

A limitation of this study is that these results are not causal. Correlations can indicate biological mechanisms, but cannot confirm them. An interesting avenue of future research

would be to determine the mechanism of axonal transection that contributes to GM atrophy. Intriguingly, oxidative stress – resulting in mitochondrial dysfunction – has been implicated in axonal loss in both MS and EAE (Nikic et al., 2011; Qi et al., 2006; Sadeghian et al., 2016; Smith et al., 2001; Smith and Lassmann, 2002). Future investigation is needed to determine if axonal mitochondrial dysfunction can induce GM atrophy both in normal mice and during EAE.

In chapter 4, I sought to investigate how a neuroprotective molecule, estriol, affected mechanisms of GM atrophy. Immunomodulatory treatments in MS have had modest success at preventing GM atrophy and the progression of long-term disability (Calabrese et al., 2012). Thus, there is a clinical need for neuroprotective therapies in MS. Treatment with estriol, an estrogen produced during pregnancy, has been shown to ameliorate disease in EAE (Kim et al., 1999; Palaszynski et al., 2004; Ziehn et al., 2012). In MS patients, estriol treatment was associated with cortical GM preservation and improvement in cognitive testing (MacKenzie-Graham et al., 2018; Voskuhl et al., 2016). In this study, I first discovered a network of pathology that contributes to GM atrophy. I then treated with estriol therapeutically, after disease onset, and found that estriol treatment disrupted this network. *In vivo* magnetic resonance imaging (MRI) revealed that therapeutic estriol treatment preserved GM volume in the cerebral cortex during EAE. Estriol treatment further prevented demyelination, microglial activation, neuronal and synaptic loss in the cerebral cortex. Additionally, estriol preserved axonal integrity in the spinal cord. I investigated a candidate mechanism for estriol-mediated GM preservation and found that ligation of ERβ induces remyelination in the cerebral cortex during EAE. Together, this demonstrates that therapeutic estriol treatment can be neuroprotective in EAE by attenuating GM pathologies and preventing cortical GM atrophy.

These results highlight an important role for estriol in remyelination and GM preservation, but are limited in that they do not establish causality. I chose to investigate cortical remyelination through ERβ as one possible mechanism through which estriol could preserve GM volume. However, it is possible that estriol treatment initiates additional neuroprotective mechanisms

that contribute to GM preservation. For example, estriol can act as an antioxidant (Mooradian, 1993) which could lead to a reduction in microglia activation and axonal damage. Further study is necessary to determine other effects of estriol treatment and the degree to which individual mechanisms can contribute to GM preservation.

In chapter 5, I, for the first time, characterized patterns of GM atrophy within each sex during EAE using *in vivo* MRI and VBM. In MS, females demonstrate increased susceptibility and an increased inflammatory response while males demonstrate faster disease progression. Human studies have shown that males with MS have increased GM atrophy compared to females (Voskuhl et al., 2020). Sex differences in GM atrophy had not previously been investigated during EAE. VBM indicated more extensive GM atrophy in males during EAE particularly in the motor cortex, visual cortex, somatosensory cortex, hypothalamus, amygdala, and cerebellum. Voxelwise-regression analysis revealed a strong association between disability and GM atrophy in the somatosensory cortex in males, but not females. Further, males demonstrated increased neuronal loss in the cerebral cortex and increased axonal transection in the spinal cord compared to females. Together, these results demonstrate that males experience worse GM atrophy and worse neurodegeneration during chronic EAE than females, mirroring clinical observations in MS. Establishing sex differences in GM atrophy during EAE will allow for the future investigation of mechanisms that contribute to increased GM atrophy in males.

This study is the first step in determining the role of sex-specific factors on disease progression and much work remains to be done to determine why males show increased neurodegeneration compared to females. My results are limited in that they do not yet indicate a mechanism. Now that I have shown that sex differences exist in the chronic EAE model, I will first investigate whether these findings are hormone-mediated. I have conducted a study where gonadectomized male and female mice with EAE are compared to sham male and female mice with EAE. If the atrophy in male and female gonadectomized mice is comparable it might

suggest a protective effect of endogenous estrogens against brain atrophy during EAE. In the longer term, utilizing the four core genotype mouse model, where the effects of sex hormones are decoupled from the effects of sex chromosomes, will be valuable in determining whether differences in sex chromosome complement are contributing to the observed sex differences in GM atrophy and cerebral cortex neurodegeneration.

GM atrophy in MS is strongly linked to irreversible disability yet its underlying mechanisms are poorly understood. The studies documented in this dissertation demonstrate the use of *in vivo* MRI to characterize GM atrophy in EAE and its associated pathology. This approach integrated cellular and anatomical information to identify mechanisms of neurodegeneration and neuroprotection. The exciting finding of increased neurodegeneration in males with chronic EAE compared to females will serve as a starting point for future studies to investigate different neurodegenerative mechanisms in the sexes. Further studies may build upon this work and aid in the development of novel neuroprotective therapies for patients with MS and potentially other neurodegenerative diseases as well.

Conclusion References

Beery, A.K., Zucker, I., 2011. Sex Bias in Neuroscience and Biomedical Research. Neuroscience and biobehavioral reviews 35, 565-572.

Bergsland, N., Horakova, D., Dwyer, M.G., Dolezal, O., Seidl, Z.K., Vaneckova, M., Krasensky, J., Havrdova, E., Zivadinov, R., 2012. Subcortical and cortical gray matter atrophy in a large sample of patients with clinically isolated syndrome and early relapsing-remitting multiple sclerosis. Ajnr. American Journal of Neuroradiology 33, 1573-1578.

Calabrese, M., Bernardi, V., Atzori, M., Mattisi, I., Favaretto, A., Rinaldi, F., Perini, P., Gallo, P., 2012. Effect of disease-modifying drugs on cortical lesions and atrophy in relapsing-remitting multiple sclerosis. Mult Scler 18, 418-424.

Clayton, J.A., Collins, F.S., 2014. Policy: NIH to balance sex in cell and animal studies. Nature 509, 282-283.

Corre, C., Friedel, M., Vousden, D.A., Metcalf, A., Spring, S., Qiu, L.R., Lerch, J.P., Palmert, M.R., 2014. Separate effects of sex hormones and sex chromosomes on brain structure and function revealed by high-resolution magnetic resonance imaging and spatial navigation assessment of the Four Core Genotype mouse model. Brain Struct Funct.

Datta, S., Staewen, T.D., Cofield, S.S., Cutter, G.R., Lublin, F.D., Wolinsky, J.S., Narayana, P.A., 2015. Regional gray matter atrophy in relapsing remitting multiple sclerosis: baseline analysis of multi-center data. Mult Scler Relat Disord 4, 124-136.

Dorr, A.E., Lerch, J.P., Spring, S., Kabani, N., Henkelman, R.M., 2008. High resolution three-dimensional brain atlas using an average magnetic resonance image of 40 adult C57Bl/6J mice. Neuroimage 42, 60-69.

Dutta, R., Trapp, B.D., 2011. Mechanisms of neuronal dysfunction and degeneration in multiple sclerosis. Prog Neurobiol 93, 1-12.

Eshaghi, A., Marinescu, R., Young, A., Firth, N., Prados, F., Jorge Cardoso, M., Tur, C., De

Angelis, F., Cawley, N., Brownlee, W., De Stefano, N., Laura Stromillo, M., Battaglini, M., Ruggieri, S., Gasperini, C., Filippi, M., Rocca, M., Rovira, A., Sastre-Garriga, J., Geurts, J., Vrenken, H., Wottschel, V., Leurs, C., Uitdehaag, B., Pirpamer, L., Enzinger, C., Ourselin, S., Gandini Wheeler-Kingshott, C., Chard, D., Thompson, A., Barkhof, F., Alexander, D., Ciccarelli, O., 2018. Progression of regional grey matter atrophy in multiple sclerosis. Brain : a journal of neurology 141.

Fan, L., Tang, Y., Sun, B., Gong, G., Chen, Z.J., Lin, X., Yu, T., Li, Z., Evans, A.C., Liu, S., 2010. Sexual dimorphism and asymmetry in human cerebellum: An MRI-based morphometric study. Brain Research 1353, 60-73.

Fisher, E., Lee, J.C., Nakamura, K., Rudick, R.A., 2008. Gray matter atrophy in multiple sclerosis: a longitudinal study. Ann Neurol 64, 255-265.

Fisniku, L.K., Chard, D.T., Jackson, J.S., Anderson, V.M., Altmann, D.R., Miszkiel, K.A., Thompson, A.J., Miller, D.H., 2008. Gray matter atrophy is related to long-term disability in multiple sclerosis. Ann Neurol 64, 247-254.

Ghione, E., Bergsland, N., Dwyer, M., Hagemeier, J., Jakimovski, D., Paunkoski, I., Ramasamy, D., Silva, D., Carl, E., Hojnacki, D., Kolb, C., Weinstock-Guttman, B., Zivadinov, R., 2018. Brain Atrophy Is Associated with Disability Progression in Patients with MS followed in a Clinical Routine. Ajnr. American Journal of Neuroradiology 39.

Giedd, J.N., Castellanos, F.X., Rajapakse, J.C., Vaituzis, A.C., Rapoport, J.L., 1997. Sexual dimorphism of the developing human brain. Prog Neuropsychopharmacol Biol Psychiatry 21, 1185-1201.

Goldstein, J.M., Seidman, L.J., Horton, N.J., Makris, N., Kennedy, D.N., Caviness, V.S., Jr., Faraone, S.V., Tsuang, M.T., 2001. Normal sexual dimorphism of the adult human brain assessed by in vivo magnetic resonance imaging. Cerebral Cortex 11, 490-497.

Kim, S., Liva, S.M., Dalal, M.A., Verity, M.A., Voskuhl, R.R., 1999. Estriol ameliorates

autoimmune demyelinating disease: implications for multiple sclerosis. Neurology 52, 1230-1238.

MacKenzie-Graham, A., Brook, J., Kurth, F., Itoh, Y., Meyer, C., Montag, M.J., Wang, H.J., Elashoff, R., Voskuhl, R.R., 2018. Estriol-mediated neuroprotection in multiple sclerosis localized by voxel-based morphometry. Brain Behav 8, e01086.

Mooradian, A., 1993. Antioxidant Properties of Steroids. The Journal of steroid biochemistry and molecular biology 45.

Nikic, I., Merkler, D., Sorbara, C., Brinkoetter, M., Kreutzfeldt, M., Bareyre, F.M., Bruck, W., Bishop, D., Misgeld, T., Kerschensteiner, M., 2011. A reversible form of axon damage in experimental autoimmune encephalomyelitis and multiple sclerosis. Nat Med 17, 495-499.

Palaszynski, K.M., Liu, H., Loo, K.K., Voskuhl, R.R., 2004. Estriol treatment ameliorates disease in males with experimental autoimmune encephalomyelitis: implications for multiple sclerosis. J Neuroimmunol 149, 84-89.

Qi, X., Lewin, A.S., Sun, L., Hauswirth, W.W., Guy, J., 2006. Mitochondrial protein nitration primes neurodegeneration in experimental autoimmune encephalomyelitis. J Biol Chem 281, 31950-31962.

Sadeghian, M., Mastrolia, V., Rezaei Haddad, A., Mosley, A., Mullali, G., Schiza, D., Sajic, M., Hargreaves, I., Heales, S., Duchen, M.R., Smith, K.J., 2016. Mitochondrial dysfunction is an important cause of neurological deficits in an inflammatory model of multiple sclerosis. Sci Rep 6, 33249.

Smith, K.J., Kapoor, R., Hall, S.M., Davies, M., 2001. Electrically active axons degenerate when exposed to nitric oxide. Ann Neurol 49, 470-476.

Smith, K.J., Lassmann, H., 2002. The role of nitric oxide in multiple sclerosis. Lancet Neurol 1, 232-241.

Spring, S., Lerch, J.P., Henkelman, R.M., 2007. Sexual dimorphism revealed in the structure of

the mouse brain using three-dimensional magnetic resonance imaging. Neuroimage 35, 1424-1433.

Voskuhl, R., Patel, K., Paul, F., Gold, S., Scheel, M., Kuchling, J., Cooper, G., Asseyer, S., Chien, C., Brandt, A., Meyer, C., MacKenzie-Graham, A., 2020. Sex differences in brain atrophy in multiple sclerosis. Biology of sex differences 11.

Voskuhl, R.R., Wang, H., Wu, T.C., Sicotte, N.L., Nakamura, K., Kurth, F., Itoh, N., Bardens, J., Bernard, J.T., Corboy, J.R., Cross, A.H., Dhib-Jalbut, S., Ford, C.C., Frohman, E.M., Giesser, B., Jacobs, D., Kasper, L.H., Lynch, S., Parry, G., Racke, M.K., Reder, A.T., Rose, J., Wingerchuk, D.M., MacKenzie-Graham, A.J., Arnold, D.L., Tseng, C.H., Elashoff, R., 2016. Estriol combined with glatiramer acetate for women with relapsing-remitting multiple sclerosis: a randomised, placebo-controlled, phase 2 trial. Lancet Neurol 15, 35-46.

Ziehn, M.O., Avedisian, A.A., Dervin, S.M., O'Dell, T.J., Voskuhl, R.R., 2012. Estriol preserves synaptic transmission in the hippocampus during autoimmune demyelinating disease. Lab Invest 92, 1234-1245.